An Antenna Specific Site Modeling Tool for Interactive Computation of Coverage Regions for Indoor Wireless Communications

Nitin Bhat

Thesis submitted to the faculty of the
Virginia Polytechnic Institute and State University
in partial fulfillment of the requirements for the degree of

Master of Science
in
Electrical Engineering

A. Lynn Abbott, Chair
Theodore S. Rappaport
Brian D. Woerner

March 2, 1998
Blacksburg, Virginia

An Antenna Specific Site Modeling Tool
for Interactive Computation of Coverage Regions
for Indoor Wireless Communications

by
Nitin Bhat
Committee Chairman: Dr. A. Lynn Abbott, Chairman
The Bradley Department of Electrical Engineering

Abstract

A goal of indoor wireless communication is to strategically place RF base stations to obtain optimum signal coverage at the lowest cost and power. Traditionally, transceiver locations have been selected by human experts who rely on experience and heuristics to obtain a near-optimum placement. Current methods depend on involved on-site communication measurements and crude statistical modeling of the obtained data which is time consuming and prohibitive in cost. Given the inherent variability of the indoor environment, such a method often yields poor efficiency. As an example, it is possible that more power than required or extra number of transceivers were used. This thesis describes an interactive software system that can be used to aid transceiver placement. The tool is easy to use and is targeted at users who are not experts in wireless communication system design. Once the transceiver locations are selected by the user within a graphical floor plan, the system uses simple path-loss models to predict coverage regions for each transceiver. The coverage regions are highlighted to indicate expected coverage. Earlier work assumed isotropic transceivers and had limited directional transmitter support. This thesis describes how the tool has been enhanced to support a wide range of 3D antenna patterns as encountered in practical situations. The tool has also been expanded to accommodate more partition types and to report area of coverage. The resulting system is expected to be very useful in the practical deployment of indoor wireless systems.

Keywords: Directional antennas, RF propagation, Site specific prediction, Wireless communication.

Acknowledgments

The acknowledgments are many, and if I ponder on including everyone, it can take the form of a thesis! My sincere appreciation goes to my academic advisor Dr. A. Lynn Abbott for his unerring guidance and support during the past three years. Thanks Sir, for patiently listening, when I used to digress and go off on tangents with my ideas! Dr. T.S. Rappaport provided the feedback and vision without which all the pieces of my work could not have fallen together. I wish to thank him for that. Appreciation is due to Dr. B. D. Woerner for serving on my graduate committee.

I got involved into this work thanks to my friend Manish Panjwani. The thesis is essentially based on what he did. Thanks are due to Roger Skidmore for his support during the initial phases of SMT 7.0 development. This research was partially supported by IBM, T.J.Watson Research Center. For this and for all the suggestions, I want to extend my thanks to Dr. Modest Oprysko.

This work also owes much to the inspiration and encouragement I received from my friend and now wife, Srilekha. Finally, my sincere appreciation to my parents and sisters for their love and support. Without them I could not have got this far in my career.

Table of Contents

List of Figures

List of Tables

Chapter 1
Introduction

1.0 Overview

This thesis describes a system which assists in the strategic placement of radio-frequency (RF) base stations within an indoor environment. Henceforth referred to as the SMT 7.0 (Site Modeling Tool, version 7.0), this system gives the user interactive capability to display graphical floor plans and select base station location, orientation and communication parameters. The system then computes and highlights estimated coverage regions for each transceiver, enabling the user to assess the total coverage within building. Simple but accurate path-loss models are used for coverage prediction with independent choice of single floor or multifloor environment. In essence, the SMT 7.0 is targeted at users with no expertise in wireless communication system design and intended to be a powerful tool in specifying indoor wireless systems.

1.1 Motivation

The design problem is as follows: Given a building, how do you position base stations so that communication is possible at all desired locations in the building, with the minimum cost and power? Traditionally a human expert studies the floor plan and uses heuristics to suggest an appropriate plan for base station placement. Unfortunately, this approach is difficult and costly. Also, such system designs are generally over-engineered [Fort95]. The indoor propagation channel is far too complicated for highly accurate modeling, and spending time and money by taking measurements at potential customer premises is not the answer. What is needed is an easy to use, accurate system that can assist someone who is not an expert in communication system design. Recently, tools such as SMT *Plus* [Skid97] and WISE [Fort95] have been developed to partially fulfill this need.

However, a wireless system design solution to satisfy the requirements of minimum power and cost is impossible without a judicious choice of directional antennas. In fact it has been often stated that any system is only as good as the antennas. The ability to fully support 3D directional antennas was absent in the earlier SMT versions (SMT [Panj95] and SMT *Plus* [Skid97]). As this thesis describes, the SMT 7.0 fulfills this need.

1.2 Contributions of this Research

SMT 7.0 is the only system available which offers the user a choice of an astonishing range of 3D antenna patterns for transceivers. This is key to satisfying the design requirements with the additional advantage of reducing signal spill over. Such a requirement is becoming quite important for security and privacy reasons.

The main contributions of this research are listed below:

1) A mathematical foundation has been developed which allows prediction coverage to include any directional antenna pattern which admits a closed form representation. The antennas patterns have been categorized as “User provided patterns”, “Omnidirectional patterns” and “Other directional patterns”.
2) A set of closed form two dimensional pattern equations for practically deployable antenna types was compiled. These equations form the basis for 3D calculations. A study was made on the most useful range of parameter values for the pattern equation variables. Some of these equations were used by the Antenna*Builder* of SMT *Plus*.
3) The standard industrial format for user generated two dimensional directional antenna patterns was used, which permits the user to input data in the same file format for SMT calculations. The SMT coverage contour resolution is independent of the resolution of the file format data.
4) The tool allows the user to work with three dimensional patterns. This implies that the user can orient the patterns in any direction by rotating them in 3D. He can also place the transmitter antenna at a different height than the receivers. A mathematical foundation based on homogeneous coordinate transformations was developed for the

same. Note that the coverage prediction is done in 2D on the receiver plane for any arbitrary orientation of 3D antenna pattern on the transmitter plane.

5) An interpolation method was developed to work with two dimensional patterns, and convert the same into three dimensional patterns. An algorithm was worked out to accomplish the same, after looking into various interpolation techniques.
6) The user interface was enhanced by addition of a directional antenna menu and icon. The tool was embellished by allowing the user to view the area of coverage. This area coverage feature was also ported to SMT *Plus* during the initial phases of its development.
7) AutoCAD features were exploited, to make the prediction models more dynamic by providing the ability to specify an increased number of partitions (from 2 to 4). This idea was used by SMT *Plus* and the number of partition types increased to 6.

1.3 Organization of Thesis

Chapter 2 presents an overview of indoor wireless communication systems and explains the relevance of the SMT. Chapter 3 gives a high level description of the SMT. This also includes an explanation on the relationship between AutoCAD and the SMT. Chapter 4 describes directional antennas. This chapter contains the mathematical development of equations to predict signal coverage, and a detailed description of various patterns in 2-dimensional planes. Chapter 5 focuses on 3-dimensional directional antenna patterns and describes the interpolation and coordinate transformation techniques employed to obtain the same from 2-dimensional ones. Chapter 6 provides operational examples. Chapter 7 presents a conclusion and suggests future work. Appendices A to D describe the minimum system requirements, provide a listing of files along with their placement, present a brief description of SMT code compilation and provide the SMT 7.0 command reference respectively.

Chapter 2
Indoor Wireless Communication Systems

2.0 Overview

This chapter provides an introduction to indoor wireless communication systems. In an indoor environment, wireless systems provide an attractive alternative to traditional wired ones. One can broadly classify indoor wireless systems as either cellular or wireless local area networks. Cellular systems are predominantly voice applications, while the other is essentially for data applications. Wireless technology has shown tremendous growth potential in both cases. The following points are noteworthy.

- Installation costs for a wired local area network is estimated to be 40% of the total cost, thus making wireless LAN an attractive alternative in situations which may involve frequent network reconfigurations or relocation [Nemz95].

- There is no doubt that a tremendous boom exists in the mobile work force. It is interesting to note that the mobile work force in the U.S. is estimated to be 45 million of the 118 million total, and approximately 8 million laptop computers are sold every year. These numbers are expected to grow phenomenally. For example, indoor wireless LAN systems are expected to yield $500 million by 1998 [Nemz95].

- The application domain for indoor wireless systems is huge. Wireless desktops, wireless laptops, cordless phones, point-of-sale devices, active badges, bar code readers are examples of devices used in indoor wireless systems. For data applications, the data rates of wireless systems are comparable to their wired counterparts. One prominent application of wireless laptops or notebook computers is in inventory control systems. Since virtual communication mobility is well on its way to being a reality, we can imagine numerous applications for portable terminals

in areas of customer service, retailing and health care. However data rates for mobile units are generally low and likely to remain so because of the direct relationship between data rate and power consumption [Mull95].

2.1 Indoor Wireless Systems

2.1.1 Cellular Systems

For completeness these systems can be categorized as wireless radio (analog or digital cellular), cordless telephone (digital cordless) and personal communication standards (PCS). Table 1 gives a listing of currently popular standards around the world. Frequency bands and the driving technology behind the standards are also mentioned. The standards and their popularity vary based on geographic location. However all standards can be thought of as flavors of an essential few. Even though the systems are primarily for voice applications, low data rate applications are also possible. For example CDPD (Cellular Digital Packet Data) takes advantage of idle time on analog AMPS (Advanced Mobile Phone Service) channels to transmit packet data at 19.2 kbps [Padg95]. The second generation cellular systems focus on [Padg95] the following:

- Digital technology (TDMA[1] or CDMA[2]) to allow natural integration with the evolving digital wireline network in contrast to the analog technology (FDMA[3]).
- Flexibility of mixed voice/data applications.
- Increased capacity (e.g. voice coding).
- Reduced RF transmit power (more battery life).
- Less complexity, encryption for communication privacy.

[1] TDMA: Time Division Multiple Access.
[2] CDMA: Code Division Multiple Access.
[3] FDMA: Frequency Division Multiple Access.

2.1.2 Wireless Local Area Networks

Popularly known as WLANs, such systems are targeted primarily for high-data-rate in-building applications (≥ 1Mbps). Less frequent are the short haul or building-to-building applications. The backbone for a WLAN is generally a wired network (e.g. Ethernet, Token Ring, FDDI). Terminology varies, but the wireless unit which forms the interface to the wired one is generally called an *access point* or a *base station* or a *hub unit*.

Table 1. *Popular cellular standards [Rapp95].*

Name	Type	Frequency range	Multiple access
AMPS	Analog cellular	824-849/869-894	FDM[4]
N-AMPS	Analog cellular	824-849/869-894	FDMA
IS - 54/ IS - 136	Digital cellular	824-849/869-894	TDMA/FDMA/FDD
GSM	Digital cellular	890-915/935-960	TDMA/FDMA/FDD
IS 95	Digital cellular	824-849/869-894	CDMA
PACS	Digital cordless	1850-1910/1930-90	FDD or TDD[5]
PHS	Digital cordless	1895-1918	TDD
CT2	Digital cordless	864-868, 944-948	TDD
DECT	Digital cordless	1880-1900	TDD
PHS	PCS standard	1895-1907	TDMA/FDMA/ TDD
DCS 1800	PCS standard	1710-85/1805-80	TDMA/FDMA/FDD

[4] FDM: Frequency Division Duplex
[5] TDD: Time Division Duplex

Figure 1 is an illustration of one possible configuration for a such a network. The most common frequency band for WLANs applications is the FCC allocated unlicensed ISM (Industrial, Scientific, Medical) band. These bands are 902-928 MHz, 2400-2483.5 MHz, and 5725-5850 MHz.

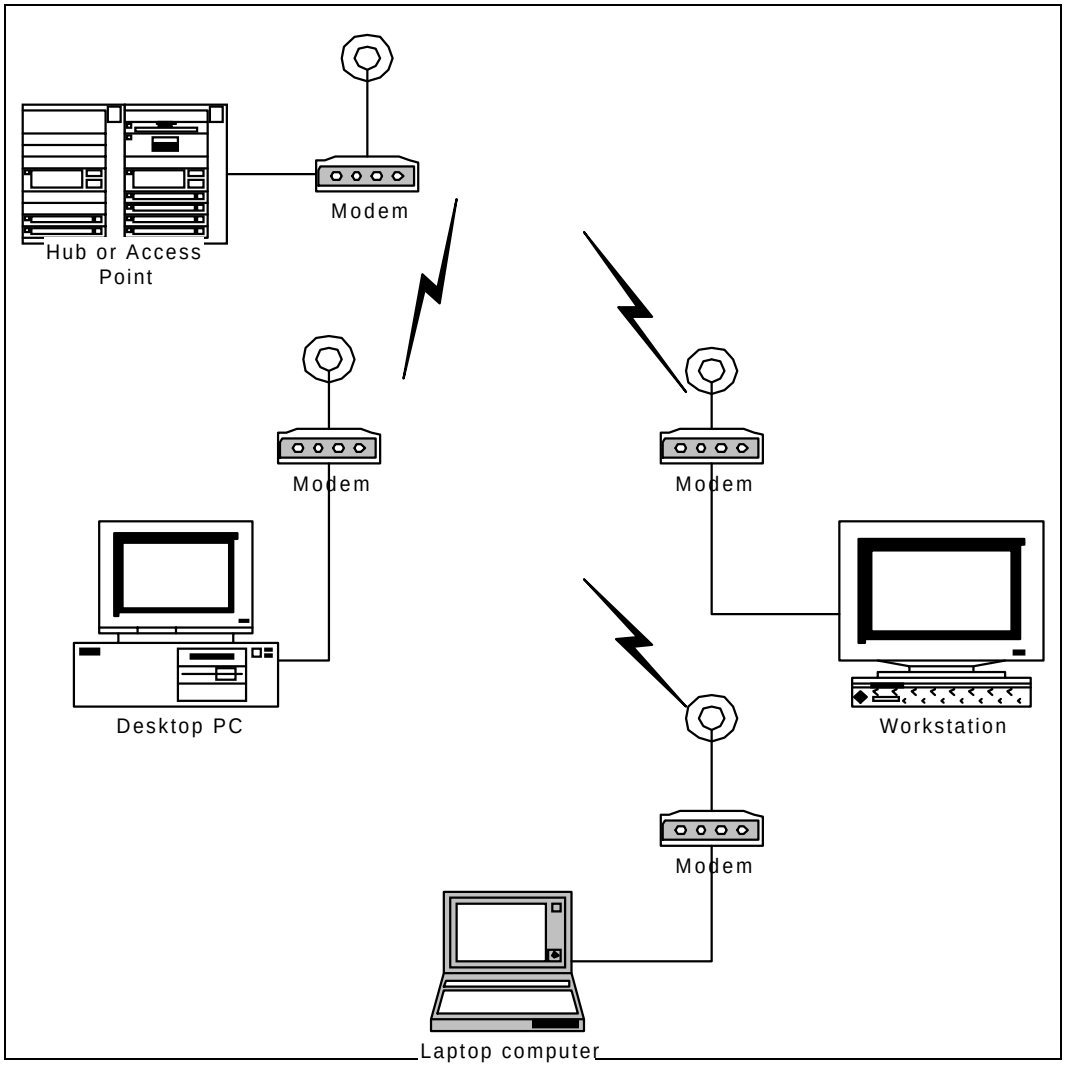

Figure 1. *An example of a wireless network with one access point and three transceivers. Each computer communicates directly with the hub. The hubs normally employ omnidirectional patterns, whereas the others can be directional.*

2.1.3 WLANs: Standardization and Vendor Profiles

With regard to LANs, the principal standards-making organization in the U.S. is the IEEE. The IEEE 802.11 standard for wireless LANs was finalized on June 26,1997 after seven years of work. Standard-conferment products are expected to make their debut by year's end, but interoperability between vendor offerings is not expected until the beginning of 1999. In Europe, HIPERLAN is the comparable standard to IEEE 802.11. HIPERLAN is focusing on data rates higher than that in 802.11. This is made possible by the allocation of large dedicated bands: 5150-5300 MHz plus 200 MHz near 17 GHz. However there are a number of similarities between the two standards. Both are intended for data rates exceeding 1 Mbps, and since it is anticipated that many terminals will be battery powered, the standards incorporate sleep mode for power management. Architectures with infrastructure will be supported, as well as "ad hoc" architectures, whereby terminals communicate directly to each other (peer-to-peer) without the mediation of a fixed base station. Point-to-point, point to multicast and broadcast services will be available. Finally, while asynchronous packet transmission will be the dominant mode, distributed time-bounded services (DTBS) will also be supported [Padg95].

As is typically the case with many technologies, vendors began marketing their own technologies before organizations like IEEE began work on standards. The following is a brief profile for wireless LAN offerings of major vendors [Mull95] [Nemz95]. Eventually all major vendors will offer complete wireless connectivity solutions that encompass Ethernet and token-ring compatibility, as well as SNMP (Simple Network Management Protocol) management.

- **WaveLAN:** It was a product originally developed by NCR Corp. until it merged with AT&T. WaveLAN provides peer-to-peer communication in the ISM Band. It uses direct sequence spread-spectrum technology with CSMA/CA (Carrier Sense Multiple Access/ Collision Avoidance) and provides a data transmission rate of two Mbps with a BER (Bit Error Rate) of better than 10^{-8}. The working range of WaveLAN in

an office setting is 100 ft to 800 ft, depending on environmental characteristics, with a typical coverage area of 50,000 square feet. The operating range can be extended to five miles using a directional antenna with the WavePOINT, a bridge that also functions as an access point to the wired network.

- **AirLAN:** Developed by Solectek Corp., AirLAN closely resembles WaveLAN in many of its features due to cooperative development. AirLAN offers a wireless Ethernet solution, which includes an internal adapter for desktop computers, a PCMCIA card for portable computers, a bridge, and a hub. It uses spread-spectrum in the ISM frequency Band and transmits data at two Mbps. Its omni-directional antenna provides coverage up to 800 ft. which translates into 50,000 square feet of office space.

- **Altair Plus II:** Developed by Motorola, Altair uses Ethernet protocol and operates in the terrestrial microwave spectrum near 18 GHz. It offers an effective data throughput of 5.7 Mbps and uses a transceiver together with a six-sector antenna. In the U.S, a site-specific FCC license is required. Depending on deployed power, a coverage of 5,000 to 50,000 square feet can be obtained.

- **ARLAN:** The family of wireless Ethernet products developed by Aironet Wireless Comminication Inc., is called ARLAN (Advanced Radio Local Area Network). ARLAN consists of two separate product lines operating at different frequency ranges using spread spectrum technology. The base product line operates in the 902-928 MHz ISM band to provide data transfer rate of 215 to 880 Kbps. The other product line offers data rate of 1 Mbps and operates in the 2.4 GHz frequency. The indoor operating radius varies according to the building structure: 300 feet in an indoor dense office; 600 feet in an indoor open office; and up to 3000 feet in any open factory or warehouse. The hub has the ability to hand off the connection to another hub as users move about the workplace from one *microcell* to another.

- **FreePort:** Developed by Windata, FreePort is a product line which offers Ethernet wireless connectivity using direct sequence spreading in the ISM band. The other product lines are AirPort for wireless interbuilding connectivity and SeePort for system management. FreePort has an aggregate data rate of 16Mbps and is capable of delivering 5.7 Mbps throughput.

- **Range LAN:** Developed by Proxim, RangeLAN offers low-speed data networking, while RangeLAN2 offers higher speed data networking. Both operate in the ISM band. RangeLAN uses direct-sequence spread spectrum, RangeLAN2 uses frequency-hopping spread spectrum. The operating range is 300 to 500 ft in normal office environments and 800 to 1000 feet in open space environments. RangeLAN products are designed for less data intensive applications as e-mail, printer sharing, terminal emulation and industry specific mobile computing applications.

2.1.4 Infrared WLANs

For the sake of completeness it is important to mention another existing WLAN technology which uses infrared light modulated to carry data between computers. The wavelength of 780 to 950 nm is typically used for infrared links due to availability of inexpensive, reliable system components. IRDA (InfraRed Data Association) is involved in the standardization process. InfraLAN is the example of a WLAN product developed by BICC Communications. There are two categories of infrared systems most commonly used for wireless LANs. One is the directed infrared and the other diffused infrared. Even though IR is virtually immune to electromagnetic interference, one major drawback of IR systems is emitted optical power. Since this is a serious limitation, any absorption, scatter and shimmer can reduce received power causing the data to be lost or corrupted. This limits the data rate and operating distance, even thought it is possible to achieve data rates of over 10 Mbps by high speed switching of optical sources (LEDs).

2.2 The Indoor Propagation Channel

2.2.1 The Physics of Propagation

A simple free-space propagation model in terms of *attenuation* (power decay based on Frii's free-space equation [Bala97]) as used in satellite communication and microwave line-of-site radio is not sufficiently accurate to model wireless radio communication. The inherent variability of an indoor channel is similar to its outdoor counterpart, and is due to the triple problem of direct-path radio wave propagation - *reflection, refraction* and *scattering*. As a result, the signal arriving at the receiver is a vectoral combination of plane waves with varying phase, angle of arrival and amplitude. This is called *multipath*. A direct consequence of multipath is random frequency modulation due to different Doppler shifts on different paths. For a narrow band systems, there is rapid signal strength fluctuation called Rayleigh fading. Figure 2 is a typical waveform to depict the fading. For wideband systems, there is a delay spread of received signal leading to ISI (Inter Symbol Interference) thus limiting the data rate for an acceptable error performance. The above problems are however intensified in the indoor environment because the distances covered are much smaller. Also there is the ubiquitous problems of *background noise* and *cochannel interference*. The cochannel interference may be severe due to the short distances separating the transmitter and receivers (users). Further, the cochannel interference due to frequencies employed in the outdoor environment will have to be considered. It is observed that the propagation within buildings is heavily dependent on the type of building, and particularly on the placement and composition of walls. Signals levels vary depending on whether the interior doors are opened or closed. Where antennas are mounted also impacts large scale propagation and sometimes it may be difficult to operate in the far-field region [Rapp95].

2.2.2 Propagation Models

Much effort has been put into propagation measurements by telecommunication companies, research laboratories and universities in order to develop reasonable design guidelines and propagation parameters for indoor environments [Ande95]. Some of the observations were listed in the earlier section.

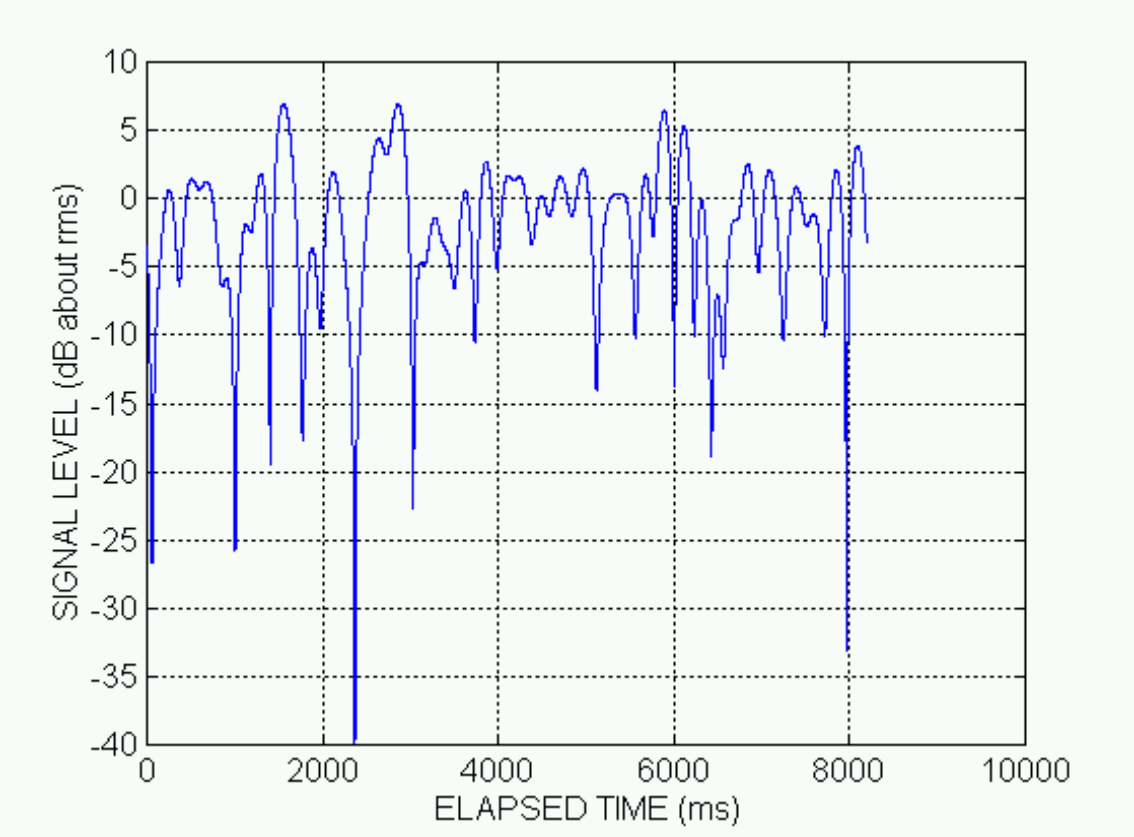

Figure 2. *Typical received signal levels for an indoor radio communication system. The carrier is at 900 MHz and the receiver speed is 20 km/hr. Notice that the small scale fading (Rayleigh) produces level changes of 20 db or more, whereas the local average signal level changes much more slowly with distance [Rapp95].*

The building layouts, and composition of partitions however remain the single most important factor in propagation prediction. Researchers have classified the buildings broadly as *open plan* or *closed plan* buildings. Open plan buildings are typically sports arenas, warehouses and distribution centers. Closed plan buildings typically

have many internal partitions, and can be further classified as residential homes in suburban areas, residential homes in urban areas, retail stores, grocery stores, factory buildings and office buildings. Whatever the nature of the building, one can think of buildings to be made up of *hard* and *soft* partitions. Hard partitions describe obstructions within the building which cannot be easily moved such as existing walls. Soft partitions on the other hand are movable obstructions such as office furniture panels. It is thus possible to classify any given building environment into a fixed number of hard and soft partitions. Table 2 gives average signal loss measurements reported by researchers for radio paths obstructed by some common building materials. This table gives a flavor of the extensive work done by researchers for a great number of partition types. A given building may be single floored or multifloored. It is important to note that propagation between floors will have to be modeled separately from that in a single floor. For a given floor inside a building, propagation geometry may be classified as LOS (Line Of Sight) or OBS (Obstructed).

Indoor propagation models can be classified as either *statistical* models or *deterministic* models. Discussion about models like the log-distance path loss model, Ericsson multiple break point model, attenuation factor model, and the Keenan Motley model can be found in [Rapp95] and [Fleu96]. A *ray launching* approach is an example of a deterministic model. Some of the key events which have to be measured or built into models before any wireless system is built are temporal fading for fixed and moving terminals, mutipath delay spread, and path loss. Discussion on these topics may be found in [Ande95].

2.2.3 Simulation and Prediction tools

The earlier two sections concentrated on theoretical analysis, measurement and modeling parameters which go into designing an indoor wireless system. Simulation

and prediction tools are very powerful in that they take into account all these factors to drastically cut system design time without compromising accuracy.

Table 2. *Average signal loss measurements reported by various researchers for radio paths obstructed by common building materials [Rapp95].*

Material Type	Loss (dB)	Frequency
Concrete wall	8-15	1300 MHz
Concrete floor	10	1300 MHz
Dry plywood (3/4 in.), 1 sheet	1	9.6 GHz
Wet plywood (3/4 in.), 1 sheet	19	9.6 GHz
Foil insulation	3.9	815 MHz
Light textile inventory	3-5	1300 MHz
Metal blanker, 12 sq. ft.	4-7	1300 MHz
Heavy machinery, > 20 sq. ft.	10-12	1300 MHz
Empty cardboard inventory boxes	3-6	1300 MHz
Semi automated assembly line	5-7	1300 MHz
Metallic inventory rack, 8 sq. ft.	4-9	1300 MHz

SIRCIM (Simulation of Indoor Radio Channel Impulse Response Models) [Rapp91] is a popular simulation tool available for PCs and Sun workstations. Developed by the MPRG (Mobile and Portable radio Research Group) at Virginia Tech, SIRCIM can be used to provide channel models for BER (bit error rate) simulations, channel access or

diversity studies, indoor system design, cochannel interference simulation, etc. It features a complex channel impulse response simulator with real-world channel models. Open and closed plan buildings are included with a 7.8 ns resolution for individual multipath signals. Both frequency-flat and frequency-selective fading indoor environments are covered.

SMT in its various forms (SMT, SMT 7.0, and SMT *Plus*) and WISE are the only indoor prediction tools available to date. Presently only SMT *Plus* is commercially available [Skid97]. Details on WISE can be found in [Fort95]. WISE stands for WIreless System Engineering Tool. WISE runs on a Unix system with X windows and in a more restricted form on PCs under Microsoft windows. Results can be visualized within the floor plan of a building. The user specifies wall locations and composition, communication system parameters, and base station locations. The system then estimates the signal strength and delay spread throughout the building or at specific points. The system is also capable of searching for optimum base station locations. Ray-tracing methods are used by the system. Although most ray-tracing systems are quite slow, often requiring hours of computation time, several simplifying assumptions and computational geometry tool have been employed within WISE to reduce the computation time to reasonable levels for an interactive system. Prediction errors within 6 dB have been reported. The user has also a choice of omnidirectional antennas to choose from for transceivers.

Chapter 3
The Site Modeling Tool

3.0 Overview

This chapter provides a high level description of the SMT 7.0. First, the relationship between SMT 7.0 and AutoCAD is explained. The simplifying assumptions made to increase computational speed of the SMT 7.0 are listed next. This is followed by an explanation of the modules of the SMT 7.0. The propagation models, the dialog boxes to choose values for the variables of a model, and equations used for communication and coverage estimation are included as part of the module description. The mathematical development of certain equations is however deferred to later chapters.

3.1 The SMT 7.0 and AutoCAD

This section describes the relationship between the SMT 7.0 and AutoCAD. Since the SMT 7.0 can be viewed as an AutoCAD application, the reasons for choosing AutoCAD is first presented. This is followed by a listing of the key features of AutoCAD that SMT 7.0 uses. The interface between AutoCAD and SMT 7.0 is explained next. Finally, a brief explanation of how to adapt AutoCAD drawings to SMT 7.0 is provided.

3.1.1 AutoCAD as a Graphical Foundation

There are several reasons that led to choosing AutoCAD as a graphical foundation. The main reasons are cited below:

- AutoCAD is one of the world's leading design and drafting software products. As it is very popular with architects, it was easy to obtain floor plans made using AutoCAD. Appendix A lists the minimum system requirements for SMT 7.0, including the AutoCAD system requirements.

- Autodesk, the manufacture of AutoCAD, also makes packages which can be used to convert non-AutoCAD file formats to AutoCAD ones. Further, floor plan blue prints may be scanned and stored in AutoCAD file formats. A plethora of third-party packages are also available to accomplish the above. Thus, it is possible to import any floor plan in any form into AutoCAD.
- AutoCAD permits third parties to develop extensions to AutoCAD. In this sense, SMT 7.0 can be viewed as an AutoCAD application program.
- Most important, the development time for the SMT 7.0 was shortened because AutoCAD provided the GUI (Graphical User Interface). Figure 3 is an example of the how the computer screen looks to an user when the SMT 7.0 is running. The SMT 7.0 screen menu is seen as a vertical bar on the right hand side. The SMT 7.0 and ANTENNA pull-down menu is an addition to the otherwise default AutoCAD pull-down menu on top. The bottom part of the screen is the AutoCAD command line. An top down view of a floor plan is shown at the screen center, with the coverage depicted around the directional antenna placed on the floor.

3.1.2 Key Features of AutoCAD

Once a floor plan is imported into AutoCAD and *modified* [see section 3.1.4] to fit the requirements of the SMT 7.0, it is not required to utilize any of the AutoCAD commands to run the SMT 7.0. This is because SMT 7.0 has its own screen and pull-down menus as seen in Figure 3. However the SMT 7.0 program itself uses certain key features of AutoCAD that may not be apparent to the user. These are highlighted below:

- AutoCAD defines a *polyline* as a set of lines that are treated as a single entity. The entire set of lines can be rotated, deleted and edited with a single command. Polylines therefore provide a convenient way to represent and manipulate arbitrary complex

objects. This is important because coverage region boundaries are represented in the SMT 7.0 as polygons.

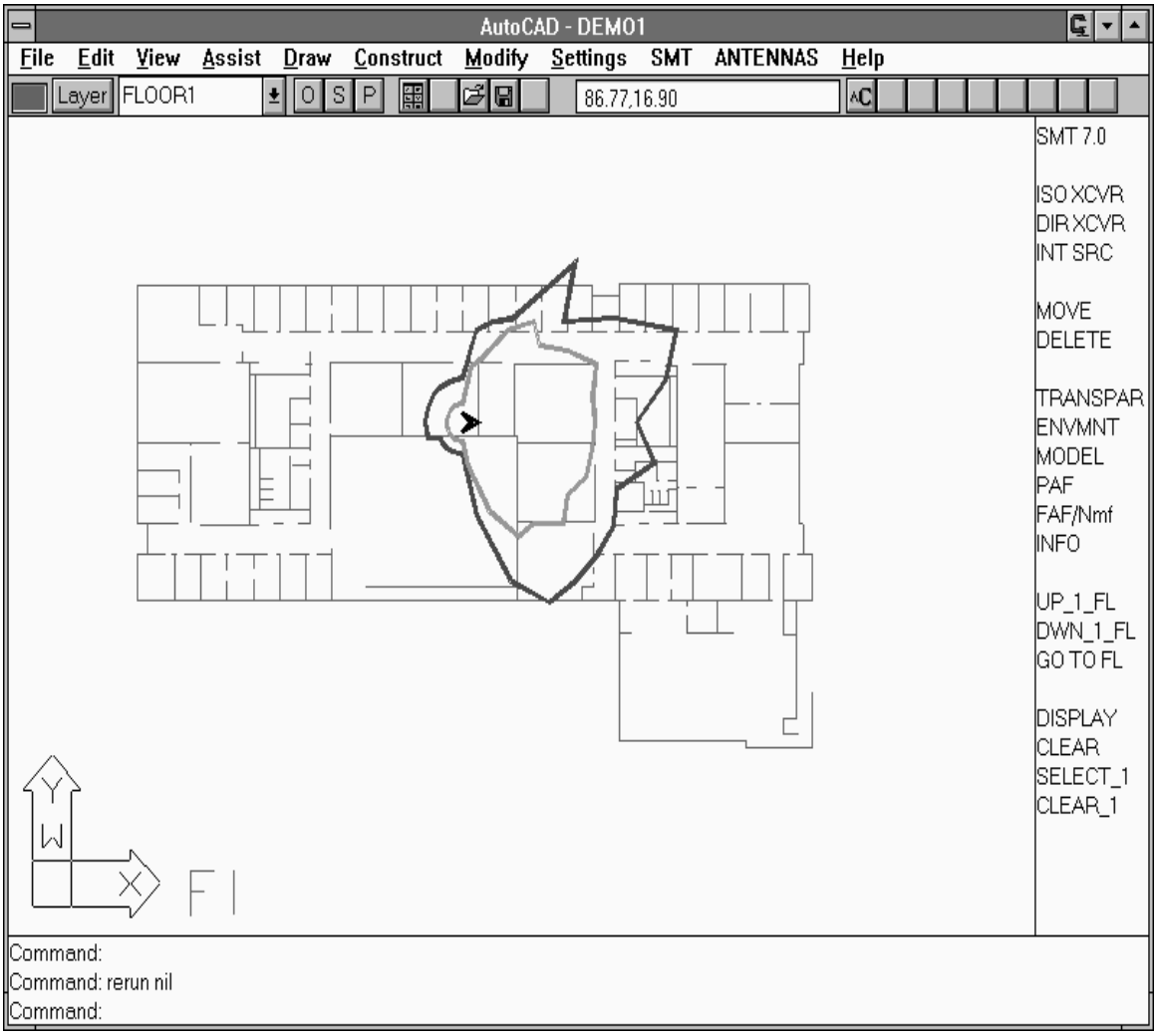

Figure 3. *An example of an AutoCAD screen running SMT 7.0. The coverage for a directional antenna is depicted. The screen menu is visible on the right hand side.*

- AutoCAD also allows separating logical portions of a drawing by defining them as *layers*. In the SMT 7.0, for example, the plan for each floor consists of four layers, each layer representing a partition type. Each layer can be distinguished from the other by assigning them different colors if the user so desires. Also, each layer can be turned *on*, *off* or may be *frozen*. The subtle difference between on and frozen layer is

that, while both do not appear on the screen, entities are not considered if a layer is frozen. This feature has been utilized by the SMT 7.0 to enhance computational speed by freezing layers not of immediate interest.

3.1.3 Developing AutoCAD Applications

The ADS (AutoCAD Development System) was used to develop the SMT 7.0. ADS and AutoLISP are two programming environments that Autodesk markets to assist third parties in developing AutoCAD applications. The choice for ADS was driven by the fact that it is a C-language interface in the form of an object library. Unlike AutoLISP it is more efficient in terms of speed and memory. The library contains approximately 85 C functions that execute standard AutoCAD commands, retrieve or set AutoCAD system variables, prompt the user for input, display and activate menus, and update screen images. The dialog boxes are defined by ASCII files written in DCL (Dialogue Control Language). ADS also provides functions for handling dialog boxes.

In order to develop an AutoCAD extension, the user writes a new function in C that invokes functions from the ADS library. This new function is compiled and linked with the ADS code. After AutoCAD is invoked, the new function can be loaded and then executed just like any standard AutoCAD command. If desired, new functions created in this manner can be placed in pull-down menus or in a menu that is permanently displayed at the side of the screen. It is important to understand that an ADS application program will not run alone; it will only function under a running session of AutoCAD. An ADS extension is event-driven, normally waiting within a control loop for a message from AutoCAD. When a user selects the new function, a message is sent and the user's software takes control. It is now the responsibility of the software to return control back to AutoCAD.

3.1.4 Adapting AutoCAD Drawings

Developing floor plans from scratch, or modifying existing drawings to meet the requirements of the SMT 7.0, requires the user to be familiar with AutoCAD. Many a times modifications are needed simply because architects do not follow a single standard while creating floor plans. To assist a user in doing so, researchers at Virginia Tech have developed a tool tailored specifically for the SMT 7.0. This is called the "Site*Planner*"[Skid97]. The modifications which are typically needed are described below:

- The SMT 7.0 expects to find at least one of the four partition types for each floor of the building. The partitions are simply called Partition1, Partition2, etc. These are maintained as separate layers for each floor. The layer that is named "Floor*f*" must contain Partition1 (concrete walls) that are located on floor *f*, where *f* = 1, 2, 3, etc. The numbering must be sequential, with *f* = 1 representing the ground floor. Similarly, the layer named "Spart*f*" must contain Partition2 (soft-cloth covered) partitions that are located on floor *f*. Partitions 3 and 4 are identified by layer names Hpart*f* and Mpart*f* respectively. All of the Floor*f*, Spart*f*, Hpart*f* and Mpart*f* layers must be provided by the user.
- All additional information is considered extraneous, and should be deleted or placed on frozen layers. This is important for improving computational speed, as mentioned earlier.
- Since the SMT 7.0 computes coverage in meters, it is necessary to make sure that other units are not used. If a conversion is required, after the conversion, the drawing may have to be magnified or shrunk to fit the screen (Note that the AutoCAD *zoom* command will have to be used for this purpose. The AutoCAD *scale* command actually scales the original drawing and is not to be used).
- Finally, it is necessary to make sure that the *x* and *y* coordinates of the floor plan are positive and the origin is the lower left hand corner of the screen. This, in AutoCAD terminology is called the WCS (World Coordinate System). This can be achieved by

using the AutoCAD *move* and *zoom* commands. As seen in later chapters, this is important, as it ensures that the 3-dimentional antenna coordinate system and the building coordinate system are identical.

3.1.5 The Process of "Abstraction"

The idea of increasing the number of partition types that the SMT 7.0 supports (from two to four) originated during field measurements of open-plan buildings. It was observed that it is difficult to categorize all obstructions by just two partition types. Further, specifying more partition types has a direct impact on improving the accuracy of coverage prediction. However this gain in accuracy may be lost if the obstructing object is improperly represented on the floor plan. A good example is a rack in a ware house. The original object in the floor plan was replaced by a single straight line, to avoid the SMT 7.0 calculating a single rack as many partitions. This process of modifying the original drawing has been termed "abstraction". Given the type of environment, it may be necessary to follow this procedure to get accurate assessments. The Site*Planner* tool mentioned in the previous section does not automatically perform this function, but can be used as an aid. Chapter 6 provides an example of abstraction carried out on a warehouse plan.

3.2 Assumptions

Even though the calculations performed by SMT 7.0 program are mathematically rigorous, it is necessary to make several simplifying assumptions to increase computational speed without sacrificing accuracy. These are listed below:

- First, only one floor is considered at a time. A base station may be present on a different floor, but its coverage region is computed for the current floor only. The coverage region for a single base station, and for a given floor, can therefore be

modeled as a set of two-dimensional points $S = \{(x, y) \mid$ communication is possible at $(x, y)\}$.

- S is assumed to form a connected set with no holes. This means that no "islands" are present within a coverage region, and a single coverage region is never subdivided into separate, connected sets. (This is a safe assumption in most practical situations. However, see [Panj96] for a discussion of cases that violate this assumption.)
- Following from the previous assumptions, the border of the coverage region can be assumed to be a simple closed curve that represents the limit of communication coverage for a given base station. The SMT 7.0 approximates this border as a polygon, $B=\{(x_i, y_i) \mid i = 1, 2,...., n\}$ where the points (x_i, y_i) represent the n vertices of polygon B given in counterclockwise order when viewed from above.
- Although the SMT 7.0 accommodates base stations with directional transceivers, it assumes that all terminal units are omnidirectional with unit gain. Within the base station, the transmitter and receiver characteristics are assumed to be the same. The base station can then be modeled as a directional transmitter, and it coverage region corresponds to locations in the building for which propagation losses are sufficiently low.

3.3 Modules of the SMT 7.0

SMT 7.0 was developed using five different modules. Figure 4 on the next page depicts these five modules. Modularity has been important for simplifying development and system maintenance. This approach permits one system module to be updated at a later time without the need to redesign the rest of the system. Also note that each of the modules may in turn be subdivided into smaller modules. For example, if a more sophisticated propagation model becomes available in the future, only this sub-module of the communication module needs to be updated. An explanation of these sub-modules forms a part of the individual module description.

3.4 User Interface Module

Since the SMT 7.0 was targeted at users who are not experts in wireless communication system design, special attention has been paid to the user interface module. The user interface module interacts with all the other modules which in turn interact among each other. The user employs the mouse or the keyboard as input devices to access the SMT 7.0 related screen and pulldown menus. The screen and the pulldown menus allow the user to set building, communication, and antenna pattern parameters;

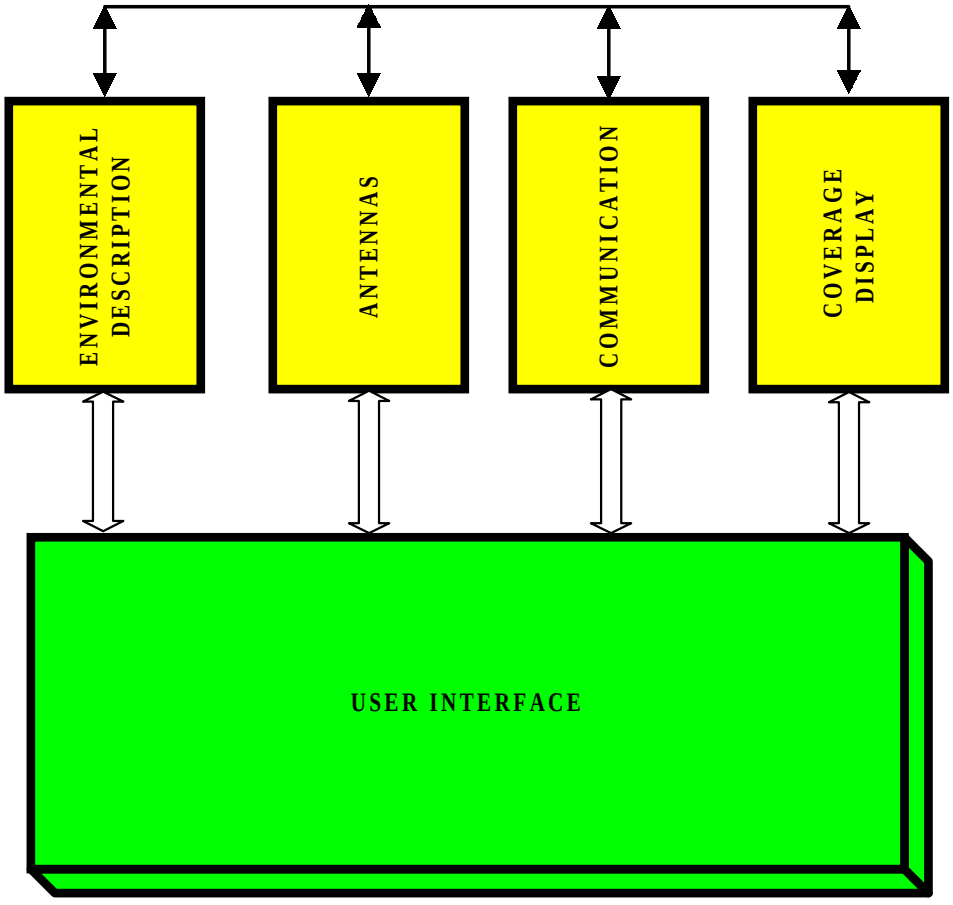

Figure 4. *Modules of the SMT 7.0. The user interface module communicates with each of the other modules which in turn internally communicate.*

place directional transmitters, omnidirectional transceivers and interference sources; move from floor to floor; and direct the calculation of coverage areas. Some of the menu items pop up dialog boxes for setting the various parameters described above. These parameters and the dialog boxes are explained under the relevant modules. The monitor of the PC serves as the output device and provides both textual and graphical feedback to the user. The area of coverage is output as text via the command line. The coverage region can be viewed graphically in color on the floor plan.

Some of the highlights of this module are as follows:

- The user can add, reposition and delete any number of omni-directional transceivers, directional transmitters and interference sources.
- The user can initiate the calculation of the coverage regions for one or all of the above sources. Similarly he can clear the coverage regions for one or all of the above sources.
- The areas of coverage may be obtained for any coverage region.
- The contour resolution and the step size for coverage calculation can be changed to increase the accuracy of coverage prediction.
- The user if free to experiment with different path-loss models, select various building types, and change the communication parameters including the attenuation factors.
- The user is free to select from a wide range of omni-directional and directional patterns, change their orientation in space, place them at different heights above the floor or even provide his own patterns to be associated with the directional transmitter.
- If the floor plan supports multiple floors, the user may move between, place the transmitting and interfering sources on, and view the resulting coverage regions on any floor.

3.5 Environmental Description Module

This module essentially serves as a database containing information that may be accessed by all other modules when needed. The stored information can be categorized as building attributes or communication parameters. There are seven dialog boxes which the user employs to choose these parameters and attributes. These then get stored as variables in the environment description module to be used by other modules. The location of transmitters and interference sources are also stored in this module and the user can view the location as an informational dialog box. All these dialog boxes are shown below. A brief description on these dialog boxes is as follows:

- The dialog box shown in Figure 5 is used to set all the communication parameters of a base station like frequency, power, bandwidth, etc.

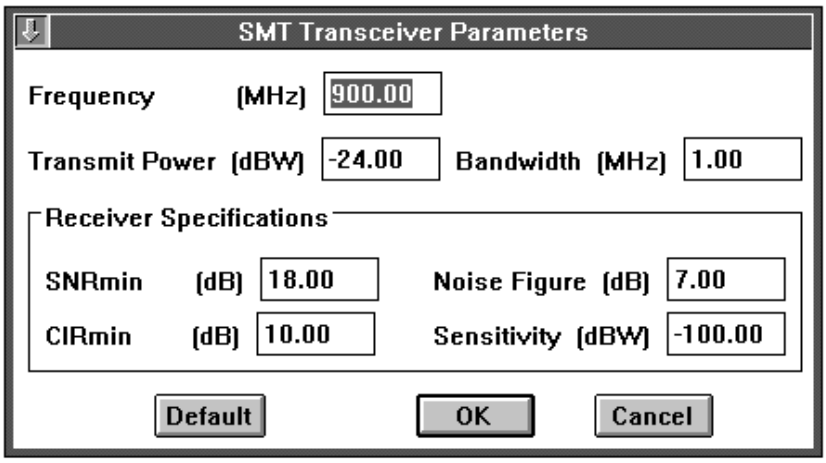

Figure 5. *Transceiver communication parameters. The user sets these parameters before placing transceivers.*

- SMT 7.0 supports a choice of four path loss models, two for each floor. The choice of the model is done via the dialog box shown in Figure 6. Based on the model selected, the appropriate dialog box (shown in Figures 7, 8, 9, and 10) will have to be used to set the parameters.

- Figure 7 depicts the environmental parameters dialog box. The *n* values of the same floor distance-dependent path loss model are set via this dialog box.
- Figure 8 depicts the dialog box to be used if the same floor partition attenuation factor model is selected. The attenuation for various partition types is set via this dialog box.

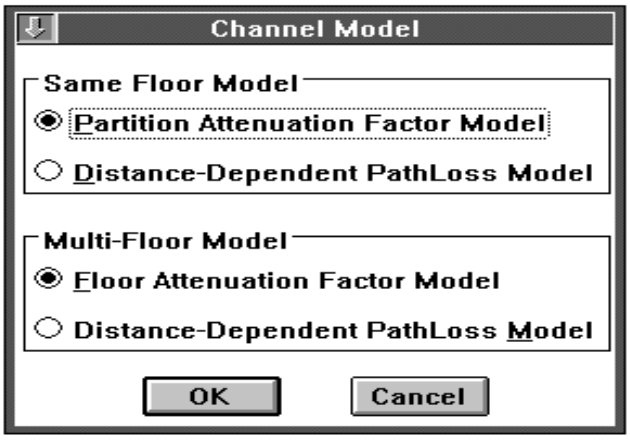

Figure 6. *Propagation model choices. There are four choices, two for each model type.*

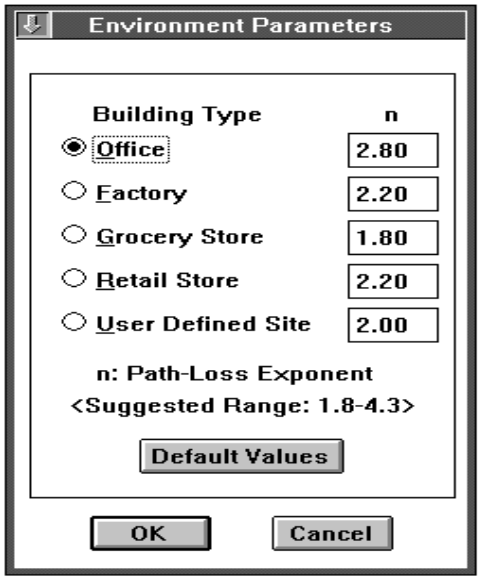

Figure 7. *Environmental parameters. The n values chosen are for the same floor distance dependent model.*

- Dialog box shown in Figure 9 sets the floor attenuation factor for the multi-floor, floor attenuation factor model.
- Dialog box shown in Figure 10 sets the *n* value for the multi-floor, distance dependent model.

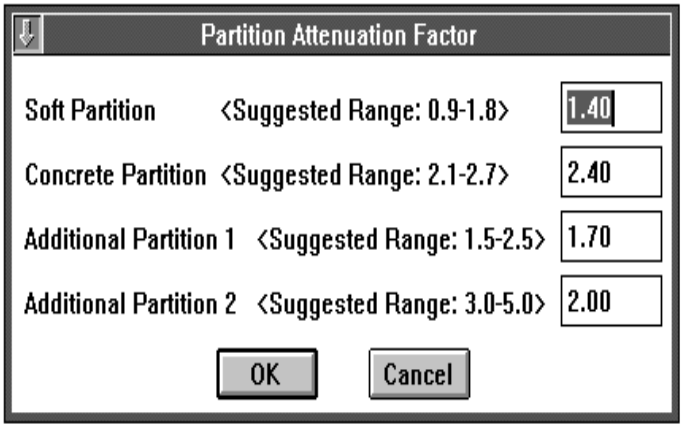

Figure 8. *Partition attenuation factors. The values chosen are used by the same floor, partition attenuation model.*

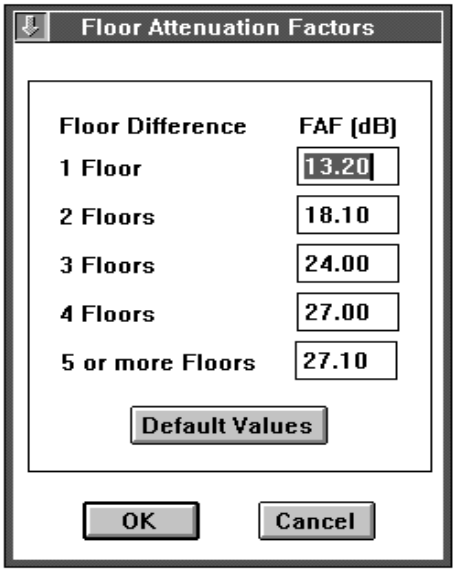

Figure 9. *Floor attenuation factors for multifloor models.*

- The contour resolution dialog box shown in Figure 11, is used to select the accuracy of coverage prediction. The minimum distance resolution is one meter and the maximum number of polygon points suggested is 72.
- Figure 12 depicts the informational dialog box related to interference sources. The user clicks on the interference source he is interested in after selecting the INFO command on the screen menu. The dialog box pops up with information on position, frequency and power levels.

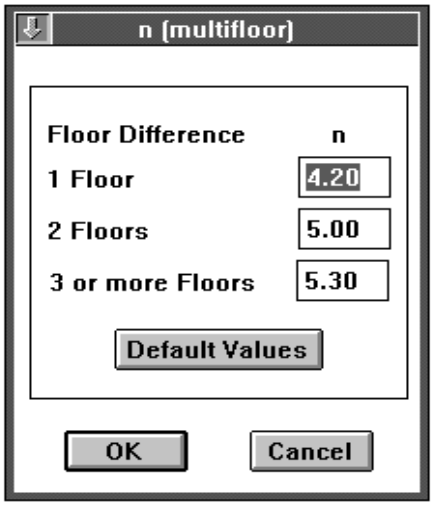

Figure 10. *n values selection for multifloor distance dependent models.*

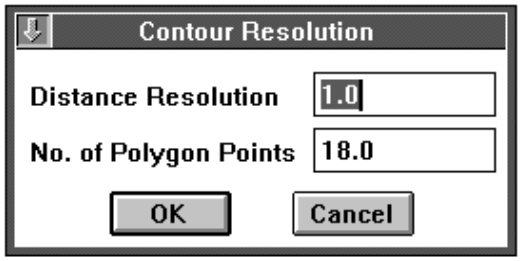

Figure 11. *Coverage contour resolution parameters to be set by the user prior to displaying coverage.*

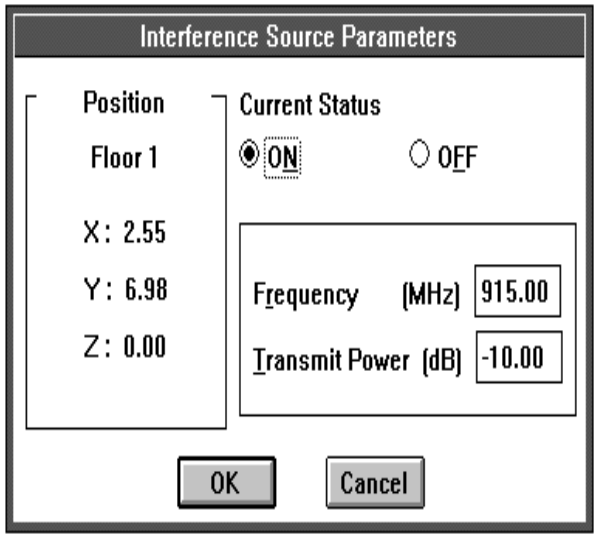

Figure 12. *Example of information displayed about an interference source. This display indicates the location, status and characteristics of an interference source chosen by the user.*

3.6 Antenna Module

This module essentially performs two functions. First, it allows the user to set various antenna parameters and choose from a variety of antenna patterns. The dialog boxes through which these are performed are shown below. Based on the patterns and parameters chosen, the corresponding values of these variables are used to calculate $G_T(\theta,\phi)$ which is the transmitter antenna gain value in dB. This value gets plugged into the path loss equation as seen in the next section 3.7.1. A detailed explanation on $G_T(\theta,\phi)$ is deferred to chapters 4 and 5 because the equation for $G_T(\theta,\phi)$ is different for different categories of antenna patterns.

Figure 13 depicts the dialog box to be used to set the height and orientation for all antenna pattern types. Section 5.1 explains how these parameter values are used to perform homogeneous coordinate transformations. Note that these values set the height and orientation for any 3D antenna pattern.

As the dialog boxes will indicate, other than the pre-existing isotropic pattern, the user has a choice of patterns from three different categories. These are 1)

"Omnidirectional patterns", 2) "User provided" antenna patterns, and 3) "Other patterns", and are depicted in Figures 14, 15 and 16 respectively. When the user selects from the menu of eight omnidirectional patterns as shown in Figure 14, it is implicit that he or she is choosing a 3D pattern. However, if the user wants the SMT 7.0 to use 3D antenna pattern for the "User" and "Other" pattern types, he or she has to explicitly choose the 3D display option on the dialog boxes in Figure 15 and 16. This is due to the fact that the tool provides the user with a choice of viewing a 2D coverage plot for the azimuth or elevation pattern for the above mentioned pattern types. The idea behind providing this additional feature is basic. Since interpolation is used for "User provided antenna patterns" and "Other directional patterns" the user may want to look at the two 2D patterns he is choosing for 3D interpolation. As an example, assume that the user has indicated the location of his Az and El data files in the dialog box shown in Figure 15. If the user wants a display of how the azimuth data looks in 2D, he or she simply chooses the "2D Az Display" option and selects the *n* value model from Figure 6. A similar explanation is valid for the "2D Az Display" and "2D El Display" options provided for the "Other pattern Menu" dialog box shown in Figure 16. The user can choose his own parameter value for various patterns presented in that dialog box and the *n* value model from Figure 6 to obtain a 2D Az or El display of the pattern. Since the SMT 7.0 assumes the *X-Y* plane for azimuth pattern and *X-Z* plane for elevation pattern, the angle parameters in Figure 13 are not relevant. The 2D calculation assumes the same height for receiver and transmitter.

Figure 17a and 17b provide information on "Other pattern types" obtained by clicking on the Info_Az and Info_El buttons shown in Figure 16. This is simply a listing of the patterns supported by SMT 7.0. The dialog box also provides the user with a recommended range for the pattern variables. 2D plots for these patterns are presented in section 4.4.4. These plots are drawn using the MATLAB tool. Extensive study was performed using this tool for a large number of variable values before this recommended range was developed. Three main points considered were: 1) Neglect values that provide multiple side lobes of high energy for these patterns. Such patterns are not useful indoor

directional patterns. They also create the problem of a pattern with multiple boresights. 2) Make sure that the beam width of the boresight is above 20^0. Smaller beam widths decrease the usefulness of the antenna for directional indoor use. 3) The pattern should retain its property of being a normalized pattern.

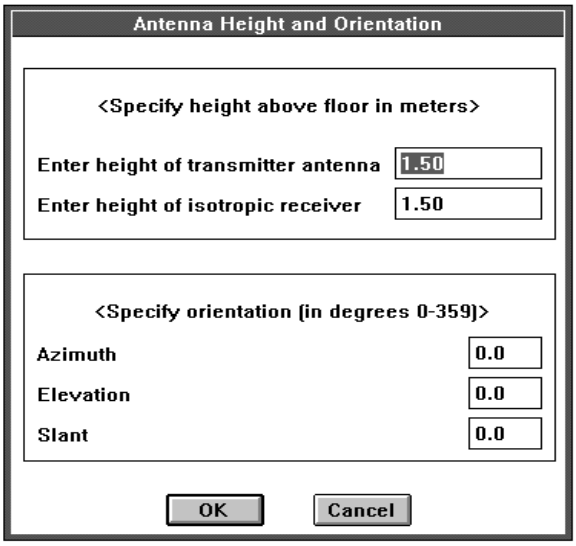

Figure 13. *Dialog box to input antenna orientation and heights. Chapter 5 describes this dialog box. The angles are specified relative to the building coordinate system.*

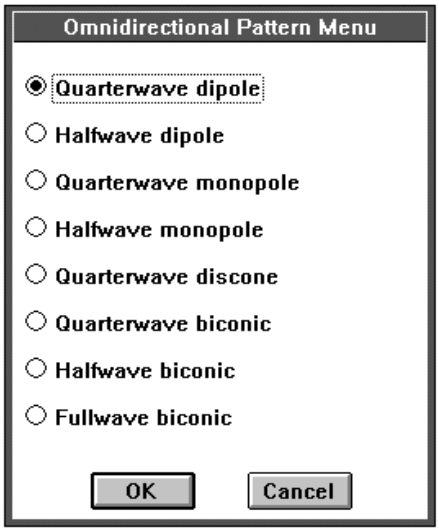

Figure 14. *A menu of omnidirectional patterns. The user can select any of the patterns that are described in detail in section 4.4.2. These patterns are inherently 3-dimensional.*

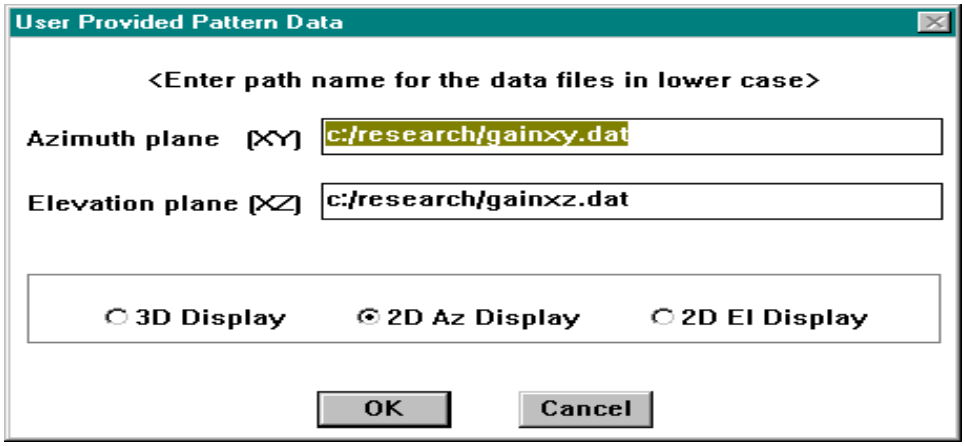

Figure 15. *The dialog box to specify location of user provided pattern files.*

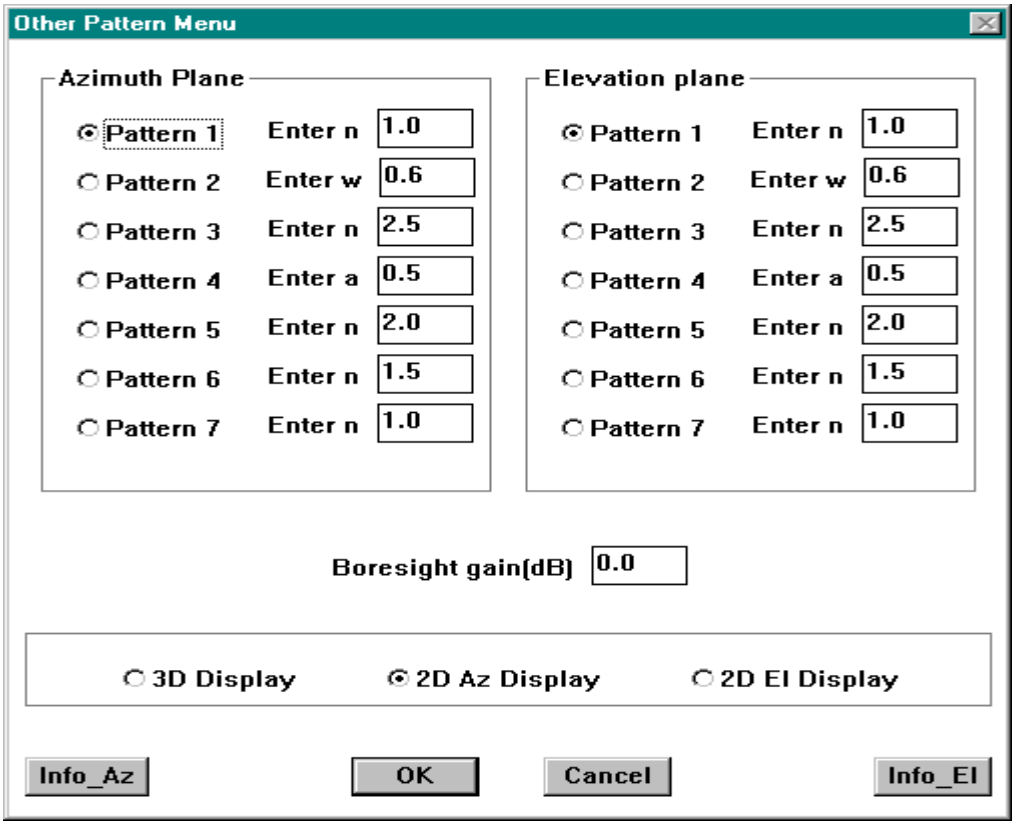

Figure 16. *A menu to select other directional patterns. The user selects two dimensional azimuth and elevation patterns independently, and defines a common boresight gain.*

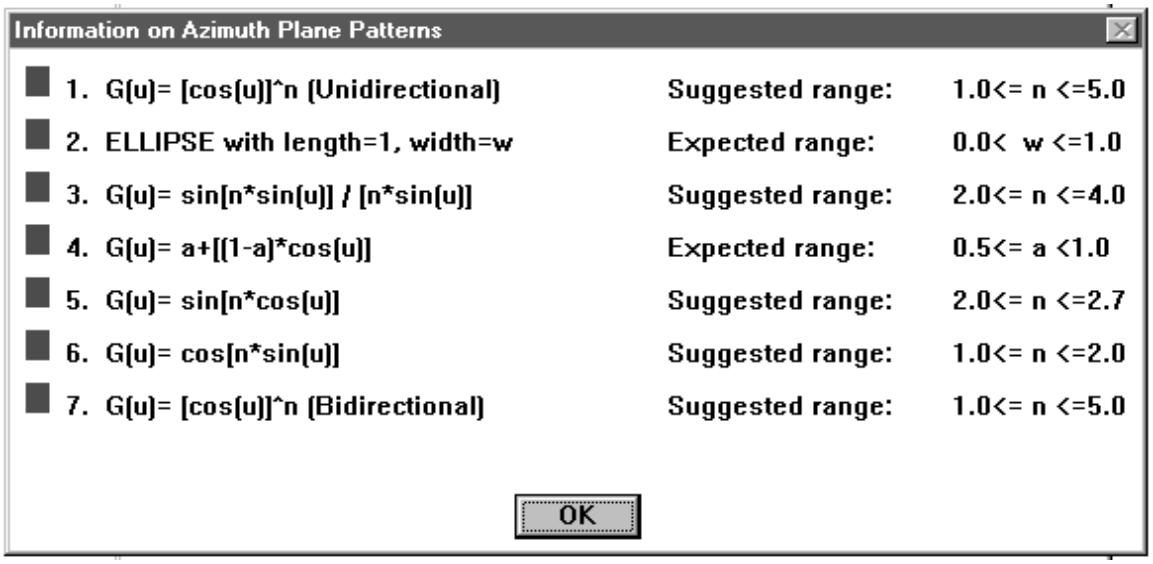

(a)

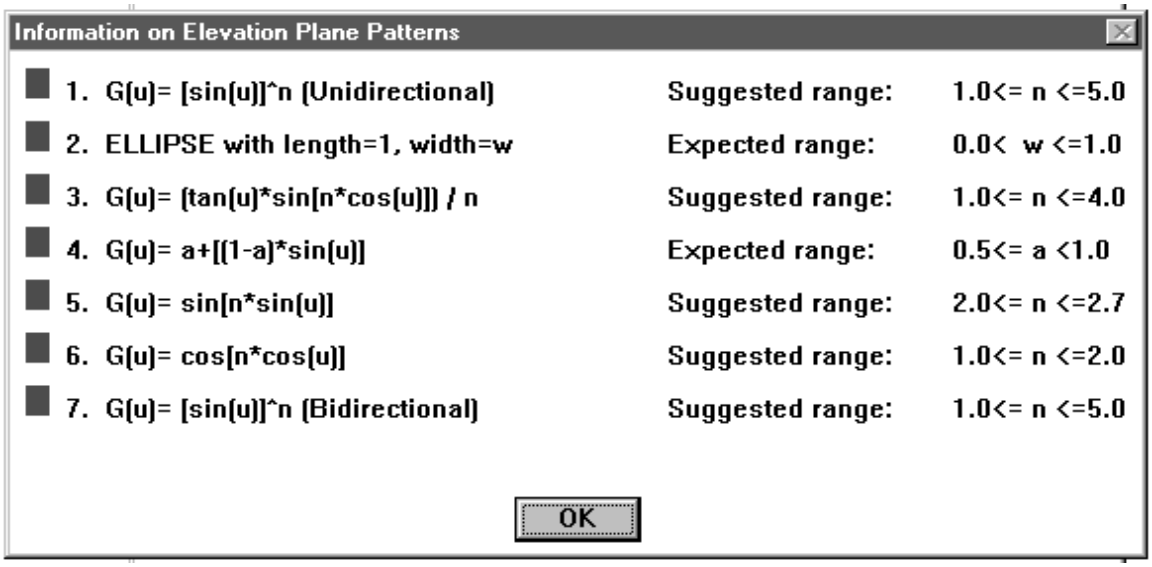

(b)

Figure 17. *Information on azimuth and elevation planes for other directional patterns than can be selected by user. Azimuth information (a) is obtained by clicking on the Info_Az button shown in Figure 16. Elevation information (b) is obtained by clicking on the Info_El button shown in Figure 16. Section 4.4.4 provides details about these patterns.*

3.7 Communication Module

The communication module is subdivided into two modules, 1) the path loss module and 2) the communication feasibility module. Both are described below:

3.7.1 Path loss Module

Based on the user selection of the antenna pattern and parameters, and the pass loss model and its parameters, the path loss module essentially computes the path loss. There are four simple but surprisingly accurate models that the SMT 7.0 uses to compute path loss. Path loss is defined as the attenuation of the transmitted signal in dB, with distance.

The variables which are used to describe these four models are listed below in the form of a table. We will simply call the four models MODEL 1, 2, 3 and 4. It is easy to see that the selections made by the user via the dialog boxes shown in the above two sections have a direct bearing on the values of these variables.

Table 3. *Listing of variables used to predict path loss.*

Variable	Description	Unit
d	Distance between transmitter and	meters
d_0	Reference distance (at least 1 meter)	meters
$\overline{PL}$	Mean path loss	dB
n	Mean path loss exponent	—
k_i	Number of partitions of type *i.*	—
AF	Partition dependent attenuation factor	dB
PL	Path loss	dB
FAF	Floor attenuation factor	dB
$G_T(\theta,\phi)$	Transmitting antenna gain	dB

MODEL 1: Single floor *n* value model

$$\overline{PL}(d)\ [\text{dB}] = PL(d_0)\ [\text{dB}] + 10\, n\, \log_{10}\left(\frac{d}{d_0}\right) - G_T(\theta,\phi)\ \ [\text{dB}]$$

MODEL 2: Single floor *PAF* (Partition Attenuation Factor) model

$$\overline{PL}(d)\ [\text{dB}] = PL(d_0)\ [\text{dB}] + 20\log_{10}\left(\frac{d}{d_0}\right) + \sum_i k_i AF_i\ \ [\text{dB}] - G_T(\theta,\phi)\ \ [\text{dB}]$$

MODEL 3: Multifloor *n* value model

$$\overline{PL}(d)\ [\text{dB}] = PL(d_0)\ [\text{dB}] + 10\, n\, \log_{10}\left(\frac{d}{d_0}\right) - G_T(\theta,\phi)\ \ [\text{dB}]$$

MODEL 4: Multifloor *PAF* (Partition Attenuation Factor) model

$$\overline{PL}(d)\ [\text{dB}] = PL(d_0)\ [\text{dB}] + 10\, n\, \log_{10}\left(\frac{d}{d_0}\right) + \text{FAF}\ [\text{dB}] - G_T(\theta,\phi)\ \ [\text{dB}]$$

Notes:

- For all the four models, $PL(d_0)\ [\text{dB}] = 20\ \log_{10}\left(\frac{4\pi d_0}{\lambda}\right)$. The distance d_0 must be at least one meter to ensure that the coverage prediction is in the far field region (see chapter 4).
- Even though the equations look similar for model 1 and 3, the *n* value for model 1 corresponds to the same floor while the *n* value for model 3 corresponds to multifloor. The *n* value for model 4 corresponds to the same floor value.
- AF_i represents the attenuation factor for partition type *i*, and k_i is the number of such partitions.
- $G_T(\theta,\phi)$ is computed by the antenna module. A detailed explanation is given in chapter 4.

3.7.2 Communication Feasibility Module

Communication feasibility at a given point is defined as the ability to receive a signal which exceeds the minimum required carrier-to-noise ratio, receiver sensitivity, and (if any interference sources are present) carrier-to-interference thresholds by a specified margin. This allows an acceptable quality communication link to be established. The mean path loss computed in the previous section is used by this module. The variables which are used by this module are listed below in the form of a table.

Table 4. *Listing of variables used to determine communication feasibility.*

Variable	Description	Unit
d	Distance between transmitter and receiver	meters
T	Absolute room temperature	^{o}K
$\overline{PL}$	Mean path loss	dB
B	RF channel bandwidth	Hz
k	Boltzmann constant (1.38×10^{-23})	J/ ^{o}K
C/N	Received carrier power to noise power ratio	—
C/I	Received carrier to interference power ratio	—
P_T	The transmit power	dBW
P_N	White noise at the receiver input = kTB	W
P_E	Environmental noise (18 dB by default)	dB
CNF	Channel noise factor specified by user	dB
m	The number of interference sources	—
n	An integer varying between 1 and m	—
P_n	Power radiated by n^{th} interference source	dBW
l_n	Coeff. based on receiver filter characteristics	—

Communication is deemed feasible at a point if the following Boolean condition is satisfied:

$$[\ (U > 0) \text{ and } (V > 3) \text{ and } (W > 0)\ ]$$

or

$$[\ (U > 3) \text{ and } (V > 0) \text{ and } (W > 0)\ ] \qquad [3.1]$$

The variables *U*, *V*, *W* are defined as follows:

$$U = \left(\frac{C}{N}\right) - \left(\frac{C}{N}\right)_{\min} \quad [\text{dB}]$$

$$V = \left(\frac{C}{I}\right) - \left(\frac{C}{I}\right)_{\min} \quad [\text{dB}]$$

$$W = C - C_{\min} \quad [\text{dB}]$$

The variables *C*, *N*, *I* in turn are defined as follows:

$$C\ [\text{dBW}] = P_T\ [\text{dBW}] - \overline{PL}(d)\ [\text{dB}]$$

$$N\ [\text{dBW}] = P_N\ [\text{dBW}] + P_E\ [\text{dB}] + CNF\ [\text{dB}]$$

$$I = \sum_{n=1}^{m} l_n I_n \quad \text{where } I_n\ [\text{dBW}] = P_n\ [\text{dBW}] - \overline{PL}(d_n)\ [\text{dB}]$$

Notes:

- The number 3 in condition [3.1] indicates a 3 dB threshold which is commonly used in industry.
- Introduction of factor P_E [Panj96] as a part of *N* is important because recent studies indicate that electromagnetic equipment such as computers, CRTs, Microwave ovens, TVs etc. contribute to the ambient noise. This noise at 900 MHz is typically 18 dB above the thermal noise floor which is given by P_N [dBW] = 10 log (*kTB*). The factor *CNF* is specified by the user and provides a means of quantifying any other noise present. The factor P_E is not used in SMT *Plus* since *CNF* is user configurable. Also, in SMT *Plus*, calculation of *I* is a bit different than in SMT 7.0.
- The concept of interference power *I* is important for two reasons. Outdoor transmitting sources spill energy into the indoor environment and it is possible they these conflict with the frequencies used in the indoor environment. Also it is possible to have indoor sources doing the same. With the likelihood of having a limited range of frequencies to choose from, for a particular indoor wireless system, frequency

reuse may become inevitable. It is in such situations that considering *I* becomes very important.

3.8 Site Coverage Module

This module displays the coverage region directly on the floor plan. The assumptions made in Section 3.2 play a role in defining the search algorithm for displaying coverage. The pseudocode for this algorithm can be found in [Panj95]. A brief explanation of how a coverage region is computed is explained in the next paragraph.

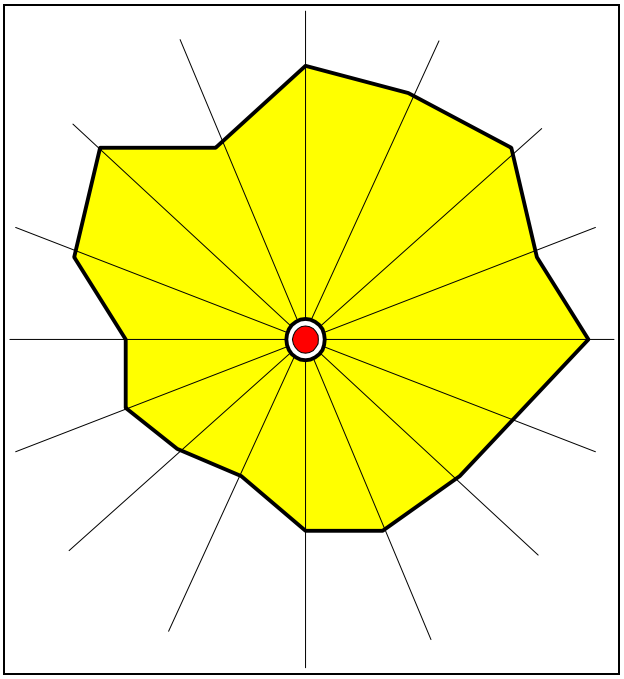

Figure 18. *Illustration of the coverage region represented by the SMT 7.0 as a polygon. A base station is located at the intersection of the radial lines that pass through the vertices of the polygon.*

The problem of estimating a coverage region *S*, given the assumptions in 3.2, reduces to a problem of computing *n* vertices of a polygon *B* that encloses a given base station. As illustrated in Figure 18, the SMT 7.0 performs a search for the end points

of a line, which form the vertices of this polygon. The number of vertices are determined by the number chosen by the user via the contour resolution dialog box (Figure 11). Thus, adjacent lines are all separated by the same angle $\Delta\alpha$. The distance d at which a vertex lies from the base station is determined by the condition [1] found in the previous section 3.7.2. In actuality the search begins and progresses in fixed steps d_0 (chosen by the user via the contour resolution dialog box) along the radial line until a point is reached when communication is no longer possible. The communication feasibility point is now chosen to lie in between the last two points. As seen in Figure 3, section 3.1, two different coverage regions are actually displayed in different colors. They are calculated as described above, but using different communication feasibility thresholds. The thresholds *U, V* and *W* for the inner contours are offset in dB from those of the outer via the command ICMARGIN. All the SMT 7.0 commands are described in Appendix D.

Chapter 4
Antennas

4.0 Overview

Section 4.1 gives a brief prelude to antennas. Section 4.2 defines key antenna terms as relevant to the SMT 7.0. The mathematical development of the gain parameter $G_T(\theta,\phi)$ is described in section 4.3. Section 4.4 describes the antenna patterns and equations the SMT 7.0 supports, and provides two dimensional plots for the same. Chapter 5 concentrates on how the SMT 7.0 converts two-dimensional patterns to three-dimensional ones.

4.1 Introduction to Antennas

It has often been said that a station is only as effective as its antenna system [Hall92]. The requirements of modern antennas in a mobile system can be summarized briefly as follows [Fuji94]:

- *The antenna must be part of the system*: The antenna cannot simply act as an isolated receive/transmit terminal.
- *The antenna must be designed to accommodate propagation effects*: Some degree of polarization and pattern diversity has to be embodied.
- *Compatibility with environmental conditions*: The antenna pattern characteristics have to match the terrain requirements and make allowances for nearby obstacles.
- *Integration of antenna with vehicle or platform*: The design should accommodate pattern changes due to hand and body effects and ensure that the vehicle/platform is safe to operate.

- *Latest manufacturing technology*: Technological advances in areas of new composite materials and VLSI/Microwave IC techniques have to be incorporated into the antenna design.
- *User-friendly and reliable performance*: The antenna design must have a minimum of moving parts and switches and high reliability of mechanical design.

4.2 Definition of Key Terms

4.2.1 Antenna

An antenna may be defined as a transducer between a *guided wave* on a *transmission line* and a *free space wave* [Bala97]. Antennas, unlike transmission lines which guide energy, radiate (or receive) energy. If the dimensions of the wire or the components in use become appreciable compared to the wavelength in use, a portion of the electromagnetic energy is no longer confined to the circuit but escapes as radiation. Most antennas are deliberately designed to ensure that the majority of energy is radiated or received [Hall92].

The theoretical foundations for antennas rest on Maxwell's equations. Once solved for the radiation problem, direct application of Maxwell's equations for antennas is warranted only in special situations. It is appropriate to mention two basic equations here. In free space, $\lambda = c / f$, where λ is the wavelength, c is the speed of light (3×10^8 meters/sec) and f is the carrier frequency. The wavelength is given by $\lambda = v / f$ where $v = c/\sqrt{\varepsilon_r}$ if the medium is a lossless nonmagnetic dielectric with relative permittivity ε_r. The intrinsic impedance of a medium is $\eta = \sqrt{\mu / \varepsilon}$, and for free space η = 376.7 Ω (a pure resistance). It is worthwhile to note that μ and ε are complex, but in a majority of antenna problems can be approximated as real constants.

4.2.2 Radiation Pattern

The IEEE standard 145-1993 defines an antenna *radiation pattern* or *antenna pattern* as "a mathematical function or a graphical representation of the radiation properties of the antenna as a function of space coordinates. In most cases, the radiation pattern is defined in the far-field region [see section 4.2.7] and is represented as a function of directional coordinates. Radiation properties include power flux density, radiation intensity, field strength, directivity phase or polarization [see section 4.2.8]".

A trace of the measured power at a constant distance from a transmitting antenna is called the *power pattern*, whereas a graph of the spatial variation of the electric field magnitude at a constant distance is called the *field pattern*. Plots of absolute power patterns are seldom made as performance of an antenna is measured in terms of gain and relative power patterns. The power is measured in dBi and the field strength is measured in volts/meter. The term dBi simply denotes power measured with reference to an isotropic radiator and since an isotropic radiator is assumed to have unit gain, the term dBi is often used interchangeably with dB. For the SMT 7.0, we will use the normalized power gain pattern as the default radiation pattern.

4.2.3 Spherical Coordinate System

All SMT 7.0 antenna patterns are represented using the spherical coordinate system. This is depicted in Figure 19. Two terms are often used to describe the geometrical planes of the coordinate system. The horizontal (*x*-*y*) plane is called the azimuth plane and mathematically denoted by $\theta = 90^0$. A vertical plane is called an elevation plane. Two elevation planes of particular interest are $\phi = 0^0$ (*x*-*z* plane) and $\phi = 90^0$ (*y*-*z* plane). The relationship between rectangular and spherical coordinates is:

$x = r\sin\theta\cos\phi,\ y = r\sin\theta\sin\phi,\ z = r\cos\theta$, where $r \geq 0$, $0^0 \leq \phi < 360^0$, $0^0 \leq \theta \leq 180^0$,

and conversely

$r = \sqrt{x^2 + y^2 + z^2}$, $\theta = \text{atan}(\sqrt{x^2 + y^2} / z)$, $\phi = \text{atan}(y/x)$.

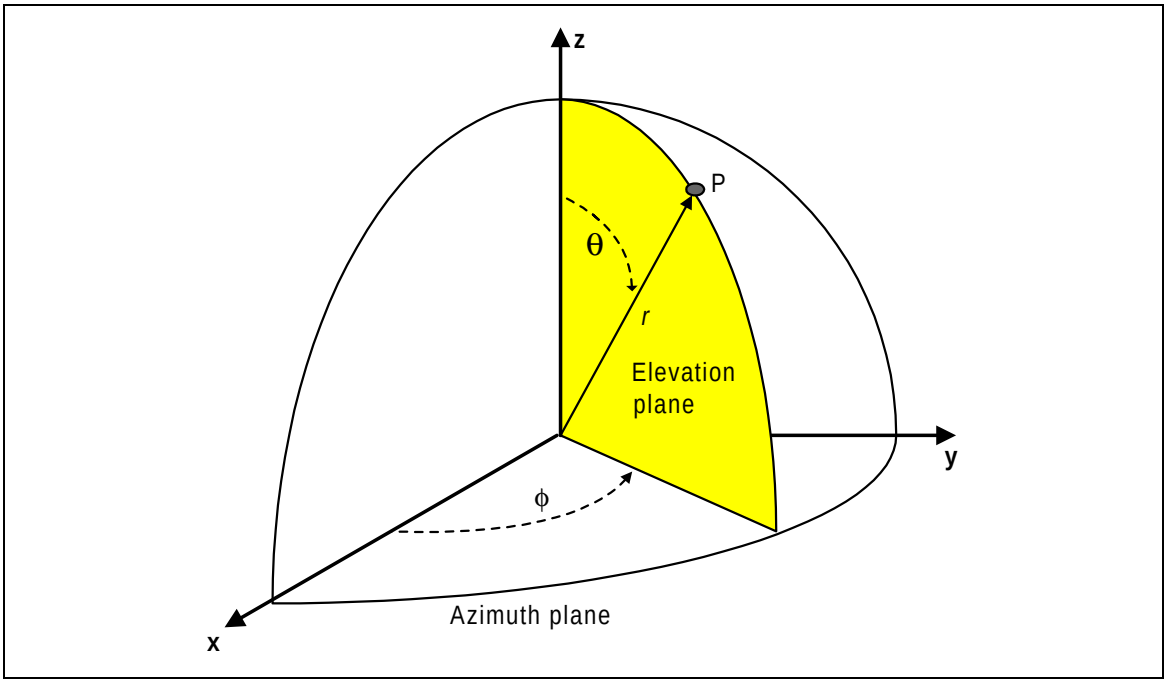

Figure 19. *Spherical coordinate system. The point P may be represented using Cartesian coordinates (x, y, z) or by using spherical coordinates (r, θ, ϕ). Also, $\phi = \phi_0$ determines a particular elevation plane.*

4.2.4 Principal Patterns

The performance of an antenna is often described in terms of its principal *E*- and *H-plane* patterns. IEEE standard 145-1993 defines the *E-plane* as the plane containing the electric-field vector and the direction of maximum radiation. Similarly, the *H-plane* is defined as the plane containing the magnetic-field vector and the direction of maximum radiation. The E- and H-planes are therefore orthogonal. It is common practice to orient antennas so that at least one of the principal plane patterns coincides with one of the Cartesian planes [Bala97]. For the SMT 7.0, the E-plane is made to coincide with the azimuth plane (*x-y* or ϕ plane) and the H-plane is made to coincide with the elevation plane determined by with $\phi = 0^0$ (*x-z* plane). Also, for the SMT 7.0 the positive *x* axis is assumed to be the direction of maximum radiation.

For nearly all situations of interest, just two *cuts* (one horizontal, one vertical) are sufficient to reconstruct the three-dimensional pattern. As stated above, the SMT 7.0 uses the *x*-*y* and *x*-*z* planes as the reference 2D planes to create a 3D pattern.

4.2.5 Radiation Pattern Lobes

Figure 20 illustrates various parts of the radiation pattern which are referred to as *lobes*. A *radiation lobe* is defined as a "portion of the radiation pattern bounded by regions of relatively weak radiation intensity". Lobes may be subclassified into major or main, minor, side and back lobes.

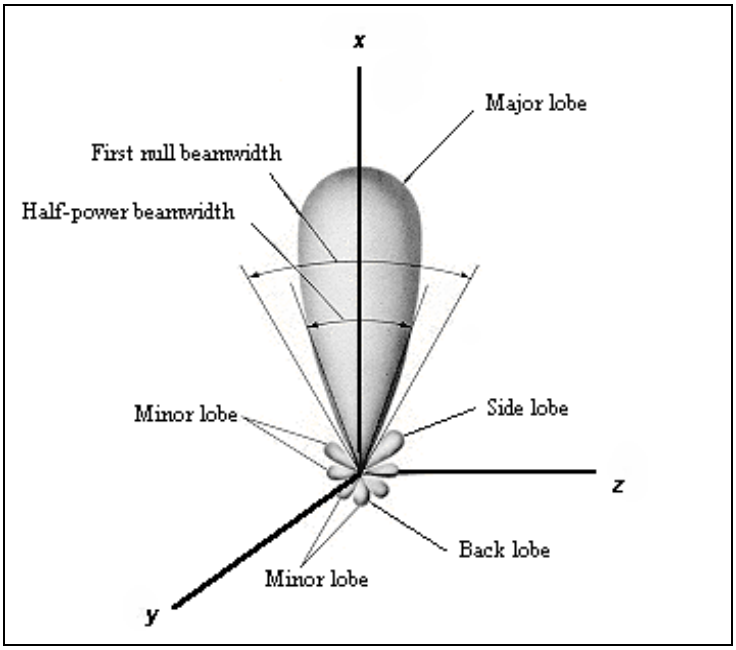

Figure 20. *Example of a radiation pattern (adapted from [Bala97]).*

The *boresight direction* is the direction of maximum radiation from the antenna. SMT 7.0 assumes the positive *x* axis to be the default boresight direction. There are two terms associated with the boresight. A *broadside antenna* is one in which the boresight direction is normal to the plane containing the antenna. An *endfire antenna* is

one in which the boresight direction is parallel to the plane containing the antenna. In practice power measurements are taken for a constant positive value (in meters) of *r* in the far-field region to plot the radiation pattern as shown in Figure 20.

4.2.6 Pattern Types

All antenna patterns can be classified into three types.

1. An ***isotropic radiator*** is defined as a hypothetical lossless antenna having equal radiation in all directions. In three dimensions the radiation pattern is spherical in shape. Although such an ideal radiator is physically impossible, it is often taken as reference to express the directional properties of other antennas. Earlier versions of the SMT 7.0 supported only this pattern type. The existing version also includes the following two types.
2. A ***directional antenna*** is one having a property of radiating and receiving electromagnetic waves more efficiently in certain directions. The SMT 7.0 in its present form supports nine such directional patterns that are not omnidirectional.
3. An ***omnidirectional antenna*** is a special type of directional antenna. IEEE Standard 145-1993 defines omnidirectional antenna as one having a non-directional pattern in a given plane and directional pattern in the orthogonal plane. For the SMT 7.0, the pattern is circular in the E-plane and directional in the H-plane. In three dimensions this pattern can be visualized as a donut. The SMT 7.0 presently supports eight omnidirectional patterns.

4.2.7 Near and Far-field Regions [Bala97]

The space surrounding the antenna can be subdivided into two regions: 1) the near-field region and 2) the far-field (Fraunhofer) region. Sometimes the near field

region is further subdivided into the a) reactive near-field region and b) radiating near-field (Fresnel) region. According to IEEE standard 145-1993, the far-field region is defined as "that region of the field of the antenna where the angular field distribution is essentially independent of the distance from the antenna". This is not true for the near field region of antenna as it contains reactive power indicating stored energy. The impedance of an antenna is in general complex, and the real part (neglecting ohmic losses of the antenna structure) represents radiation, while the imaginary part corresponds to the reactive near-field power [Stut81].

The criterion commonly used to define the boundary between the near and far field region is $r=2D^2/\lambda$, where D is the largest dimension of the antenna. Also note that additionally the following must be satisfied: $r>>D$, and $r>>\lambda$. A commonly used standard in the wireless industry is to consider distances more than 1 meter from the antenna, for an indoor environment, to constitute the far-field distance. To ensure that coverage calculations are carried out in the far-field region, the SMT 7.0 does not allow step size definitions of less than 1 meter (Figure 11, Section 3.5).

4.2.8 Polarization

Polarization is a property of a single frequency electromagnetic wave, and describes the shape and orientation of the locus of the extremity of field vectors as a function of time [Bala97]. The following are some of the terms used to describe various polarization states: linear vertical polarization, linear horizontal polarization, right circular polarization, left circular polarization, right elliptical polarization, left elliptical polarization. The polarization of the transmitting and receiving antenna in VHF and UHF regions need not be the same at both ends of a communication circuit, though generally for short distances (miles) there may be no appreciable change. Therefore, the design of a receiving antenna for an optimal wave reception will have to match that of the transmitter. In cases where incoming waves may have unpredictable

polarization, the design of the receiving antenna should be such as to respond equally to all polarizations. What polarization to choose (to avoid interference) for a given antenna type is dictated by the height of antenna supports, man-made RF noise in the area and other interferences.

Polarization is *not* supported in the present version of the SMT 7.0. However, if needed, it is a simple matter to modify calculations by introducing a "polarization mismatch factor" in the form of a dialog box parameter which can be used to scale the antenna gain during coverage calculations. A more elaborate and very accurate method would be to include this as a part of the antenna pattern equation itself.

4.2.9 Frequency dependent and independent antennas

Typically, radiation from an antenna has a spread of frequencies around a carrier frequency. The spread is due to some form of modulation associated with the radiation. Its important to note that for analysis purposes, a single frequency equal to the carrier frequency is generally used [Stut81]. For the SMT 7.0, the frequency bands of interest are the VHF (30 - 300 MHz) and the UHF (300 - 3000 MHz) regions. The term broadband or frequency-independent is used to describe antennas whose patterns and impedance do not change over a large frequency range of operation (at least one octave). If it does, the antenna is frequency dependent [Stut81].

4.3 Mathematical Development of $G_T(\theta,\phi)$

Derivation of each equation mentioned below can be found in [Stut81]. Only the logical progression of results are utilized to explain the significance of $G_T(\theta,\phi)$.

4.3.1 Radiation Power Density [Bala97] [Stut81]

The results mentioned below are essentially solutions of Maxwell's equations to the problem of finding the power radiated by a surface under certain boundary conditions. The quantity used to describe the power associated with an electromagnetic wave is the instantaneous Poynting vector defined as:

$$\mathcal{W} = \mathcal{E} \times \mathcal{H}$$

where,

$\mathcal{W}$ = Instantaneous Poynting vector (W/m^2),

$\mathcal{E}$ = Instantaneous electric field intensity (V/m), and

$\mathcal{H}$ = Instantaneous magnetic field intensity (A/m).

For sinusoidally varying signals it is common to define complex fields **E** and **H** that are related to their instantaneous real counterparts $\mathcal{E}$ and $\mathcal{H}$ by equations:

$$\mathcal{E}(x, y, z; t) = \mathrm{Re}[\mathbf{E}(x, y, z)\, e^{j\omega t}]$$
$$\mathcal{H}(x, y, z; t) = \mathrm{Re}[\mathbf{H}(x, y, z)\, e^{j\omega t}]$$

Using the above two definitions and the identity $\mathrm{Re}[\mathbf{E}\, e^{j\omega t}] = 0.5\, [\mathbf{E}\, e^{j\omega t} + \mathbf{E}^* e^{-j\omega t}]$ where **E*** is the complex conjugate of **E,** the equation for $\mathcal{W}$ can be rewritten as

$$\mathcal{W} = 0.5\, \mathrm{Re}[\mathbf{E} \times \mathbf{H}^*] + 0.5\, \mathrm{Re}[\mathbf{E} \times \mathbf{H}\, e^{j2\omega t}]$$

The first term is not a function of time, and the time variation of the second term is twice the given frequency. Hence the time average Poynting vector (*average power density*) can be written as

$$\mathbf{W}_{av}(x, y, z) = 0.5\, \mathrm{Re}[\mathbf{E} \times \mathbf{H}^*] \quad (\mathrm{W/m^2}) \qquad [4.1]$$

The total power P crossing a closed surface can be obtained by integrating the normal component of the Poynting vector over the entire surface s. Therefore, the instantaneous total power P is given by

$$P = \oiint_s \mathbf{W} \bullet d\mathbf{s} = \oiint_s (\mathbf{E} \times \mathbf{H}) \bullet d\mathbf{s} \qquad [4.2]$$

and using [4.1] the time averaged power P_{av} can be written as

$$P_{av} = \oiint_s \mathbf{W}_{av} \bullet d\mathbf{s} = \frac{1}{2} \oiint_s \mathrm{Re}(\mathbf{E} \times \mathbf{H}^*) \bullet d\mathbf{s} \qquad [4.3]$$

As explained in section 4.2.7, the average power in the far field region is simply the power radiated by the antenna. Therefore, $P_{av} = P_{rad}$. Similarly, $\mathbf{W}_{rad}$ represents the time averaged power density in the far field region and termed as *radiation density* [Bala97] and $\mathbf{W}_{av} = \mathbf{W}_{rad}$.

4.3.2 Directive Gain and Directivity

The P_{rad} and $\mathbf{W}_{rad}$ defined in the above section are used in this section to define U. The time averaged radiation intensity U is defined as the time averaged power radiated per unit solid angle and has units WATTS/steradian. By definition, [Bala97] U can be mathematically expressed as

$$U = r^2 \left\| \mathbf{W}_{rad} \right\| \qquad [4.4]$$

where r is the distance in the far field the radiation intensity is measured. Further, from the above definition it follows that total power radiated can be obtained by integrating the radiation intensity over all directions (solid angle 4π steradians). Hence,

$$P_{rad} = \oiint_\Omega U \, d\Omega \qquad [4.5]$$

where $d\Omega = \sin\theta \, d\theta \, d\phi$. Even though the above relations are useful, we are interested in finding the relation of radiation intensity to field or power patterns. This is because SMT uses field or power patterns as input data to obtain gain. Before we proceed to find this

relationship, lets describe for the sake of completeness, how radiation intensity is related to the electric field components in the far field region. Equation [4.7] describes the same.

The power pattern of an antenna is just a trace of the received power at a constant radius, and normally expressed relative to the power of an isotropic radiator. Given a sphere of radius r, η the intrinsic impedance of the medium and solid angle $d\Omega$, P_{rad} defined in [4.3] can also be derived to be [Stut81]:

$$P_{\text{rad}} = \frac{1}{2\eta} \oiint \left[\left| E_\theta \right|^2 + \left| E_\phi \right|^2 \right] r^2 d\Omega \qquad [4.6]$$

where E_θ and E_ϕ represent the θ and ϕ components of the far-zone electric field. Note that **E** and **H** fields are perpendicular to each other and to the direction of propagation. Each field in general can be described by θ and ϕ field components. The approximation used to derive equation [4.6] is given by: $\left\| \mathbf{E}(r,\theta,\phi) \right\|^2 \cong \left| E_\theta(r, \theta, \phi) \right|^2 + \left| E_\phi(r, \theta, \phi) \right|^2$ [Bala97]. θ and ϕ refer to the spherical coordinate angles as described in sections 4.2.3 and 4.2.4. Comparing [4.5] and [4.6] we can also represent U as:

$$U(\theta, \phi) = \frac{r^2}{2\eta} \left[\left| E_\theta \right|^2 + \left| E_\phi \right|^2 \right] \qquad [4.7]$$

Note that from [4.4] and [4.7] it is also evident that:

$$\left\| \mathrm{W}_{\text{rad}} \right\| = \frac{1}{2\eta} \left[\left| E_\theta \right|^2 + \left| E_\phi \right|^2 \right]$$

Let us now take a key relationship from [Stut81] which represents $U(\theta, \phi)$ in the form

$$U(\theta,\phi) = U_m \left| F(\theta,\phi) \right|^2 \qquad [4.8]$$

where U_m is the maximum radiation intensity and $\left| F(\theta,\phi) \right|$ is the magnitude of the normalized electric field. $\left| F(\theta,\phi) \right|^2$ has a maximum value of unity in the direction of $(\theta_{\max},\phi_{\max})$, that is $U_m = U(\theta_{\max},\phi_{\max})$. For the SMT 7.0 since the positive X axis represents the direction of boresight, we have $(\theta_{\max},\phi_{\max}) = (90^0, 0^0)$. As we will see from the definition of directive gain below, equation [4.8] is an important relationship used by

the SMT 7.0 as all the pattern files used, are normalized electric field or power pattern in dB. If [4.8] is compared to [4.7] it is easy to see that

$$U_m \left| F(\theta,\phi) \right|^2 = \frac{r^2}{2\eta} \left[\left| E_\theta \right|^2 + \left| E_\phi \right|^2 \right]$$

[Stut81] has shown the above relationship.

Directive gain is defined as the ratio of radiation intensity in a certain direction to the average radiation intensity. i.e.

$$D(\theta,\phi) = \frac{U(\theta,\phi)}{U_{ave}} = \frac{U_m \left| F(\theta,\phi) \right|^2}{U_{ave}}$$

Directivity is defined as $D_0 = U_m / U_{ave}$ where U_{ave} is the radiation intensity of an isotropic source and is constant in all directions. Figure 21 below is an illustration of directivity. Directivity is a figure-of-merit to describe the directional properties of an antenna. Therefore, the equation for directive gain can be rewritten as:

$$D(\theta,\phi) = D_0 \left| F(\theta,\phi) \right|^2 \qquad [4.9]$$

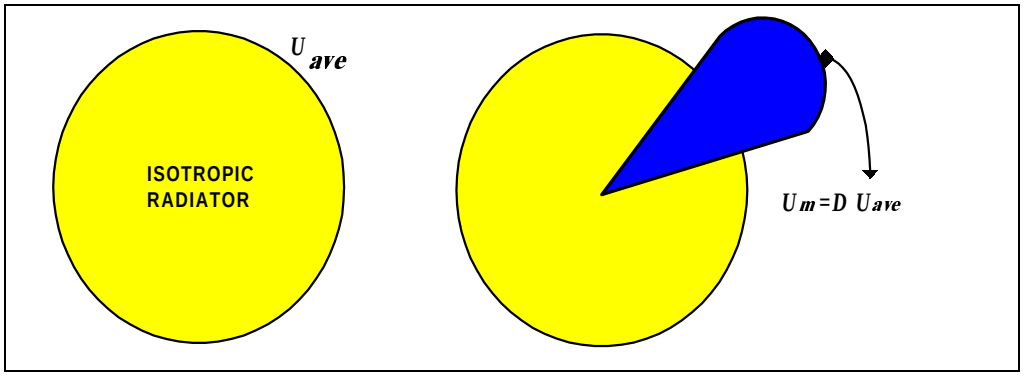

Figure 21. *Illustration of directivity. Both circles represent the average radiation intensity of an isotropic source. The darker region represents the directional property of the antenna.*

4.3.3 Field Pattern and Power Pattern

SMT 7.0 uses the field or the power radiation pattern as the reference. Therefore, we introduce $P(\theta, \phi)$ (not to be confused with instantaneous power P defined in equation [4.2] to be the normalized power counterpart of $F(\theta,\phi)$ described in the earlier section. The relationship between the field and the power patterns has been proved by [Stut81] to be

$$P(\theta, \phi) = |F(\theta, \phi)|^2 \qquad [4.10]$$

It is important to recognize that the field magnitude pattern $F(\theta, \phi)$ and the power pattern $P(\theta, \phi)$ are the same when plotted in dB. This follows directly from the definitions.

$|F(\theta, \phi)|$ [dB] = 20 log $|F(\theta, \phi)|$

$P(\theta, \phi)$ [dB] = 10 log $P(\theta, \phi)$ = 10 log $|F(\theta, \phi)|^2$ = 20 log $|F(\theta, \phi)|$ = $|F(\theta, \phi)|$ [dB]

4.3.4 Gain Equation for SMT 7.0

The directive properties of an antenna are solely determined by the radiation pattern. However, when an antenna is used in a system, the efficiency of the antenna in converting the power applied to its terminals comes into play and the equation $G(\theta,\phi) = eD(\theta,\phi)$, $0 \le e \le 1$ is often used to indicate this. The SMT 7.0 assumes e =1. Thus the gain for a transmitting antenna can be written as:

$$G_T(\theta, \phi) = D(\theta,\phi)$$

Using equation [4.9] the above can be rewritten as:

$$G_T(\theta, \phi) = D_0 |F(\theta,\phi)|^2$$

Plugging in the value from equation [4.10] we also have,

$$G_T(\theta, \phi) = D_0 P(\theta, \phi)$$

Note that D_0 is nothing but the boresight gain which we will call as G_B. $P(\theta, \phi)$ will be replaced by the term $G_M(\theta, \phi)$ which is normalized and hence lies in the range [0,1]. As will be described later, the procedure for obtaining $G_M(\theta, \phi)$ is different for different pattern types.

Hence the generalized equation for SMT 7.0 in terms of dB can be written as:

$$G_T(\theta, \phi)\ [\text{dB}] = G_B\ [\text{dB}] + m \log_{10} \left| G_M(\theta, \phi) \right| [\text{dB}]$$

The following points are important:

- The value of m in the above equation is either 10 or 20. Since "Omnidirectional patterns" and "Other directional patterns" use normalized field patterns, m = 20. The user provided data is a power pattern and hence m = 10.
- As will be evident later, the value of G_B is user provided for other directional patterns. For omnidirectional patterns this value is a pattern dependent constant. As described later, for user provided patterns both G_B and $G_M(\theta, \phi)$ are together input as a single dB value.
- $G_M(\theta, \phi)$ is a value between 0 and 1 which in dB converts to the range (- ∞, 0]. To circumvent the problem of - ∞, values less than 0.001 are limited to -60 dB by the SMT 7.0 program. This is small enough to avoid any loss in accuracy.
- Principal plane patterns (2D) are described for θ or ϕ in a range from 0^0 to 360^0. Strictly speaking, θ is limited to the range $[0^0, 180^0]$ in spherical coordinates and ϕ is limited to $[0^0, 360^0)$. This is because, (θ, ϕ) in the above range is sufficient to locate the unique position of any point in 3D space. However, the situation for the SMT 7.0 is different. A) We have two independent 2D gain files in terms of θ and ϕ respectively in the $[0^0, 360^0)$ range. B) Based on the search algorithm on the receiver plane and homogeneous co-ordinate transformations, we also obtain a set of θ and ϕ values. One of the things the interpolation algorithm does is to effectively combine the above two situations. Section 5.4.3 describes the same in detail. (θ, ϕ) values are mapped onto a octant which avoids any ambiguity in determining a unique 3D point.

4.4 Explanation of patterns in SMT 7.0

The SMT 7.0 in its present form supports four types of antenna patterns. The four pattern types supported are 1) isotropic, 2) omnidirectional, 3) user provided,

and 4) other directional patterns. Principal pattern plots are shown in this thesis for all types. The $G_T(\theta, \phi)$ equation is presented in each instance. The last two pattern types however require an interpolation of values from the two principal patterns. The techniques employed to perform interpolation along with 3D orientation techniques are explained in chapter 5.

4.4.1 Isotropic Pattern

As described before, this is the simplest possible antenna pattern. For the SMT 7.0, the screen menu item to choose this antenna type is "ISO XCVR" (Figure 3, Chapter 3). The gain equation is described by: $G_T(\theta, \phi) = 0$ [dB]

4.4.2 Omnidirectional Patterns

Antennas with these patterns are perhaps the most widely used in indoor communications. Most of the omnidirectional patterns can be visualized as donuts. An omnidirectional pattern is a constant in the azimuth plane and directional in any elevation plane. Hence the generalized gain equation for SMT 7.0 may be written as:

$$G_T(\theta, \phi) \text{ [dB]} = G_{AZ}(\phi) \text{ [dB]} + G_{EL}(\theta) \text{ [dB]}$$

where $G_{AZ}(\phi)$ is a constant. Thus, $G_{AZ}(\phi) = G_B$ and $G_{EL}(\theta) = G_M(\theta, \phi)$. Figure 22 is a simple illustration of the pattern with the donut

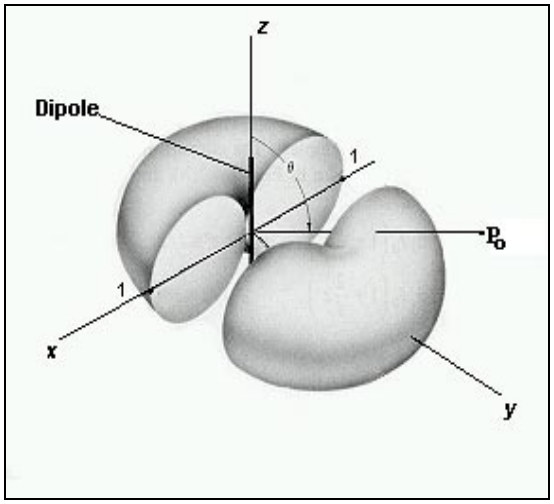

Figure 22. *An omnidirectional pattern [Bala97].*

sliced to show an elevation plane pattern. Even though there are many gain pattern equations which may yield an omnidirectional pattern, the SMT 7.0 supports eight patterns which are commonly used. A menu of these patterns is shown in Figure 14, Chapter 3. The antenna types supported are dipole, monopole, discone and biconic.

Dipole antennas [Elli81] [Bala97]

The SMT 7.0 supports the quarter wave and the halfwave dipole patterns. The dipole is physically assumed to be placed along the *z* axis as illustrated in Figure 22.

1) Halfwave dipole

The antenna is called a halfwave dipole because its physical length is $\lambda/2$. Note that this is the shortest possible length of a resonant wire simply because it corresponds to the shortest time in which an electric charge can travel from one end of the wire and back, in one RF cycle. A major reason for the wide acceptance of the halfwave dipole is because its radiation resistance is 73Ω, very near the 75Ω characteristic impedance of some transmission lines. The halfpower beamwidth of a halfwave dipole is 78^0 and the peak directivity is 1.64 or 2.15 dB. Since the pattern is constant in the azimuth plane, only the elevation plane pattern [$G_{EL}(\theta)$] is shown in Figure 23.

In the azimuth plane: $G_{AZ}(\phi) = 2.15$ [dB]

In the elevation plane: $G_{EL}(\theta) = 20 \log_{10} \left| \dfrac{\cos(0.5\pi \cos\theta)}{\sin\theta} \right|$ [dB] for all $\theta \in (0^0, 180^0)$

Note 1: In software, a very small value of $G_{EL}(\theta) = -60$ dB is assumed for all cases when $G_{EL}(\theta)$ approaches $-\infty$. This case is encountered for $\theta = 0^0$ and 180^0.

Note 2: The closed form equations are described here as normalized electric field variations (V/m) and hence convert to dB as $20\log_{10}|\bullet|$. However the peak directivity is treated as power (dB) and hence converts to dB as $10 \log_{10}|\bullet|$. Notice that 1.64 = 2.15 dB. The above two notes are valid for all the remaining patterns in this section.

2) <u>Quarterwave dipole</u>

The antenna is called quarterwave dipole because its physical length is $\lambda/4$. The pattern is similar to the halfwave dipole except that the halfpower beamwidth of a quarterwave dipole is 87^0 and the peak directivity is 1.57 or 1.96 dB. Figure 23 depicts the elevation plane pattern.

In the azimuth plane: $G_{AZ}(\phi) = 1.96$ [dB]

In the elevation plane: $G_{EL}(\theta)=20\log_{10}\left|\dfrac{\cos(0.25\pi\cos\theta)-\cos(0.25\pi)}{\sin\theta}\right|$ [dB] for $\theta \in (0^0, 180^0)$

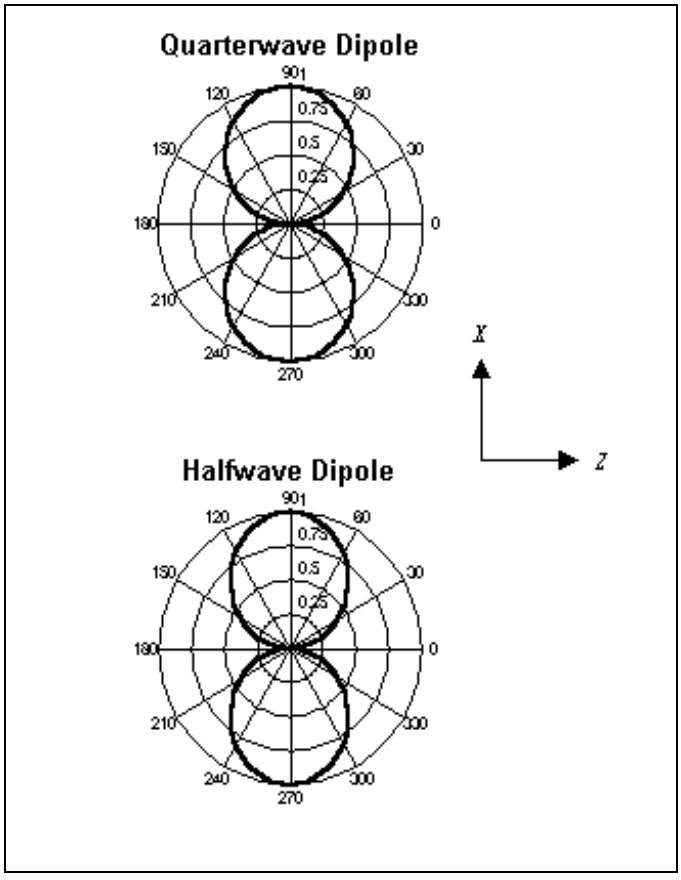

Figure 23. *Elevation plane polar plots of dipole type omnidirectional antennas. For convenience, θ is shown lying in the range $[0^0, 360^0)$.*

Monopole antennas **[Elli81] [Bala97]**

The SMT 7.0 supports the quarter wave and the halfwave monopole patterns. The monopole is assumed to be physically placed along the *z* axis. The monopole is simply a dipole divided in half at its center feed point, and fed against a ground plane as shown in Figure 24a. However, high frequency monopoles are often fed from behind the ground plane as shown in Figure 24b. A monopole above the ground plane radiates one-half the total power of a similar dipole in free space, and thus the directivity of a monopole is double that of a similar size dipole.

Since the monopole is one half of a dipole, we can expect the pattern to be similar to the top half of a dipole pattern. Thus we can imagine the donut chopped along the azimuth plane to be the three dimensional pattern of a monopole. This is however the ideal case because we are assuming the ground to be infinite and a perfect electrical conductor. In reality this is never the case, and we can imagine the pattern to be a function of varying ground plane sizes $m\lambda$, where m is a real number. [Elli81] and [Bala97] discuss how the closed form equations for a dipole may be modified to fit ground plane effects for a monopole. This consists of multiplying the closed form equations for the dipole by the

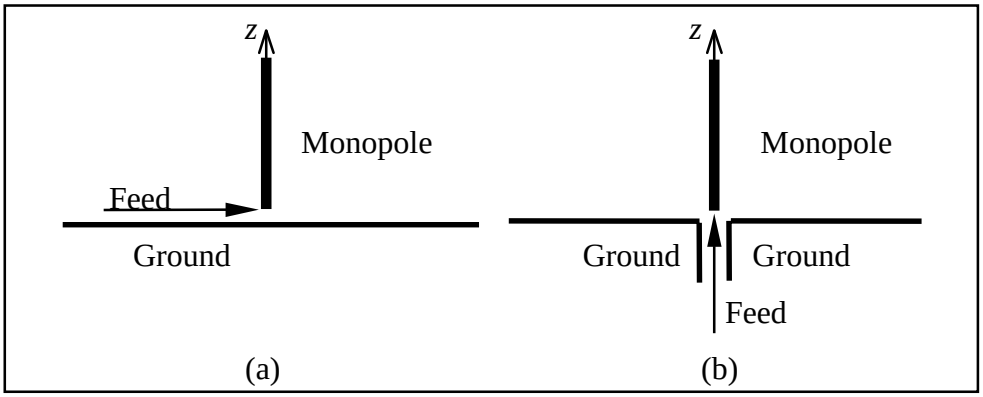

Figure 24. *An illustration of a monopole antenna. The figure depicts two ways energy can be fed into the antenna.*

factor "$k \sin(n \sin\theta)$", where n and k are determined by the size of the ground plane and the size of the monopole antenna [Bala97]. This factor is called the "ground plane correction factor".

3) Quarterwave monopole

The antenna, called the whip antenna, is considered the fundamental mobile antenna. As we discussed earlier, directivity is 2×1.57, twice that of a quarterwave dipole. Also the equation for the elevation plane is same as a halfwave dipole multiplied by the "ground plane correction factor" we mentioned in the previous paragraph. The values for n and k have been chosen based on the observed half power beamwidth for ground plane sizes typically found an indoor environment. The elevation pattern plot is shown in Figure 25.

In the azimuth plane: $G_{AZ}(\phi) = 4.97$ [dB]

In the elevation plane: $G_{EL}(\theta) \cong 20 \log_{10} \left| \frac{\cos(0.5\pi \cos\theta)}{\sin\theta} \right| \; | k \sin(n \sin\theta) |$ [dB]

for $\theta \in (0^0, 90^0]$ with $n = 2.5$ and $k = 1.4782$.

Elsewhere, $G_{EL}(\theta) = -60$ dB.

4) Halfwave monopole

The directivity is 2×1.64, twice that of a halfwave dipole. Also the equation for the elevation plane is same as a fullwave dipole multiplied by the "ground plane correction factor". The half power beamwidth of a halfwave monopole is 47.8^0. The elevation pattern is shown in Figure 25.

In the azimuth plane: $G_{AZ}(\phi) = 5.16$ [dB]

In the elevation plane: $G_{EL}(\theta) \cong 20 \log_{10} \left| \frac{\cos(\pi \cos\theta + 1)}{\sin\theta} \right| \; | k \sin(n \sin\theta) |$ [dB]

for $\theta \in (0^0, 90^0]$ with $n = 2.75$ and $k = 1.2015$.

Elsewhere, $G_{EL}(\theta) = -60$ dB.

5) <u>Quarterwave Discone</u>

A discone is a frequency independent antenna as discussed in section 5.2 and therefore offers acceptable pattern and impedance properties over several octaves of frequency. The antenna itself is a inverted cone with a disk shaped ground plane on top. The base of the cone is placed to be parallel to the azimuth plane, such that the *z* axis

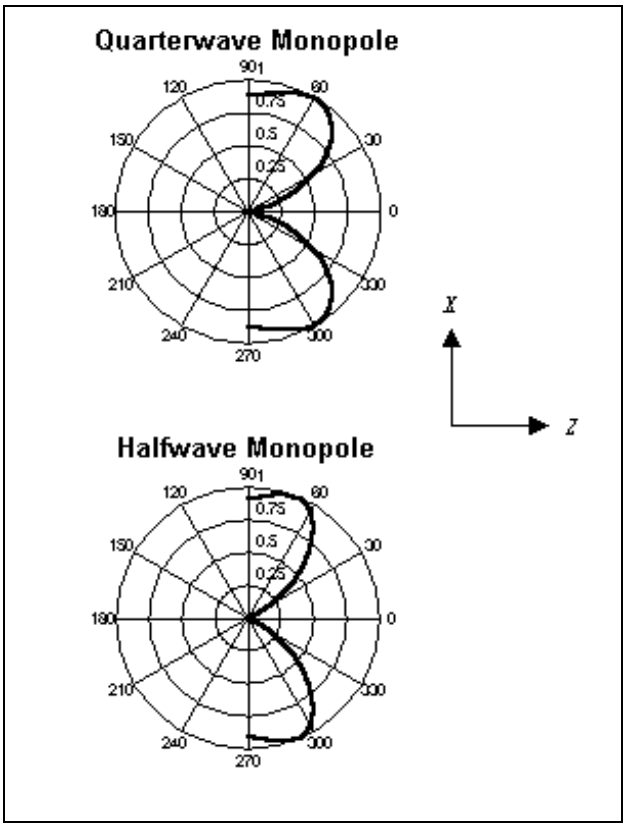

Figure 25. *Elevation plane polar plots of monopole type omnidirectional antennas. For consistency, the x-axis is still used as the boresight direction, though the gain is slightly less than the maximum due to ground plane effects.*

passes through the cone vertex and is perpendicular to the ground plane disk. The gain pattern equation is same as a quarterwave monopole for a different θ range so that the pattern is a mirror image of that of a quarterwave monopole. The elevation plane pattern is shown in Figure 26.

In the azimuth plane: $G_{AZ}(\phi) = 4.97$ [dB]

In the elevation plane: $G_{EL}(\theta) \cong 20 \log_{10} \left| \frac{\cos(0.5\pi \cos\theta)}{\sin\theta} \right| \; | k \sin(n \sin\theta) |$ [dB]

for $\theta \in [90^0, 180^0)$ with $n = 2.5$ and $k = 1.4782$

$G_{EL}(\theta) = -60$ [dB] elsewhere.

Biconical antennas [Stut81] [Bala97]

The SMT 7.0 supports three types of biconical antennas. The biconical antenna is a broadband antenna. A biconical antenna consists of two cones, a cone on top of an inverted cone with the energy fed between the two vertices. The *z* axis passes through the center of both cones. For an infinite biconical antenna the equation for the pattern in the elevation plane is $\sin\theta_h / \sin\theta$ for $\theta_h < \theta < \pi - \theta_h$. θ_h is the angle between the *z* axis and the slant surface of the cone and is called the cone angle. However for a finite biconical antenna with small cone angles, the pattern is similar to that of an ordinary dipole antenna of the same length, where length refers to the total vertical height of the bicone.

6) Quarterwave biconic

The pattern equations are the same as that for a quarterwave dipole. The elevation plane pattern is shown in Figure 26.

7) Halfwave biconic

The pattern equations are the same as that for a halfwave dipole. The elevation plane pattern is shown in Figure 26.

8) Fullwave biconic

The pattern equations are the same as that for a fullwave dipole. The fullwave dipole has a physical length of λ and a boresight gain of 3.8 dB. The elevation plane pattern is shown in Figure 26.

In the azimuth plane: $G_{AZ}(\phi) = 3.80$ [dB]

In the elevation plane: $G_{EL}(\theta) = 20 \log_{10} \left| \frac{\cos(\pi \cos\theta + 1)}{\sin\theta} \right|$ [dB] for $\theta \in (0^0, 180^0)$

$G_{EL}(\theta) = -60$ [dB] elsewhere.

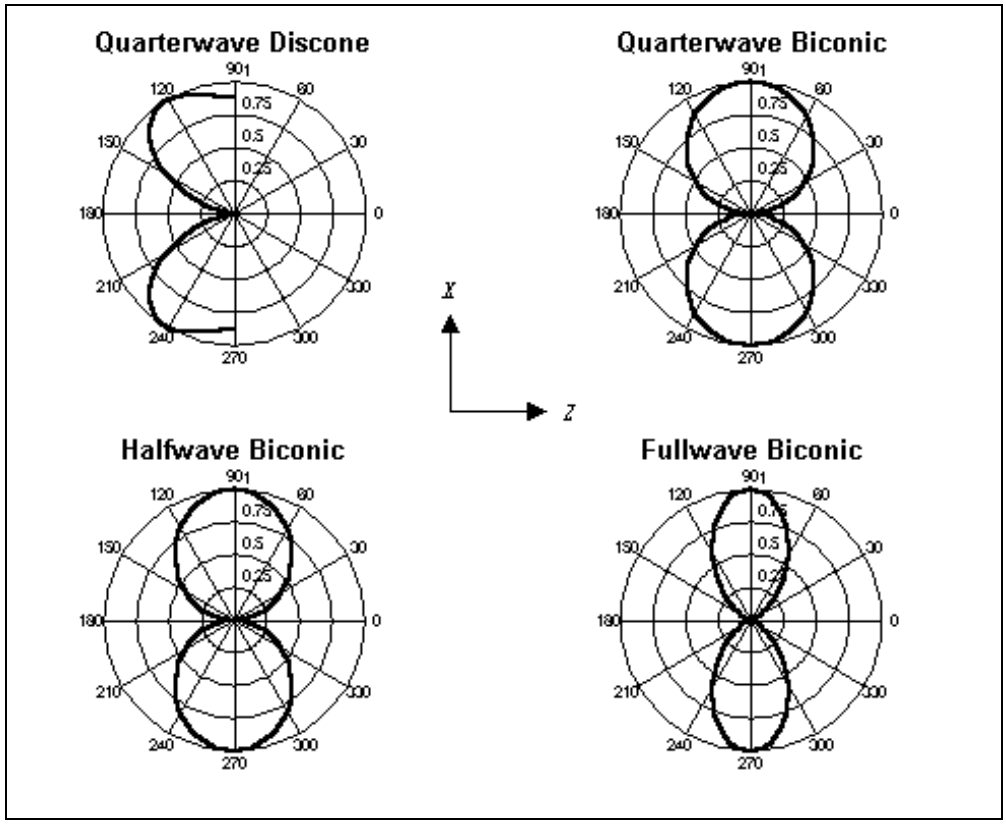

Figure 26. *Elevation plane polar plots of some omnidirectional antennas. For consistency, the x-axis is called the boresight direction for the quarterwave discone, even thought this is not the direction of maximum gain.*

4.4.3 User Provided Patterns

To select user provided patterns the user selects the "User patterns" dialog box under the "Antennas" pull-down menu [Figure 15, chapter 4]. The user is required to specify the location for the ASCII files which contain the azimuth and elevation plane data. The data itself is required to be stored in a column format in 5^0 increments in dB.

This seems to be a de facto industrial standard in which antenna pattern measurement data is stored when measurements are taken with a power meter for any directional antenna pattern. Since the SMT 7.0 assumes the *x* axis to be the default boresight direction as discussed earlier, the user has to ensure that his pattern data meets this requirement. Figure 27 gives polar plots of an actual antenna for the elevation [$G_{EL}(\theta)$] and azimuth [$G_{AZ}(\phi)$] planes. As can be seen, the maximum gain in the boresight direction is around 10 dB.

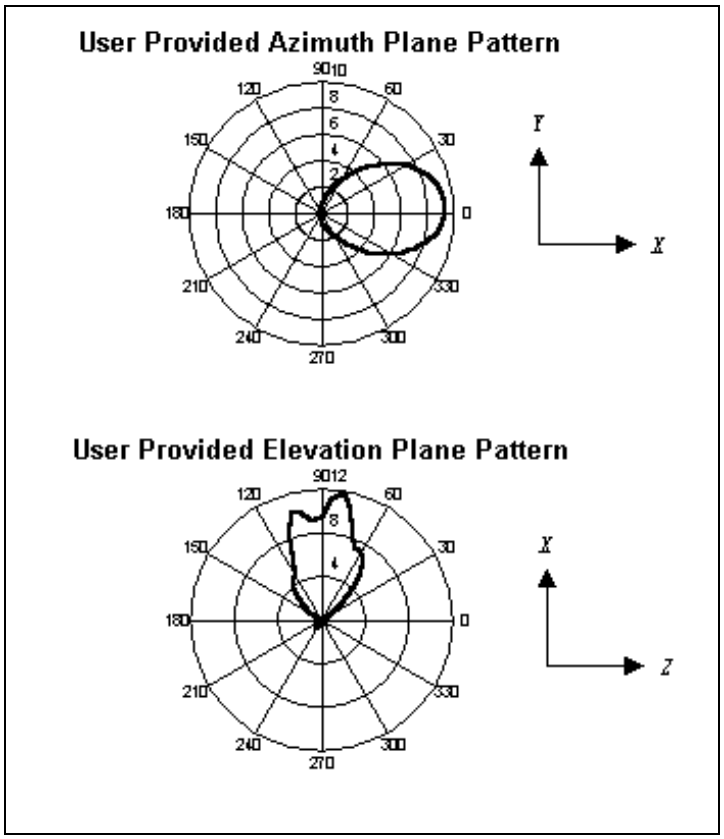

Figure 27. *Example of user provided polar pattern plots. For consistency, x-axis continues to be used as the boresight, even though the maximum gain is not exactly on the x-axis.*

The gain in the boresight direction is given by G_B [dB], and therefore the generalized equation in three-dimensions is:

$$G_T(\theta, \phi)\ [\text{dB}] = G_B\ [\text{dB}] + 10 \log_{10} \left| G_M(\theta, \phi) \right| [\text{dB}]$$

where $G_M(\theta, \phi)$ represents the interpolated value between normalized patterns $G_{EL}(\theta)$ and $G_{AZ}(\phi)$ and is described in the next chapter. Given the pattern data for the elevation and azimuth plane, the software internally calculates the boresight gain G_B and normalized gain pattern data for $G_{EL}(\theta)$ and $G_{AZ}(\phi)$.

4.4.4 Other Directional Patterns

To view the menu for other directional patterns the user selects the "Other patterns" dialog box under the "Antennas" pull-down menu [Figure 16 and 17, Chapter 4]. Given the wide range of shapes and physical dimensions that are possible, many closed form equations are needed to describe the antenna patterns. A menu of fourteen two-dimensional pattern equations (seven for the azimuth plane and seven for the elevation plane) are supported by the SMT 7.0. These include such important indoor antennas such as horn and patch antennas. The reason for specifically choosing these 14 equations from a huge list of closed form equations is two folds. 1) For reasons of practicality choose only those closed form equations that depict typical directional indoor antenna patterns. 2) Allow flexibility in the equations to change variables to obtain an impressive variety of antenna patterns. *By judiciously choosing patterns for the azimuth and elevation plane with the appropriate parameters, it is possible to create nearly any practical antenna pattern.* Before we list these pattern equations, a brief description of horn and patch antennas is given for the sake of completeness. Note that generalized representation of these antenna pattern equations can be found in the menu described later in the section.

Horn antennas **[Jasi84] [Bala97]**

Horn antennas are by far the most popular aperture antennas, with electromagnetic fields being radiated through physical apertures. This is not to be

mistaken for the effective aperture of an antenna which is simply the effective area which can radiate or receive energy. A horn antenna may also be described as a open ended (or flared out) waveguide. Since it produces a uniform phase front, directivity is high. Figure 28 shows three aperture antenna configurations. A brief mention of the patterns generated by horn antennas is as below. Note that all the pattern types form a part of the pattern menu for "Other antennas".

- *Sectoral horn*: This can be further categorized as E-plane sectoral horn or H-plane sectoral horn. The horn end is similar to the rectangular aperture shown in Figure 28, but the body tapers down like the pyramidal horn. The classification of E and H planes is based on the direction in which the rectangular aperture is placed with reference to the spherical coordinate system. The patterns are the transpose of each other. i.e. the elevation plane pattern of a H-plane sectoral horn is a *cardioid* [see type 5, other pattern menu], which is the azimuth plane pattern for a E-plane sectoral horn. Similarly the azimuth plane pattern for the H-plane sectoral horn is a $\cos^n\theta$ function [see type 1, other pattern menu] which is the pattern equation for the elevation plane pattern for the E-plane sectoral horn. Here *n* is real number between 2 and 5.
- *Pyramidal horn*: This is probably the most popular form of rectangular horn used. The radiation field expression is a combination of E and H plane sectoral horns. Thus both the E and H field expressions can be approximated by $\cos^n\theta$.
- *Uniform rectangular aperture*: For a uniform rectangular aperture of size $L_x \times L_y$ the normalized principal plane patterns are:

$$G_{EL}(\theta) = 20 \log_{10} \left| \frac{\sin[(\beta L_y / 2)\sin\theta]\cos\theta}{(\beta L_y / 2)\sin\theta} \right| \quad \text{[dB]}$$

$$G_{AZ}(\phi) = 20 \log_{10} \left| \frac{\sin[(\beta L_x / 2)\sin\phi]\cos\phi}{(\beta L_x / 2)\sin\phi} \right| \quad \text{[dB]}$$

For large apertures (L_x, L_y >> λ) the factor $\cos\theta$ is negligible. The half power beamwidth for the elevation plane is .886 (λ/L_y) and for the azimuth plane is .886 (λ/L_x). With $\text{sinc}(z) \equiv \sin(\pi z)/\pi z$, the three dimensional gain pattern equation is:

$$G_T(\theta,\phi)\ [\text{dB}] = 20 \log_{10} \left| \text{sinc}(L_x \sin\theta \cos\phi) \times \text{sinc}(L_y \sin\theta \sin\phi) \right|$$

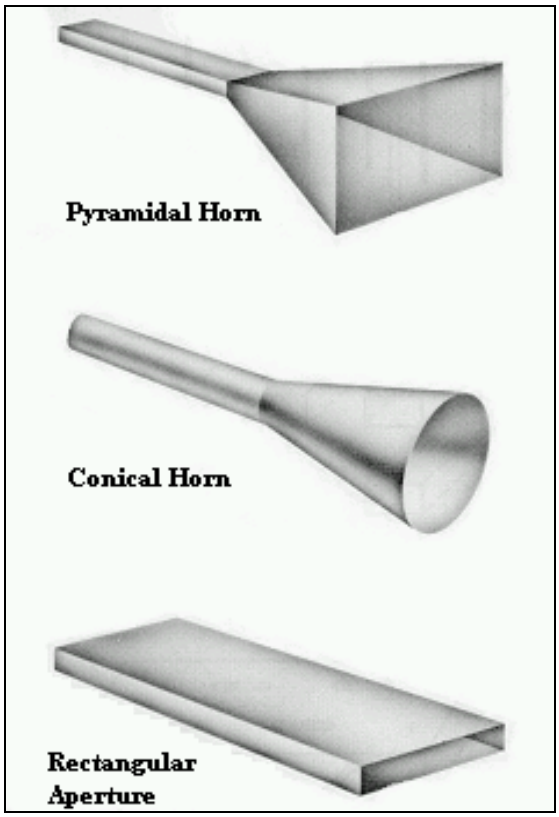

Figure 28. *Example of aperture antennas [Bala97].*

Microstrip and Patch antennas [Jasi84]

The terminology for this class of antennas is highly misleading, with names like patch antennas and microstrip antennas being used to essentially denote the same thing.

A patch antenna in its simplest form consists of a thin metallic film bonded to a grounded dielectric substrate (essentially a printed circuit board [PCB]). The advantage of such a construction is a low profile, lightweight, and economical

construction. The patch can be of any shape, but regular geometric shapes like a rectangle or circle are most popular. Feeding is achieved via a microstrip, or through a coaxial line. The placement of the feed is important to the operation of the antenna. More sophisticated antennas of this type would be a *microstrip array*, but they are omitted from discussion as a closed form solution is not available. The flow of electromagnetic power in easy to visualize, with the fed energy spreading out into the region of the patch, some of which crosses the boundary to be radiated into space. The drawback of this antenna stems from the fact that it is narrowband, but patches in arrays (microstrip array) can alleviate this problem.

The rectangular patch antenna is quite popular. These antennas are generally operated in various electrical modes of excitation and the patterns are different depending on the modes. Further, depending on the resonant frequency, the equations would vary. For $w << \lambda$, the directivity D of the microstrip is ≈ 3 (4.77 dB) and for $w >> \lambda$, $D \approx 4$ (6.02 dB) where w is the width of the rectangular patch [Bala97]. The pattern equations for the principal planes for certain types of microstrip antennas is listed below. Note that all these equations are available in a generalized form in the SMT 7.0 "other pattern" menu.

- Rectangular quarter wave, where θ is the angle in the elevation plane and w is the width of the antenna:

  $G_{EL}(\theta) = 20 \log_{10} | \tan\theta \ \sin([\pi w/\lambda_0] \cos\theta) |$ [dB]

- Rectangular, full wavelength resonant, with $0^0 < \phi < 180^0$, where K is a constant:

  $$G_{AZ}(\phi) = 20 \log_{10} \left| K \sin \left(\left(\pi \Big/ \sqrt{\varepsilon_r} \right) \cos\phi \right) \right| \text{ [dB]}$$

- Rectangular, half wavelength resonant, with $0^0 < \phi < 180^0$, where K is a constant:

  $$G_{AZ}(\phi) = 20 \log_{10} \left| K \cos \left(\left(\pi \Big/ 2\sqrt{\varepsilon_r} \right) \cos\phi \right) \right| \text{ [dB]}$$

Patterns in the "Other pattern" menu

The explanation and figures of the fourteen patterns which form a part of this menu are as follows. Note that each pattern equation is described as an elevation $G_{EL}(\theta)$ or an azimuth plane $G_{AZ}(\phi)$ equation depending on its boresight direction. As discussed before, all 2D pattern plots are defined for the range $[0^0, 360^0)$ although these values are mapped to the values in $[0^0, 180^0]$ for the case of elevation angle. The equations themselves are normalized and have values ranging from 0 [dB] to -60 [dB], which represents gain values between 1 and 0. The gain in the boresight direction is a user configurable parameter and is given by G_B [dB], and therefore a generalized equation in three-dimensions is:

$$G_T(\theta, \phi)\ [\text{dB}] = G_B\ [\text{dB}] + 20\log_{10} \left| G_M(\theta, \phi) \right| [\text{dB}]$$

where $G_M(\theta, \phi)$ represents the interpolated value between $G_{EL}(\theta)$ and $G_{AZ}(\phi)$ and is described in the next chapter. Also, note that each of the patterns described below have user modifiable variables like n and w as part of the pattern equation. The SMT 7.0 recognizes two decimal places of accuracy.

1) ***The unidirectional cosine function*****:** The equation is as follows:

$G_{AZ}(\phi) = 20 \log_{10} \left| \cos^n(\phi) \right|$ [dB] for $\phi \in [0^0, 90^0)$ and $(270^0, 360^0)$

$= -60$ [dB] for all other ϕ.

A plot of this is shown in Figure 29. The value of n is suggested to be between 1 and 5. This is because, as the value of n becomes larger the beam width becomes smaller until it becomes a pencil beam, and ceases to be an useful pattern. Aperture antennas like the horn antennas generate unidirectional cosine patterns, which explains why ϕ has a restricted coverage range.

2) *The unidirectional sine function*: The equation is as follows:

$G_{EL}(\theta) = 20 \log_{10} |\sin^n(\theta)|$ [dB] for $\theta \in (0^0, 180^0)$

$= -60$ [dB] for all other θ.

The plot is shown in Figure 29. The explanation given for the unidirectional cosine pattern is also valid for the unidirectional sine pattern.

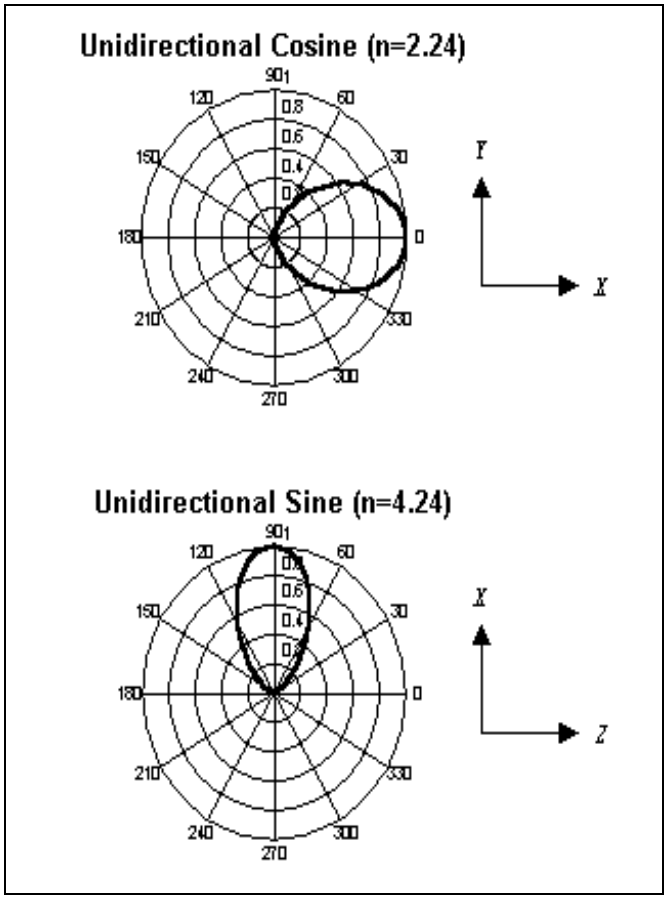

Figure 29. *Polar plots of Other pattern types 1) and 2).*

3) *The ellipse function for azimuth plane*: The plot for this pattern is shown in Figure 30. The equation for the pattern on the azimuth plane is given by:

$$G_{AZ}(\phi) = 20 \log_{10} \left| \frac{\cos\phi}{\cos^2\phi + \left(\sin^2\phi / w^2 \right)} \right| \text{ [dB] for } \phi \in [0^0, 90^0) \text{ and } (270^0, 360^0]$$

$$= -60 \text{ [dB]} \qquad \text{for all other } \phi.$$

The value of the width w is $0 < w \leq 1$. This equation can be derived from the more common ellipse equation which represents an ellipse centered at $(x, y) = (0.5,0)$. The major-axis length is 1 and the minor-axis length is w.

$$\frac{(x-0.5)^2}{(0.5^2)} + \frac{y^2}{(0.5w)^2} = 1$$

By substituting $x = G_{AZ}(\phi)\cos\phi$ and $y = G_{AZ}(\phi)\sin\phi$, the above equation for $G_{AZ}(\phi)$ can be obtained.

4) *The ellipse function for elevation plane*: The plot for this pattern is shown in Figure 30. Using the same derivation scheme as above, the equation for the pattern on the elevation plane is given by:

$$G_{EL}(\theta) = 20 \log_{10} \left| \frac{\sin\theta}{\sin^2\theta + \left(\cos^2\theta / w^2 \right)} \right| \text{ [dB] for } \theta \in (0^0, 180^0)$$

$$= -60 \text{ [dB]} \qquad \text{for all other } \theta.$$

5) *The sinc function*: The plot for this pattern for two different values of n is shown in Figure 31. This equation can be used to approximate patterns generated by uniform rectangular apertures. The equation which describes this pattern for the azimuth plane is given by:

$$G_{AZ}(\phi) = 20 \log_{10} \left| \frac{\sin(n \sin\phi)}{n \sin\phi} \right| \text{[dB]} \qquad \text{for } \phi \in (0^0, 180^0) \text{ and } (180^0, 360^0)$$

$$= -60 \text{ [dB]} \qquad \text{for all other } \phi.$$

A n value range of $2 \le n \le 4$ is suggested to obtain patterns of practical interest.

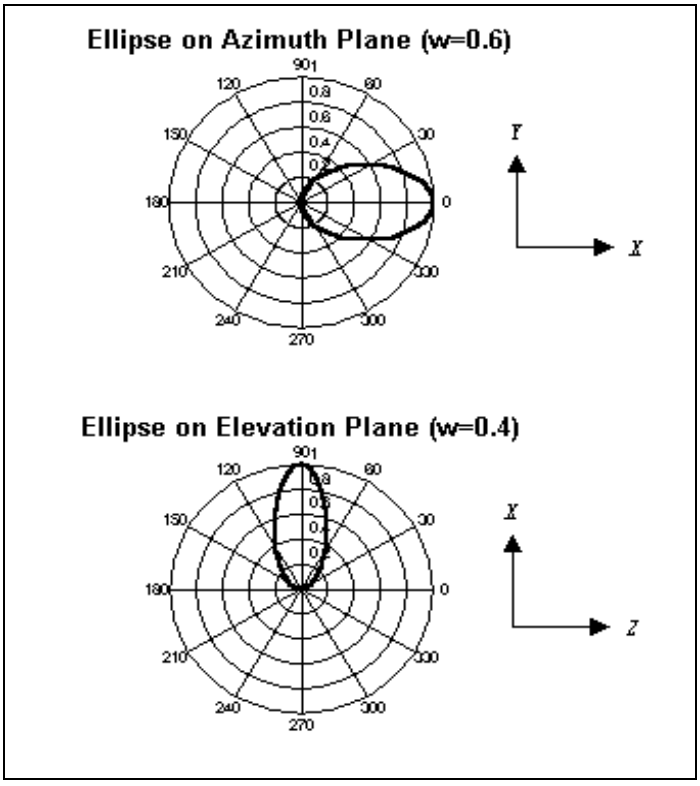

Figure 30. *Polar plots of elliptical patterns.*

6) *Function 6*: The pattern generated by this function is shown in Figure 31. The equation which describes this pattern on the elevation plane is given as:

$$G_{EL}(\theta) = 20 \log_{10} \left| \frac{\tan\theta \sin(n \cos\theta)}{n} \right| \text{ [dB]} \qquad \text{for } \theta \in (0^0, 180^0) \text{ and } (180^0, 360^0)$$

$$= -60 \text{ [dB]} \qquad \text{for all other } \theta.$$

A n value range of $1.0 \le n \le 4.0$ is suggested to obtain patterns of practical interest.

7) ***The limacon function for the azimuth plane***: The patterns generated by this function for two different values of *a* is shown in Figure 32. Recall that the equation can be used

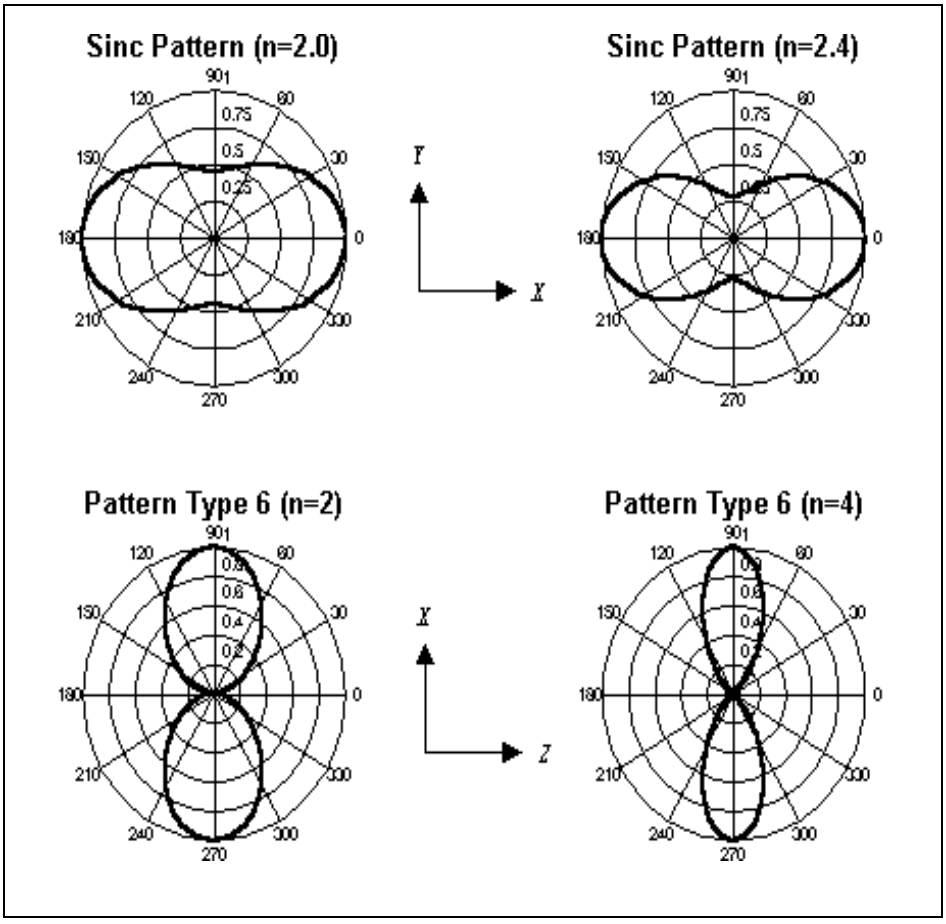

Figure 31. *Polar plots for patterns generated by the sinc function and by function 6.*

to represent patterns generated by various horn antennas. Note that if a = 0.5, then the pattern is a *cardiod*, which is a special case of a limacon. The equation which describes this pattern for the azimuth plane is given as:

$G_{AZ}(\phi) = 20 \log_{10} \left| a + (1-a)\cos\phi \right|$ [dB] for $\phi \in [0^0, 360^0)$

$= -60$ [dB] for $\phi = 180^0$, when $a = 0.5$.

The valid range for a is $0.5 \leq a < 1.0$.

8) ***The limacon function for the elevation plane***: The patterns generated by this function for two different values of *a* is shown in Figure 32. The equation which describes this pattern for the elevation plane is given as:

$G_{EL}(\theta) = 20 \log_{10} |a + (1-a)\sin\theta|$ [dB] for $\theta \in [0^0, 360^0)$

$= -60$ [dB] for $\theta = 270^0$, when $a = 0.5$.

The valid range for *a* is $0.5 \leq a < 1.0$.

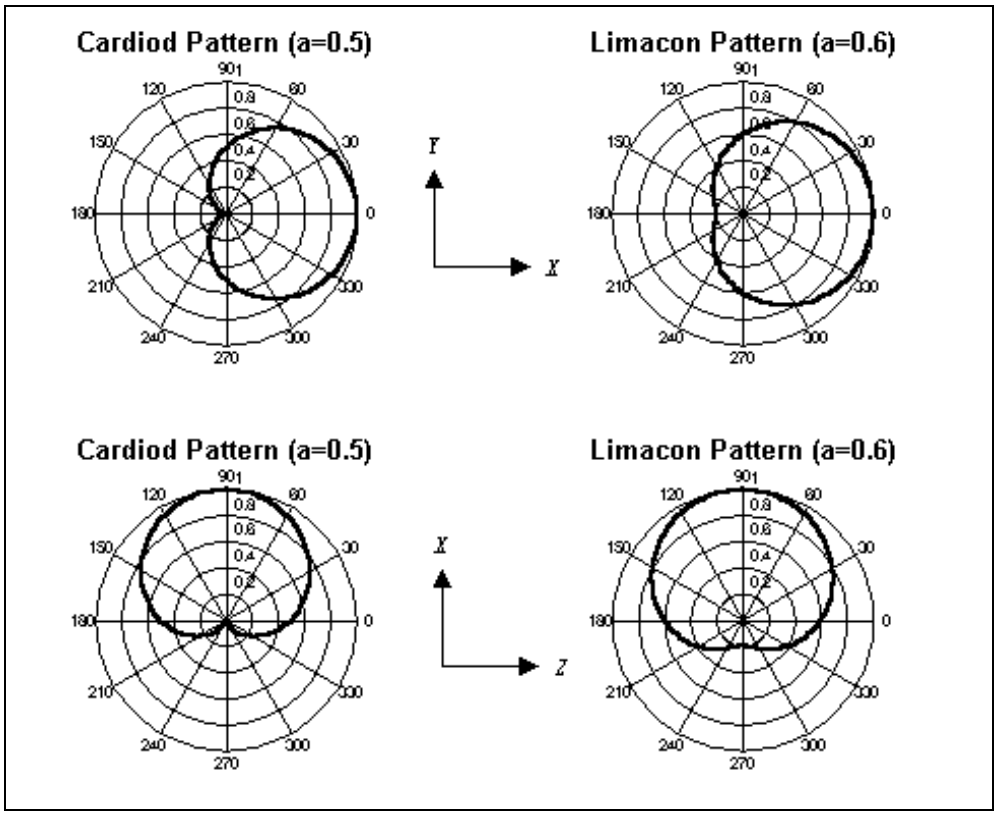

Figure 32. *Polar plots of limacon functions for the azimuth and elevation planes.*

9) ***Function 9***: The pattern generated by this function is shown in Figure 33. The equation which describes this pattern on the azimuth plane is given as:

$G_{AZ}(\phi) = 20 \log_{10} |\sin(n\cos\phi)|$ [dB] for $\phi \in [0^0, 90^0)$, $(90^0, 270^0)$ and $(270^0, 360^0)$

= - 60 [dB] for all other ϕ.

A n value range of $2.0 \le n \le 2.7$ is suggested to obtain patterns of practical interest.

10) *Function 10*: The pattern generated by this function is shown in Figure 33. The equation which describes this pattern on the elevation plane is given as:

$G_{EL}(\theta) = 20 \log_{10} | \sin(n \sin\theta) |$ [dB] for $\theta \in (0^0, 180^0)$ and $(180^0, 360^0)$

= - 60 [dB] for all other θ.

A n value range of $2.0 \le n \le 2.7$ is suggested to obtain patterns of practical interest.

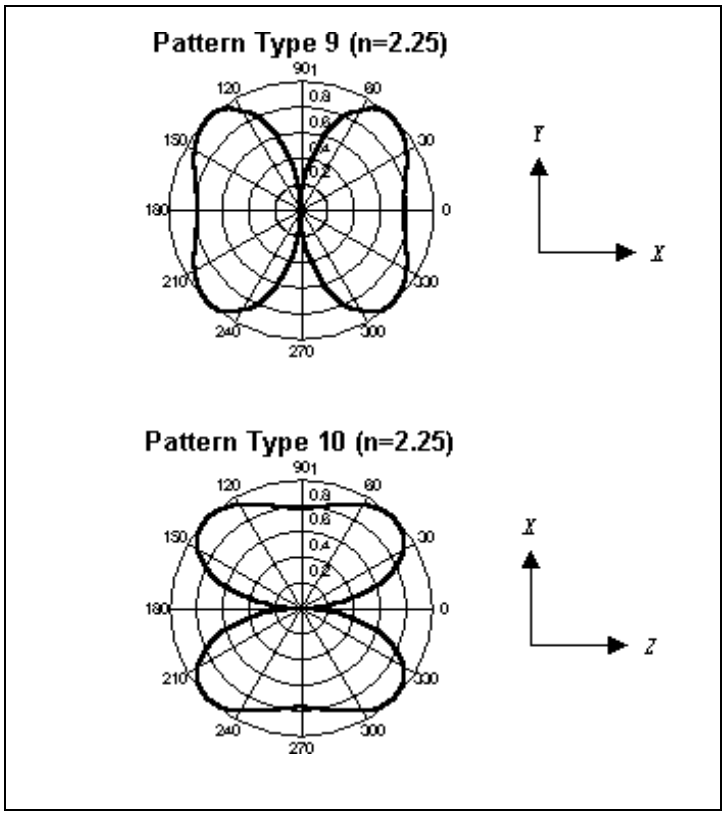

Figure 33. *Polar plots of patterns generated by functions 9 and 10.*

11) *Function 11*: The pattern generated by this function is shown in Figure 34. The equation which describes this pattern on the azimuth plane is given as:

$G_{AZ}(\phi)$ =- 60 [dB] when $|\cos(n\sin\phi)| < 0.001$

= 20 $\log_{10}$ $|\cos(n\sin\phi)|$ [dB] otherwise, for $\phi \in [0^0, 360^0)$.

A n value range of $1.0 \le n \le 2.0$ is suggested to obtain patterns of practical interest.

12) *Function 12*: The pattern generated by this function is shown in Figure 34. The equation which describes this pattern on the elevation plane is given as:

$G_{EL}(\theta)$ = - 60 [dB] when $|\cos(n\cos\theta)| < 0.001$.

= 20 $\log_{10}$ $|\cos(n\cos\theta)|$ [dB] otherwise, for $\theta \in [0^0, 360^0)$.

A n value range of $1.0 \le n \le 2.0$ is suggested to obtain patterns of practical interest.

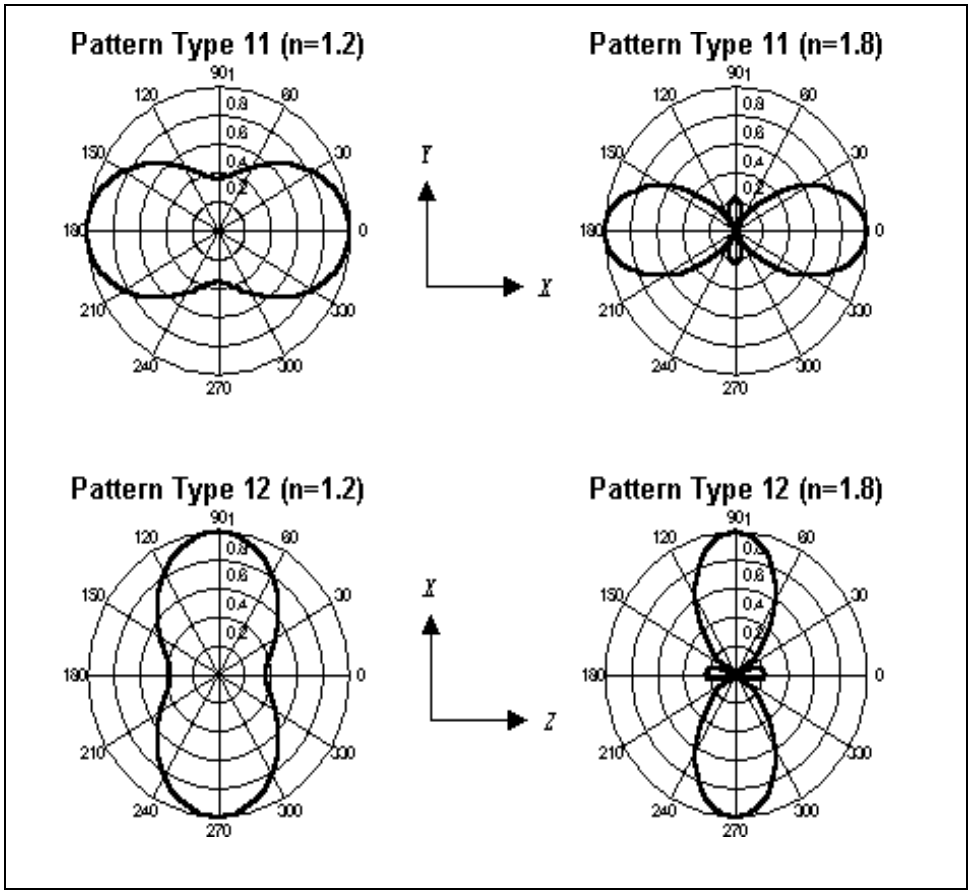

Figure 34. *Polar plots of patterns generated by functions 11 and 12.*

13) ***The bidirectional cosine function*****:** The equation for the azimuth plane is as follows:

$G_{AZ}(\phi) = 20 \log_{10} |\cos^n(\phi)|$ [dB] for $\phi \in [0^0, 90^0)$, (90,270) and $(270^0, 360^0)$.

$= -60$ [dB] for all other ϕ.

A plot of this is shown in Figure 35. The value of *n* is suggested to be between 1 and 5.

14) ***The bidirectional sine function*****:** The equation for the elevation plane is as follows:

$G_{EL}(\theta) = 20 \log_{10} |\sin^n(\theta)|$ [dB] for $\theta \in (0^0, 180^0)$ and $(180^0, 360^0)$

$= -60$ [dB] for all other θ.

A plot of this is shown in Figure 35. The value of *n* is suggested to be between 1 and 5.

To recap, patterns 1, 3, 5, 7, 9, 11 and 13 are to be selected by user as azimuth plane patterns, and patterns 2, 4, 6, 8, 10, 12 and 14 are to be selected as elevation plane patterns.

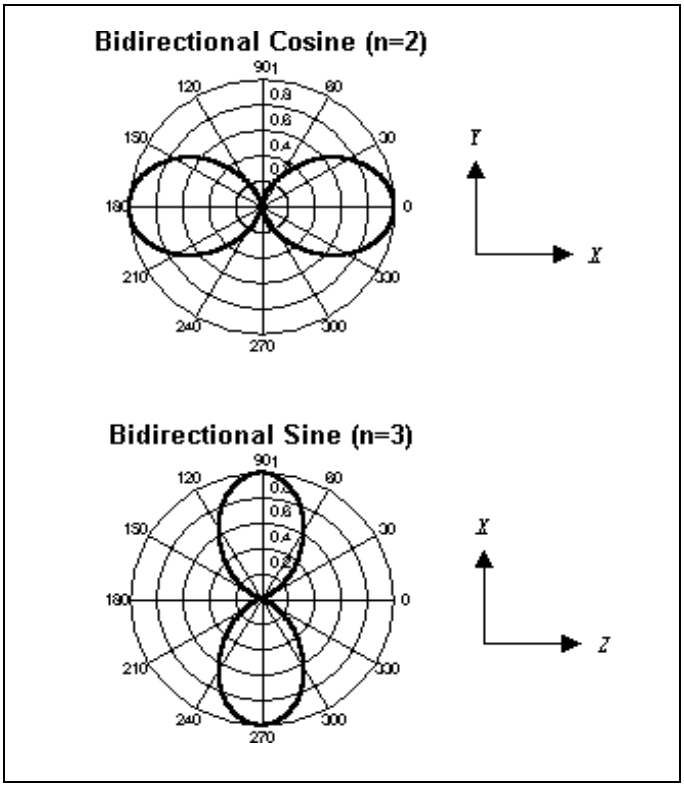

Figure 35. *Polar plots of patterns generated by functions 13 and 14.*

Chapter 5
3D Antenna Patterns

5.0 Overview

This chapter describes the methodology involved in finding the gain of an arbitrarily oriented 3D antenna pattern located on the transmitter plane, as seen by a search point [*X*,*Y*] on the receiver plane. Note that the receiver plane can be at a different height than the transmitting plane. Thus, the user obtains the coverage contour on the receiver plane in 2D corresponding to a 3D antenna pattern. The chapter has the following four main sections. Section 5.1 describes homogeneous coordinate transformations. This technique allows one to obtain (θ, ϕ) on the transmitting plane as seen by a corresponding point [*X*,*Y*] on the receiver plane. This is followed by section 5.2 which explains the steps involved in obtaining $G_T(\theta, \phi)$ for each pattern type. Section 5.3 provides an introduction to interpolation. Interpolation techniques are employed by "Other pattern types" and "User provided pattern types". Here, the user selects two 2D patterns, one for the azimuth plane and one for the elevation plane. He also decides the orientation of the final 3D pattern that would be obtained by interpolating the two chosen 2D patterns. The section also introduces the reader to some relevant terms from computer vision and computer graphics. Finally, section 5.4 describes in detail the interpolation algorithm for SMT 7.0. The results obtained in section 5.1 form a starting point for the interpolation algorithm. The algorithm essentially returns $G_T(\theta, \phi)$ given the two 2D patterns the user has chosen. This section also makes a passing mention to various interpolation techniques that were considered to convert two dimensional patterns into three dimensional ones.

5.1 Homogeneous Coordinate Transformations

As stated above, homogeneous coordinate transformation allows one to obtain (θ, ϕ) on the transmitting plane as seen by a corresponding point [X,Y] on the receiver plane. The first step to accomplish the same is to define two coordinate systems. This is explained in Step 1 below. We define one coordinate system for the receiver plane and one for the transmitter plane. The receiver plane is the plane where the coverage contour calculations are taking place and communication feasibility is being determined. The transmitter plane is the one where the transmitting antenna is located. To make the tool generic, SMT 7.0 allows one to have the plane of the receiving antenna to be different than the plane of the transmitting antenna. Also, the 3D pattern for the antenna on the transmitting plane can be arbitrarily oriented in SMT 7.0 from its boresight which is the positive X_A axis. Hence, the orientation of the coordinate system for the transmitting plane, as shown in Figure 36, can be much different from that of the receiving plane. Finding the relationship between two such coordinate systems involves a transformation matrix and this is explained in Step 2 below. Step 3 defines and explains how the roll, pitch and yaw terms normally used in homogeneous coordinate transformations relate to the azimuth, elevation and slant defined for SMT 7.0. These three angles allow the user to arbitrarily orient the 3D pattern and hence define the position of the transmitting coordinate system. Step 4 explains how the transformation matrix in Step 2 is used to reference one coordinate system with respect to the other. Finally, Step 5 gives the equation for obtaining (θ, ϕ) as seen by the receiver plane for a search point [X,Y] on its plane.

STEP 1: Defining the coordinate systems for transmitting and receiving planes

Define two coordinate systems, one for the transmitting antenna, the other for the receiver. The former will be called *ACS* to denote the *A*ntenna *C*oordinate *S*ystem and the later will be called *RCS* to denote *R*eceiver *C*oordinate *S*ystem. Figure 36 depicts these two coordinate systems. Note that the origin for the RCS is shown right under ACS. This is attributed to the way the search algorithm for coverage contour calculation works

in SMT 7.0 and other SMT versions. The search always starts from the origin out for a given transmitting antenna whose coverage is to be determined [see section 3.8].

The coordinate axes for the ACS will be denoted by (X_A, Y_A, Z_A). Similarly the coordinate axes for RCS will be denoted by (X_R, Y_R, Z_R). O_A and O_R are the respective origins. Note that O_A lies on the Z_R axis, at location $[0, 0, Z_{DIFF}]^T$ in RCS coordinates. Z_{DIFF} denotes the difference in height between the two planes. Note that even though the ACS is shown above the RCS, this need not always be the case as coverage calculations can be carried out even when the receiver plane is the same or above the transmitter plane for a given floor.

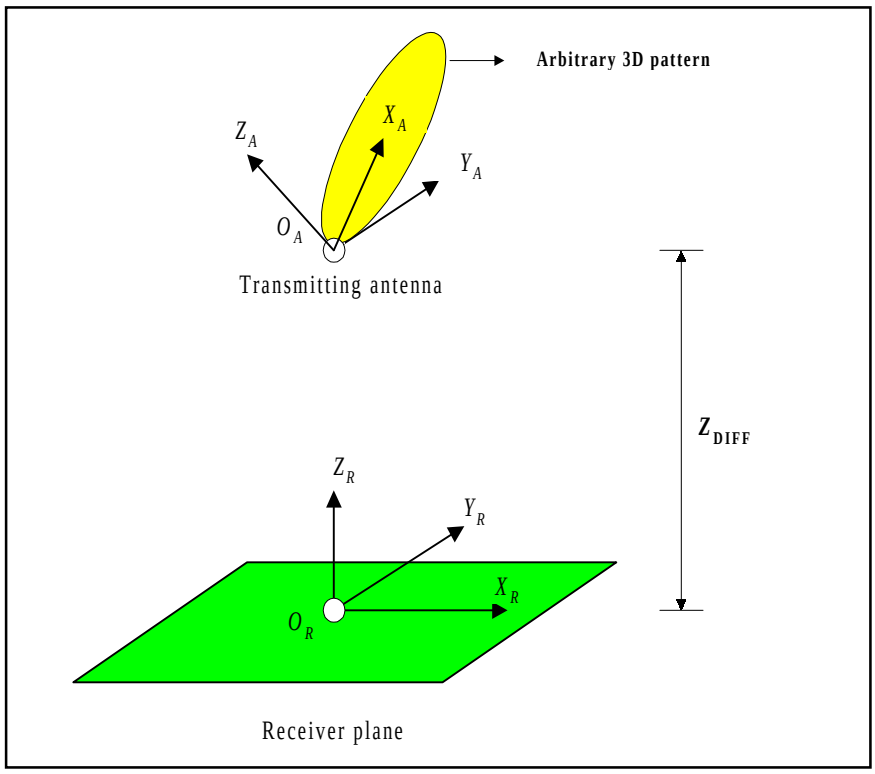

Figure 36. *The relationship between ACS and RCS. The search for the coverage contour takes place on the receiver plane.*

STEP 2: Defining the transformation matrix for ACS [Nagy87] [Crai86].

This step defines a transformation matrix which will be used later in step 4 to describe the relationship between ACS and RCS. Using rigid transformations, one can obtain the relationship of an object attached to coordinate system as a translated and rotated version of the other. Such transformations are widely used in robotics, so lets us now take a detour to robotics! In robotics, rotation is stated in terms of a set of angles: (α_A, β_A, γ_A) called *Euler angles*. In these terms, α_A can be called *roll*, β_A can be called *pitch*, and γ_A called *yaw*. α_A is commonly defined to represent rotation about the Z_A axis, β_A to the rotation about the new Y_A axis, and γ_A to rotation about the newest X_A axis. The rotations conform to a RHCS (Right Hand Coordinate System). There is a transformation matrix associated with each rotation. We will call the transformation matrix associated with the rotation α_A as $[R_\alpha]$. Similarly the transformation matrix associated with the rotation β_A will be called $[R_\beta]$ and the one associated with γ_A will be called $[R_\gamma]$. Note that the sequence of rotations is important as the multiplication of rotation matrices is *not* commutative. Also note that by performing *three successive rotations in proper sequence* it is possible to reach *any* orientation. There are many valid rotation sequences possible, but we will use the roll-pitch-yaw sequence to define the *rotation matrix*. As described later, this rotation matrix will be used to describe the rotations performed on the 3D pattern associated with the ACS. The roll-pitch-yaw sequence is the most comprehensive robotics convention, as all three rotations in their positions are involved.

The transformation matrices are given by:

$$\mathbf{[R_\alpha]} = \begin{bmatrix} \cos\alpha_A & -\sin\alpha_A & 0 \\ \sin\alpha_A & \cos\alpha_A & 0 \\ 0 & 0 & 1 \end{bmatrix} \qquad \mathbf{[R_\beta]} = \begin{bmatrix} \cos\beta_A & 0 & \sin\beta_A \\ 0 & 1 & 0 \\ -\sin\beta_A & 0 & \cos\beta_A \end{bmatrix}$$

$$\mathbf{[R_\gamma]} = \begin{bmatrix} 1 & 0 & 0 \\ 0 & \cos\gamma_A & -\sin\gamma_A \\ 0 & \sin\gamma_A & \cos\gamma_A \end{bmatrix}$$

The matrix product which gives the rotation matrix for ACS is given by:

$[R_{\alpha\beta\gamma}] = [R_\alpha]\,[R_\beta]\,[R_\gamma] =$

$$\begin{bmatrix} \cos\alpha_A \cos\beta_A & \cos\alpha_A \sin\beta_A \sin\gamma_A - \sin\alpha_A \cos\gamma_A & \cos\alpha_A \sin\beta_A \cos\gamma_A + \sin\alpha_A \sin\gamma_A \\ \sin\alpha_A \cos\beta_A & \sin\alpha_A \sin\beta_A \sin\gamma_A + \cos\alpha_A \cos\gamma_A & \sin\alpha_A \sin\beta_A \cos\gamma_A - \cos\alpha_A \sin\gamma_A \\ -\sin\beta_A & \sin\gamma_A \cos\beta_A & \cos\beta_A \cos\gamma_A \end{bmatrix} \quad [5.1]$$

Please note that an equation of the form

$$\begin{bmatrix} X_{new} \\ Y_{new} \\ Z_{new} \end{bmatrix} = [R_{\alpha\beta\gamma}] \begin{bmatrix} X_A \\ Y_A \\ Z_A \end{bmatrix}$$

maps a point $[X_A\ Y_A\ Z_A]^T$ from ACS to a new coordinate system. This is shown later in [5.3]. A special roll-pitch-yaw geometry is obtained when the rotation matrix $[R_{\alpha\beta\gamma}]$ becomes degenerate, that is when pitch rotation is equal to $\beta_A = \pm 90^0$. We can restrict to the range of $(-90^0, 90^0)$ since beyond this range no new rotation matrices are obtained. The matrix specified for $(\alpha_A\text{-}90^0, -\beta_A, \gamma_A\text{+}90^0)$ is the same as the $[R_{\alpha\beta\gamma}]$ matrix for positive β_A.

STEP 3: User defined variables.

This step essentially maps the roll, pitch and yaw used in the above step to the requirement for SMT 7.0. It also puts the parameter Z_{DIFF} which we defined in Step 1 in the right context. The "Antenna height and orientation" dialog box is used to input variables related to homogeneous coordinate transformations. The dialog box is shown in Figure 13, Chapter 3. The five variables which the user defines through the dialog box are discussed next. For analysis purposes, the 3D transmitting antenna pattern can be considered to be a rigid object associated with the ACS.

1) Angle variables:

Note that the angles α_A and $-\beta_A$ which we defined as roll and pitch earlier, can be viewed as azimuth and elevation respectively when considering the RCS. We will call angle γ_A as slant instead of yaw. Note that, as described earlier the sequence of rotation expected from the user is (α_A, $-\beta_A$, γ_A). Hence the three angles which define the rotation of the antenna pattern from its default position (boresight along positive X_A axis) are:

- The *azimuth* angle (roll) in degrees (α_A)
- The *elevation* angle (pitch) in degrees ($-\beta_A$)
- The *slant* angle (yaw) in degrees (γ_A)

2) Height variables:

Recollect that in section 3.1.4, we discussed the AutoCAD WCS. This World Coordinate System has its origin at the lower left hand corner of the screen and the building represented such that it has positive X and Y coordinates in the WCS. A two dimensional view of the floor plan is visible on the screen for a particular floor. The Z coordinate used for a particular floor however is the bottom of that floor, with every floor in a multistory building assumed to have ceilings of the same height above the given floor. Therefore, $Z = f \times h$ meters, where f is the floor number starting with 0, and h is the height of the ceiling which by default is 3 meters. This value may be changed with the command "FLOORHT". We can therefore represent the Z coordinate for the antennas as

- (a) Height of transmitting antenna in meters = $Z + h_t = f\,h + h_t$
- (b) Height of the receiving antenna(s) in meters = $Z + h_r = f\,h + h_r$
- The parameters h_t and h_r are input in meters by the user into the dialog box. Both h_t and h_r are less than h. For analysis purposes Z_{DIFF} in Figure 36 represents the value (h_t–h_r). Note that Z_{DIFF} can be positive or negative or zero.

STEP 4 **:** Establishing relationship of ACS with RCS [Nagy87] [Crai86].

Now that we have the transformation matrix for ACS given by equation 1.0 in step 2, we can proceed to establish a relationship with RCS. For this, let us utilize an established generalized equation for relative transformations.

Let the transformation matrix $H_{j,n}$ describe the position and orientation of the nth coordinate system relative to the jth one. Then,

$$H_{j,n} = \prod_{i=j}^{n-1} H_{i,\,i+1} = H_{i,\,i+1} \bullet H_{i+1,\,i+2} \bullet . \ . \ . \ . \ . \bullet H_{n-1,\,n}$$

where j is any integer less than n.

$$\boldsymbol{H_{i,i+1}} = \left[\begin{array}{ccc|c} & \boldsymbol{R_{i,i+1}} & & \boldsymbol{T_{i,i+1}} \\ \hdashline & & & \\ 0 & 0 \ . \ . \ . & 0 & 1 \end{array}\right]$$

The resultant transformation matrix $H_{i,n}$ describing the state of the nth coordinate system relative to any jth component's coordinate frame is the product of sequentially constituted transformations for $j<n$. $T_{i,i+1}$ is the position vector. This position vector describes the translation of the $(i+1)^{th}$ coordinate system with respect to the i^{th} one. With reference to O_R, since $O_A = [0 \ 0 \ Z_{DIFF}]^T$ this describes the position vector in our case. Thus the coordinates of the any target point P_t in the nth coordinate system relative to any ith component's coordinate frame can be expressed as:

$$\boxed{P_t^{(i)} = H_{i,n} \bullet P_t^{(n)}} \qquad [5.2]$$

Plugging in values, we can rewrite equation 5.2 as follows:

$$\begin{bmatrix} X_R \\ Y_R \\ Z_R \\ 1 \end{bmatrix} = \begin{bmatrix} R_{11} & R_{12} & R_{13} & 0 \\ R_{21} & R_{22} & R_{23} & 0 \\ R_{31} & R_{32} & R_{33} & Z_{DIFF} \\ 0 & 0 & 0 & 1 \end{bmatrix} \begin{bmatrix} X_A \\ Y_A \\ Z_A \\ 1 \end{bmatrix} \qquad [5.3]$$

Here R_{ij} denotes the corresponding elements of $[R_{\alpha\beta\gamma}]$ from equation [5.1].

***STEP 5*:** Stating the relationship between ACS and RCS.

The expression in equation 5.3 can be rewritten as

$$X_R = (R_{11})\, X_A + (R_{12})\, Y_A + (R_{13})\, Z_A$$
$$Y_R = (R_{21})\, X_A + (R_{22})\, Y_A + (R_{23})\, Z_A$$
$$Z_R = (R_{31})\, X_A + (R_{32})\, Y_A + (R_{33})\, Z_A + Z_{DIFF}$$

However, the SMT 7.0 search for communication feasibility is *only* on the X_R-Y_R receiver plane. Hence, $Z_R = 0$. Further, we are interested in knowing the coordinate values for the ACS for every search point in the RCS plane. Therefore we will rewrite the above equations as follows:

$$\begin{bmatrix} X_A \\ Y_A \\ Z_A \end{bmatrix} = \left[R_{\alpha\beta\gamma}{}^{-1}\right] \bullet \begin{bmatrix} X_R \\ Y_R \\ -Z_{DIFF} \end{bmatrix} \qquad [5.4]$$

But the rotation matrix has the property of orthogonality. Therefore,

$$X_A = (R_{11})\, X_R + (R_{21})\, Y_R - (R_{31})\, Z_{DIFF}$$
$$Y_A = (R_{12})\, X_R + (R_{22})\, Y_R - (R_{32})\, Z_{DIFF}$$
$$Z_A = (R_{13})\, X_R + (R_{23})\, Y_R - (R_{33})\, Z_{DIFF} \qquad [5.5]$$

***STEP 6*:** Calculating θ_0 and ϕ_0.

Let θ_0 and ϕ_0 denote the elevation and azimuth values [section 4.2.3] of any arbitrary point (X_A, Y_A, Z_A). These values will be used later by the interpolation algorithm to return the morphed gain for the 3D pattern.

The θ_0 and ϕ_0 values are as given below:

$$\theta_0 = \tan^{-1}\left(\frac{\sqrt{X_A^2 + Y_A^2}}{Z_A}\right)$$

$$\phi_0 = \tan^{-1}\left(\frac{Y_A}{Z_A}\right) \qquad [5.6]$$

Note that the values of θ_0 and ϕ_0 can also be expressed in terms of sine and cosine values. However it is important to use the atan2 function provided in the C programming environment for the following reasons:

1. Accuracy is maintained for the whole range over (-180^0, 180^0), specifically under situations when the Z_A value is close to zero and the situation of undefined sine, and cosine values does not arise.
2. The atan2 function however becomes undefined when both arguments are zero and programming language libraries handle such a situation of domain error via definitions in its errno.h file. However the SMT program search always starts and continues in the far field region and this case is not encountered.

Example of homogeneous coordinate transformation for SMT 7.0

- Let the transmitting antenna be at height of 2 meters above the first floor. Let the omnidirectional receiver on that floor be located at a height of 1.5 meters above the floor. Therefore, Z_{DIFF} = 2-1.5 = 0.5 (see Step 3).
- Assume the transmitting antenna to be oriented with an azimuth = 30^0, elevation=-60^0 and slant=0^0. Since the rotations are in the sequence of azimuth, elevation, slant and confirm to the RHCS, the transmitting antenna would be oriented as shown in Figure 36. Therefore, (α_A, β_A, γ_A) = (30^0, -60^0, 0^0).
- From equation 5.1, the transformation matrix associated with this orientation is given by

  $[R_{\alpha\beta\gamma}] = [R_\alpha]\,[R_\beta]\,[R_\gamma] =$

$$\begin{bmatrix} \cos 30\cos(-60) & \cos 30\sin(-60)\sin 0 - \sin 30\cos 0 & \cos 30\sin(-60)\cos 0 + \sin 30\sin 0 \\ \sin 30\cos(-60) & \sin(30)\sin(-60)\sin 0 + \cos 30\cos 0 & \sin 30\sin(-60)\cos 0 - \cos 30\sin 0 \\ -\sin(-60) & \sin 0\cos(-60) & \cos(-60)\cos 0 \end{bmatrix}$$

$$= \begin{bmatrix} 0.433 & -0.5 & -0.75 \\ 0.25 & 0.866 & -0.433 \\ 0.866 & 0 & 0.5 \end{bmatrix}$$

- Assume a value for a search point on the receiver plane. Say $(X_R, Y_R) = (10, 3)$
- Hence, from equation 5.5, (X_A, Y_A, Z_A) is given by (4.647, -2.402, -9.049).
- Form equation 5.6 we have the value of $(\theta_0, \phi_0) = (150^0, 14.86^0)$. Thus, the point on the receiver plane sees a point with the above angle (per spherical coordinate system) on the transmitter plane whose gain is to be calculated.

5.2 Obtaining $G_T(\theta, \phi)$ for Each Pattern Type

Section 5.2.1 basically provides a recap of essential details for all pattern types supported in SMT 7.0. Sections 5.2.2, 5.2.3, 5.2.4 provide a high level description of the steps involved in obtaining $G_T(\theta, \phi)$ for omnidirectional patterns, user provided patterns and other directional patterns. Section 5.4 exclusively deals with the interpolation algorithm. This algorithm explains in detail the mathematics involved in obtaining the $G_M(\theta, \phi)$ part of the $G_T(\theta, \phi)$ equation.

5.2.1 Recap of Essential Details

1. There are three pattern types, omnidirectional patterns, other directional patterns and user provided patterns. Recall from chapter 4 that the gain parameter for these pattern types can be described by the following equations:

$G_T(\theta, \phi)$ [dB] = $G_{AZ}(\phi)$ [dB] + 20 $\log_{10}$ | $G_{EL}(\theta)$ | [dB] for omnidirectional patterns,

$G_T(\theta, \phi)$ [dB] = G_B [dB] + 10 $\log_{10}$ | $G_M(\theta, \phi)$ | [dB] for user provided patterns, and

$G_T(\theta, \phi)$ [dB] = G_B [dB] + 20 $\log_{10}$ | $G_M(\theta, \phi)$ | [dB] for other directional patterns.

2. As explained earlier, to uniquely determine a point in 3D, for the spherical coordinate system, the $\phi \in [0^0, 360^0)$, $\theta \in [0^0, 180^0]$ range is sufficient. However, the principal plane patterns for both "user provided patterns" and "other pattern types" have been defined for the range $[0^0, 360^0]$. This is because in practice, all 2D cuts are specified for the range $[0^0, 360^0]$. Checks will have to be introduced in software while using these patterns to depict elevation plane patterns.
3. $G_{EL}(\theta)$ for omnidirectional patterns is a closed form equation with gain values varying between 1 (0 dB) and 0 ($\cong$ -60 dB). The value of $G_{AZ}(\phi)$ for omnidirectional patterns is a constant and varies based on the omnidirectional pattern type.
4. For other directional patterns, both $G_{EL}(\theta)$ and $G_{AZ}(\phi)$ which are used to obtain the interpolated value $G_M(\theta, \phi)$ are closed form equations with gain values varying between 0 dB to -60 dB. G_B, the gain in the boresight direction, is a user configurable parameter which simply scales the normalized value of $G_M(\theta, \phi)$.
5. For user provided patterns, the value of G_B is *not* user provided. The dB values input for the principal patterns are normalized to obtain G_B. Also, the normalized gain values of the principal plane patterns $G_{EL}(\theta)$ and $G_{AZ}(\phi)$, are used to obtain $G_M(\theta, \phi)$.
6. The initial position of the 3D pattern is assumed to have its boresight in the direction of the positive X_A axis. The user is required to keep this in mind before orienting the pattern by changing the azimuth, elevation and slant via the "Antenna Height and Orientation" dialog box.
7. Omnidirectional patterns do not require interpolation as the azimuth plane gain is a constant (circle). However, for the other two pattern types, to reconstruct the 3D pattern with reasonable accuracy, it is sufficient to use the pattern information for the (X_A - Y_A) plane and the (X_A - Z_A) plane. This is because, nearly all radiation from the antenna is concentrated in the these two principal planes which includes the boresight direction. The (Y_A - Z_A) plane information will not be used. This is in line with our assumption that the default boresight direction is the positive X_A axis. Since (Y_A - Z_A)

plane is not used the elevation plane now specifically refers to the (X_A - Z_A) plane. As described before, (X_A - Y_A) plane is still the azimuth plane.

5.2.2 Obtaining $G_T(\theta, \phi)$ for Omnidirectional Patterns

Objective: Obtain $G_T(\theta, \phi)$ for the 3D antenna pattern attached to the ACS for every search point on the receiver plane described by a set of (X_R, Y_R) coordinates.

1. For every search point on receiver plane, given the above coordinates and the three rotation angles, use the transformation matrix (use equation 5.6) to obtain the value of θ_0 on the transmitter plane.
2. Plug this value of θ_0 into the closed form equation for the elevation plane pattern of the user selected omnidirectional pattern.
3. Convert the normalized gain value into dB (0 to -60 dB) and add this value to the constant $G_{AZ}(\phi_0)$ [dB] for the chosen pattern to obtain $G_T(\theta_0, \phi_0)$.

5.2.3 Obtaining $G_T(\theta, \phi)$ for User Provided Patterns

Objective: Obtain $G_T(\theta, \phi)$ for the 3D antenna pattern attached to the ACS for every search point on the receiver plane described by a set of (X_R, Y_R) coordinates.

1. For every search point on receiver plane, given the above coordinates and the three rotation angles, use the transformation matrix (use equation 5.6) to obtain the value of θ_0 and ϕ_0 on the transmitter plane.
2. Find G_B [dB] and store this value separately. This value will then be used in step 5. Store the user provided pattern information in a normalized voltage table form. Normalizing is done by converting the dB values to voltage, finding the maximum value and dividing each entry by this value. Make 360 entries in the table for both azimuth and elevation pattern data. This indicates a 1^0 increment user data, immaterial of whether the data was provided by user in 5^0, 4^0, 3^0, 2^0 or 1^0 increments.

2D linear interpolation is used to generate 360 entries for azimuth and 360 entries for elevation from the provided user data. This can be mathematically explained as follows: Let e_i denote the entries in the user provided table (if the table has 73 entries then i =1, 2,…73). Let k denote the angle increment for the table (if the table has 73 entries it means that data is provided in 5^0 increments. Hence, k is 5). Then we define $\Delta_i = (e_{i+1} - e_i) / k$. Each Δ_i is then used to construct a set of k entries for the final table. If f_j, j = 0, 2,3, …359 denotes the final 360 entries for the table, then [f_0 f_1 f_2 f_3 f_4] corresponding to Δ_1 is given by [e_1 $e_1+\Delta_1$ $e_1+2\Delta_1$ $e_1+3\Delta_1$ $e_1+4\Delta_1$] and so on.

3. For the values of θ_0 and ϕ_0 obtained in step 1, find the right value of normalized gain in the elevation and azimuth plane respectively.
4. Use the 3D interpolation algorithm in section 5.4.3 to find gain value for (θ_0 , ϕ_0).
5. Convert the normalized gain value into dB (0 to -60 dB) to obtain $G_M(\theta_0, \phi_0)$, and add this value to the constant G_B [dB] for the chosen pattern to obtain $G_T(\theta_0, \phi_0)$.

5.2.4 Obtaining $G_T(\theta, \phi)$ for Other Directional Patterns

Objective: Obtain $G_T(\theta, \phi)$ for the 3D antenna pattern attached to the ACS for every search point on the receiver plane described by a set of (X_R, Y_R) coordinates.

1. For every search point on receiver plane, given the above coordinates and the three rotation angles, use the transformation matrix (use equation 5.6) to obtain the value of θ_0 and ϕ_0 on the transmitter plane.
2. Plug the values of θ_0 and ϕ_0 into the corresponding closed form principal plane equations to obtain the normalized gain values.
3. Use the 3D interpolation algorithm in section 5.4.3 to find gain value for (θ_0, ϕ_0).
4. Convert the normalized gain value into dB to obtain $G_M(\theta_0, \phi_0)$, and add this value to the constant, user configurable G_B [dB] for the chosen pattern, to obtain $G_T(\theta_0, \phi_0)$.

5.3 Introduction to Interpolation

This section describes the areas which were considered to find an interpolation technique for the SMT 7.0. Areas of computer graphics, computer vision and solid computational geometry were researched in an attempt to find useful techniques to describe surfaces. The section below gives a brief overview of surface-modeling systems. These systems describe methods of representing 3D objects. Of the available methods, the one applicable to our situation is chosen.

5.3.1 Surface-modeling Systems

There are an infinite number of different 2D patterns that correspond to the same 3D object. To make a 3D object unique for given 2D information, a wide variety of techniques are employed by surface-modeling systems. These techniques may be broadly classified into two types: 1) Surface-modeling by employing surface patches and 2) surface-modeling by employing sweep operations. Sections 5.3.2 and 5.2.3 briefly describe both these techniques.

5.3.2 Surface Patches

Curved surfaces may be approximated by a variety of surface patches. Some popular patches with practical applications are described below.

One method is to approximate a curved surface by small planar facets. These facets are often triangular and linear interpolation techniques may be readily employed. One example is generation of fractal surfaces. Fractal surfaces are not smooth and hence Euclidean-geometry methods cannot be employed. These surfaces are first approximated by mesh of triangles. A recursive method is then employed to randomly break down each triangle into smaller number of triangles until a microstructure of tiny irregular facets are produced. Topographic surfaces can be represented by sampling and interpolation. One common technique is to record elevation of arbitrary points employ a

triangulation procedure to construct a mesh of planar facets known as TIN (Triangulated Irregular Network).

Another approach is to approximate the surface by a mesh of quadrilaterals instead of triangles. Since the vertices of the quadrilateral are coplanar, a related representation can be used if the vertices do not lie on the same plane. In that case, a linear interpolation between them will produce a bilinear curved surface. A generalization of the bilinear patch is a patch bounded by four arbitrary curves and called the Coons patch. This is commonly used by boat and aircraft designers. A specialization of the Coons patch is the bicubic patch which has parameteric cubic polynomials as the four boundary curves. Another type of patch called the Bezier patch is often used by CAD systems for design of automobile bodies. NURBS is another curved surfaced modeler with practical applications. NURBS (Non-Uniform Rational B-spline) is a particular type of a surface called B-spline surface. A particular concern in using the above patches however is maintaining a smooth curvature.

5.3.3 Sweep Operations

As we will see, surface-modeling by sweep operations is quite an attractive method for modeling 3D antenna patterns. The next paragraph briefly explains the various types of sweep operations.

One way to look at a straight line is that of a path swept out by a translated point. Similarly, a rectangular surface may be regarded as a shape swept out by a translated straight line. More generally, we can specify assemblages of surfaces by sweeping arbitrary chains of lines. Such a translational sweep operation for surface insertion, is a powerful technique employed by surface-modeling systems. In addition to translation, surface-modeling systems also provide rotational sweep operations. Translational and rotational sweep operations are the essence of surface-modeling systems employing sweep operations.

A good example of above operations is an open ended cylinder. Such a cylinder may be constructed by sweeping a circle, but can also be produced by sweeping straight lines. This brings us to a very popular representation of solids bounded by curved surfaces, termed *generalized cylinders*. A generalized cylinder is the solid obtained by sweeping a planar region, its cross-section, along a space curve, its axis, or spine [Ponc89]. The cross-section is not necessarily circular, or even constant; its deformation is governed by the sweeping rule. A special class of generalized cylinders is obtained by scaling an arbitrary cross section along a straight axis. These are called SHGC (Straight Homogeneous Generalized Cylinders). As seen in section 5.4, SMT 7.0 models 3D antenna patterns as a SHGC in cases where the patterns have no side lobes. Instances of patterns having sides lobes can be considered to be modeled as an extension of the SHGC concept. Another popular representation of solids bounded by curved surfaces are generalized cones. An example of generalized cone operation is defining a complex surface like a human limb by sweeping arbitrary changing curves along arbitrary curves.

5.3.4 Terms from Computer Graphics

Even though the process of using two principal plane antenna patterns to find the pattern gain at any 3D point is essentially interpolation, it is interesting to recognize related term definitions as used in computer graphics. The two commonly used terms are Morphing and Tweening [Scot93].

Morphing A vaguely sinister term and actually a shortened version of metamorphosis, it refers to a sequence of smooth changes between two different images. Technically, morphing combines a *warp* and a *dissolve*. Warping is essentially a technique of stretching or squashing an image. Dissolving is essentially *tweening* in steps. The process involves fading out an image while fading in another.

Tweening It is a silly shorthand for in-be*tweening*. It refers to a series of images that connect two other images. Mathematically this is interpolation. The simplest form of interpolation would be linear interpolation. This is commonly used for similar images. However the interpolation technique may not be linear to do perform morphing. In this case the warping and dissolving algorithm would utilize non-linear interpolation techniques.

5.4 Interpolation Technique for the SMT 7.0

Section 5.4.1 describes the interpolation approach for SMT 7.0. Section 5.4.2 mentions the other techniques which were tried and their drawbacks. This section also covers some drawbacks of the chosen approach. Section 5.4.3 explains the interpolation technique in detail by breaking it down into steps, and mathematically describing each step.

5.4.1 Interpolation Approach

The 3D antenna gain is modeled as an infinite number of ellipses that are centered on the X_A axis. This can be viewed as an instance of SHGC or the extension of the SHGC concept, (depending on whether the patterns modeled have side lobes or not) by viewing it as an elliptical cross section being scaled along a straight axis (X_A). The major and minor axes of the ellipse are parallel to the Y_A and Z_A axes respectively.

The choice of an elliptical cross-section is very appealing for various reasons. Ellipses are well known, and both lines and circles are special cases of an ellipse. Also, a SHGC with elliptical cross section was considered a reasonably accurate representation of a 3D antenna pattern. Note that as stated before, the key assumption is that the positive X_A axis is the boresight direction. Even if a user provided pattern is not

symmetrical with the boresight that is fine with the SMT 7.0, as long as it has its boresight in and around the X_A axis.

5.4.2 Drawbacks of Interpolation Techniques

Other morphing techniques (like Lagrange polynomial, and trignometric functions) were tried, but the interpolation did not match realistic 3D patterns. The Lagrange polynomial as we know is a linear interpolation technique and the simplest. The interpolating function can be simply described as $G_T(\theta, \phi) = [G_{EL}(\theta) \times \alpha] + [G_{AZ}(\phi) \times (1-\alpha)]$ [dB] with α varying between 1 and 0. The use of simple trignometric functions in sine and cosine to represent interpolation, also yielded poor results. The polar plots of 2D planes obtained by using the above interpolation techniques was impractical. The primary reason for failure of these techniques is due to lack of a reference plane for interpolation.

Even the approach presently employed by the SMT 7.0 is not without drawbacks. Patterns with multiple major lobes will not be realistically modeled. Also, this is not a practical approach to model YAGI antenna patterns. However, YAGI antennas are not typically used in the indoor environment. YAGI antennas are outdoor antennas with very high gain in the boresight direction. The technique employed to produce very high gain in the boresight, leads to generation of many unnecessary side lobes which will not get properly modeled by the approach chosen for SMT 7.0.

5.4.3 Interpolation Process

Given

1. For the (X_A - Z_A) plane, $G_{EL}(\theta) \in [0, 1]$ for $\theta \in [0^0, 360^0)$.
2. For the (X_A - Y_A) plane, $G_{AZ}(\phi) \in [0, 1]$ for $\phi \in [0^0, 360^0)$.

3. For a specific search point on the receiver plane given by $[X_R, Y_R]$, let $P_0=(X_A, Y_A, Z_A)$ denote the point with reference to ACS. In spherical coordinates this will be represented by $P_0=(r_0, \theta_0, \phi_0)$. $G_M(\theta_0, \phi_0)$ represents the interpolated gain corresponding to P_0.

Required

Find $G_M(\theta_0, \phi_0) \in [0, 1]$ given the above information. Let us define $Q_0=(r, \theta_0, \phi_0)$ to describe the point for which $G_M(\theta_0, \phi_0)$ is to be computed. As we will see later, one of the key things the algorithm accomplishes is finding the right Q_0 within a unit sphere for any given P_0. Figure 37 is an illustration of the interpolation approach.

Interpolation Process

A description of various steps which constitute the interpolation process is given below. At the end of this section is a snapshot of the interpolation process which puts all these steps into perspective.

STEP 1: For every $[X_A, Y_A, Z_A]$ obtained by coordinate transformations, find P_0 where θ_0 and ϕ_0 are given by:

$$\theta_0 = \tan^{-1}\left(\frac{\sqrt{X_A^2 + Y_A^2}}{Z_A}\right)$$

$$\phi_0 = \tan^{-1}\left(\frac{Y_A}{Z_A}\right)$$

STEP 2: Ensure that θ_0 and ϕ_0 values are within valid limits.

The software has to check that the value returned for θ_0 and ϕ_0 is within the valid range for θ and ϕ . The C function atan2 returns the value in the range $[-\pi, \pi]$. Therefore, all negative values of ϕ_0 are converted to positive values by adding that negative value to 2π. Thus we have a $\phi_0 \in [0^0, 360^0)$. This coincides with the 2D gain data available for the

range [0^0, 360^0) for user or other pattern for the azimuth plane. However, from step 1 it is clear that the numerator argument for $\tan^{-1}$ to calculate θ_0 is never negative and hence the value of $\theta_0 \in [0^0, 180^0]$. The next step describes how this situation is handled.

STEP 3: Find out the octant $P_0=(r_0, \theta_0, \phi_0)$ belongs to.

As we know, the 2D data for azimuth and elevation cuts are in the range [0^0, 360^0). However, as seen in step 2 we have $\theta_0 \in [0^0, 180^0]$. Therefore, we will have to map certain values of θ_0 to lie in the range (180^0, 360^0). To do so, we look at the value of ϕ_0. If $\phi_0 \in (90^0, 270^0)$ then modify the value of θ_0 to be $(2\pi-\theta_0)$. Any 3D point in the

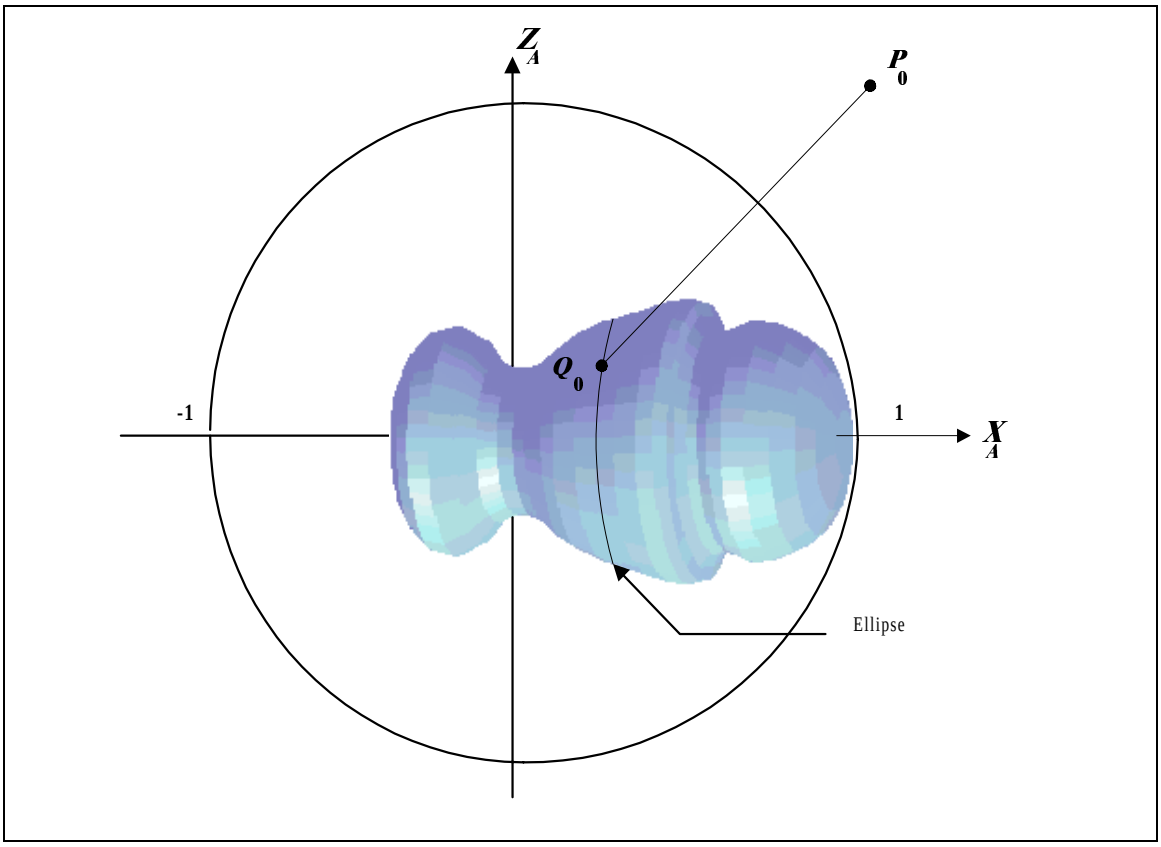

Figure 37. *Side view of a 3D pattern to illustrate the interpolation approach. Q_0 denotes the unique point inside the unit sphere. Q_0 lies on the elliptical gain surface and has coordinates ($G_M(\theta_0, \phi_0)$, θ_0, ϕ_0).*

spherical coordinate system can be described to lie in one of the 8 octants as described by Table 5. The table describes each octant by a set of quadrants for θ and ϕ. These quadrants ensure that the right set of gain values from the range $[0^0, 360^0)$ are selected for a given P_0. Angles for the elevation cut are measured from the positive Z_A axis to the positive X_A axis (boresight direction). Also note that the quadrant ranges do not include angle values like 0^0, 90^0, 180^0 and 270^0. These are treated as special cases by the software and handled separately and explained in step 4.

Table 5. *Octant description for* θ and ϕ ranges.

Octant	**Description**	**θ_0 range in degrees for pattern data**	**ϕ_0 range in degrees for pattern data**
1	+X +Y +Z	$(0^0 \sim 90^0)$	$(0^0 \sim 90^0)$
2	-X +Y +Z	$(270^0 \sim 360^0)$	$(90^0 \sim 180^0)$
3	-X -Y +Z	$(180^0 \sim 270^0)$	$(180^0 \sim 270^0)$
4	+X -Y +Z	$(0^0 \sim 90^0)$	$(270^0 \sim 360^0)$
5	+X +Y -Z	$(90^0 \sim 180^0)$	$(0^0 \sim 90^0)$
6	-X +Y -Z	$(270^0 \sim 360^0)$	$(90^0 \sim 180^0)$
7	-X -Y -Z	$(180^0 \sim 270^0)$	$(180^0 \sim 270^0)$
8	+X -Y -Z	$(90^0 \sim 180^0)$	$(270^0 \sim 360^0)$

STEP 4: Handle special cases.

As seen in the earlier step, θ_0 and ϕ_0 values within the following ranges are treated as special cases: $(89.9^0 \sim 90.1^0)$, $(179.9^0 \sim 180.1^0)$, $(269.9^0 \sim 270.1^0)$, and $(359.9^0 \sim 0.1^0)$. Any value of θ and ϕ within the above range is approximated to 90^0, 180^0, 270^0 and 0^0 respectively. Once this is done, the normalized morphed gain value $G_M(\theta_0, \phi_0)$ for these cases is calculated as follows

- IF $[\theta_0 == (90^0 \,||\, 270^0)$ && $(\phi_0 != 0^0 \,||180^0)]$ $G_M(\theta_0, \phi_0) = G_{AZ}(\phi_0)$.

- ELSE IF $[\phi_0 == (0^0 \| 180^0)]$ $G_M(\theta_0, \phi_0) = G_{EL}(\theta_0)$.
- ELSE IF $[\phi_0 == (90^0 \| 270^0)$ && $(\theta_0 == 0^0 \| 180^0)]$ $G_M(\theta_0, \phi_0) = G_{EL}(\theta_0)$.
- ELSE IF $[\phi_0 == (90^0 \| 270^0)]$ point will be morphed to lie on ellipse.

Note that in dB the value of $G_M(\theta_0, \phi_0)$ is given by $m\log_{10}|\bullet|$ where m = 10 or 20 based on whether the pattern is chosen from the "other" menu or the "user" menu. For any set of θ_0 and ϕ_0 values which are not special cases the algorithm continues with step 5.

STEP 5: Describe point Q_0 defined earlier.

The gain patterns are normalized, hence $-1 \le X_A \le 1$, $-1 \le Y_A \le 1$ for $G_{AZ}(\phi)$ and $-1 \le X_A \le 1$, $-1 \le Z_A \le 1$ for $G_{EL}(\theta)$. The r_0 value for the point P_0 is given by $\sqrt{X_A^2 + Y_A^2 + Z_A^2}$, and is greater than 1 meter, and hence lies outside a unit sphere. Given the normalized value for the patterns, we will have to find a unique $Q_0 = (r, \theta_0, \phi_0)$ such that Q_0 represents the first point to intersect the 3D pattern, within a unit sphere. Note that $|r| \le 1$ and $|r| \cong G_M(\theta_0, \phi_0)$. By intersect, we simply mean that the projection of Q_0 onto the azimuth and elevation patterns on the principal planes must lie within the maximum 2D gain pattern value for that intercept (see Figure 38). The process for finding the same is described at the end of this section which is titled "Snapshot of Interpolation Process".

STEP 6: Obtain a relationship between the elevation plane and azimuth plane.

Since the approach is to model (θ_0,ϕ_0) to lie on an ellipse perpendicular to the X_A axis, let us define the equation for the ellipse. An ellipse on the $(Y_A - Z_A)$ plane is given by: $\frac{Y_A^2}{b^2} + \frac{Z_A^2}{c^2} = 1$, where $2b$ and $2c$ are the lengths of major and minor axes respectively. To obtain the interpolated gain value for every point $Q_0=(r,\theta_0, \phi_0)$, we will need to find b and c in terms of the pattern gain value and angle. Also, note that both the azimuth and elevation patterns share the same X_A value. We will call the unique X_A value corresponding to every (θ_0,ϕ_0) returned by the SMT 7.0 search program described in step

7 as X_{REF}. This X_{REF} defines the relationship between the elevation plane and azimuth plane and hence the right set of θ and ϕ values for a given Q_0. To obtain b, c and X_{REF} we will look at the projection of this point Q_0 onto the azimuth and elevation plane. Let us consider octant 1.

- Projecting onto the azimuth plane, the sides of the triangle in bold in Figure 38a are given by:
  Hypotenuse = $|G_{AZ}(\phi)|$
  Perpendicular = b, the *semi major axis* for the ellipse whose plane is perpendicular to X_A axis.
  Base $X_{REF} = b / \tan(\phi)$ or $|b| = |G_{AZ}(\phi)||\sin(\phi)|$
  Therefore $|X_{REF}| = |G_{AZ}(\phi)||\cos(\phi)|$

- Projecting onto the elevation plane, the sides of the triangle in bold in Figure 38b are given by:
  Hypotenuse = $|G_{EL}(\theta)|$
  Perpendicular = c, the *semi minor axis* for the ellipse whose plane is perpendicular to X_A axis.
  Base $X_{REF} = c / \tan(90^0-\theta)$ or $|c| = |G_{EL}(\theta)||\sin(90^0-\theta)|$
  Therefore, $|X_{REF}| = |G_{EL}(\theta)||\sin(\theta)|$

It turns out that taking the absolute value avoids having different values of b, c and X_{REF} for different octants. Since the software notes down the octant for Q_0 taking absolute values is not a problem. Also, since we expect only the absolute gain value to be returned as the outcome of morphing, taking absolute values speeds up the search algorithm.

The values for $|b|$, $|c|$ and $|X_{REF}|$ for all octants are given in table 6.

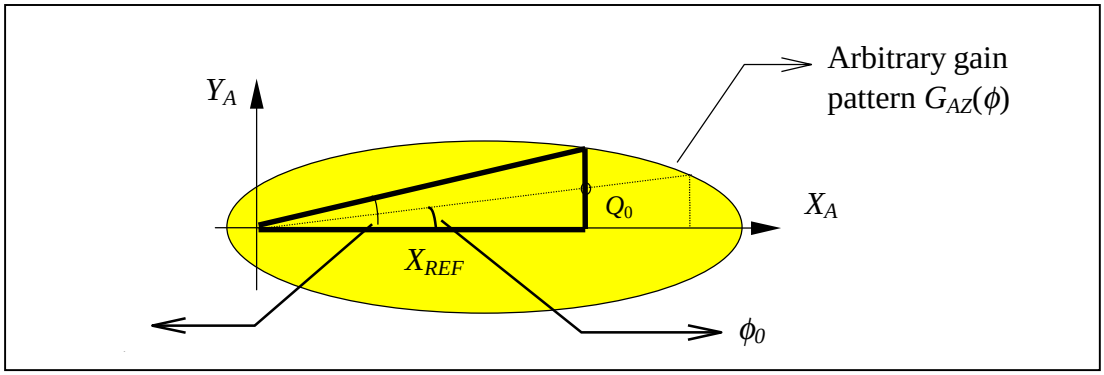

(a)

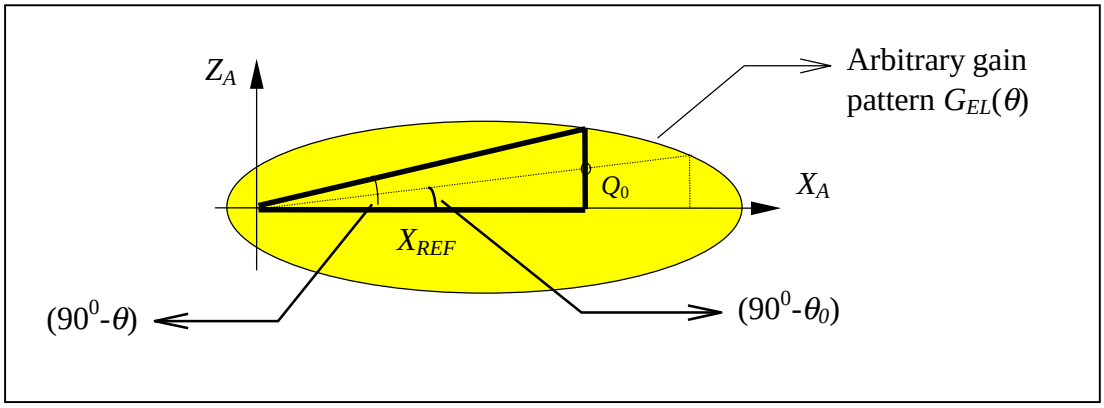

(b)

Figure 38. *(a) indicates the projection of Q_0 onto azimuth plane. (b) indicates the projection of Q_0 onto azimuth plane.*

Table 6. *$|b|$, $|c|$, and $|X_{REF}|$ values in terms of θ and ϕ.*

Octants 1 ~ 8	Value
X_{REF} for azimuth plane	$\lvert G_{AZ}(\phi)\rvert \times \lvert\cos(\phi)\rvert$
b for azimuth plane	$\lvert G_{AZ}(\phi)\rvert \times \lvert\sin(\phi)\rvert$
X_{REF} for elevation plane	$\lvert G_{EL}(\theta)\rvert \times \lvert\sin(\theta)\rvert$
c for elevation plane	$\lvert G_{EL}(\theta)\rvert \times \lvert\cos(\theta)\rvert$

STEP 7: Obtain $G_M(\theta_0, \phi_0)$ for every $Q_0=(\theta_0,\phi_0)$

To obtain the morphed value for gain in dB we first have to find the gain returned by the following equation with b and c values returned by the search algorithm.

$$G = \left| \frac{1}{\sqrt{\left(\frac{\cos^2\theta_0}{b^2}\right)+\left(\frac{\sin^2\theta_0}{c^2}\right)}} \right|$$

$G_M(\theta_0, \phi_0)$ [dB] = $m\log_{10}\sqrt{G^2 + X_{REF}^2}$ gives the gain from the origin which is the required gain. Finally, $G_T(\theta_0, \phi_0)$ [dB] = G_B [dB] + $G_M(\theta_0, \phi_0)$ [dB] gives the antenna gain corresponding to point on the receiver plane.

Algorithm for the Interpolation Process

1. **algorithm** Return_3D_Antenna_Gain (*gain_3d*)

2. User selects two patterns from dialog box (az_pattern and el_pattern) from the menu for "Other directional patterns" or "User provided patterns"

3. **sub-algorithm** Find boresight gain (*gain_bs*)

   if "Other directional pattern" select *gain_bs* from entry in dialog box

   if "User provided pattern"
   calculate *gain_bs* from procedure in section 5.2.3
   normalize user pattern az_pattern data and el_pattern data
   store az_ and el_pattern data in 1^0 increments, interpolate per section 5.2.3

4. **sub-algorithm** Prepare two search tables (ϕ_table and θ_table) in 1^0 increments

   make ϕ_table with columns $|b|$ and $|X_{REF}|$, 356 entries in 1^0 increments
   make θ_table with columns $|c|$ and $|X_{REF}|$, 356 entries in 1^0 increments
   (use table 5 and table 6 to calculate the above)
   store $|b_{max}|$ and $|c_{max}|$ the maximum value of $|b|$ and $|c|$ for each 90 entries
   (there will be four values of $|b_{max}|$ and $|c_{max}|$, one for each quadrant)

5. User selects DISPLAY or SELECT_1 command to initiate contour coverage calculation on the receiver plane.
   Repeat steps 6 to 9 until the contour coverage display is complete

6. **sub-algorithm** Find $P_0(\theta_0,\phi_0)$ for every $[X_R, Y_R]$ on the receiver plane
   $X_R = (R_{11})\ X_A + (R_{12})\ Y_A + (R_{13})\ Z_A$
   $Y_R = (R_{21})\ X_A + (R_{22})\ Y_A + (R_{23})\ Z_A$
   $Z_R = (R_{31})\ X_A + (R_{32})\ Y_A + (R_{33})\ Z_A + Z_{DIFF}$

$$\theta_0 = \tan^{-1}\left(\frac{\sqrt{X_A^2 + Y_A^2}}{Z_A}\right)$$

$$\phi_0 = \tan^{-1}\left(\frac{Y_A}{Z_A}\right)$$

7. **sub-algorithm** Coarse search for a $Q_0(\theta_0, \phi_0)$ for every $P_0(\theta_0,\phi_0)$ obtained above
   This ensures that $Q_0(\theta_0, \phi_0)$ is within extremities of 3D pattern

   if (ϕ_0 || θ_0 == 0^0 || 90^0 || 180^0 || 270^0)
   calculate *gain_morph* per step 4, section 5.4.3
   gain_3d [dB] = *gain_bs* [db] + *gain_morph* [dB]
   end Return_3D_Antenna_Gain

   else if
   $|r| = 1$
   $|Y_A| = |r| \times |\sin\theta_0 \sin\phi_0|,\ |Z_A| = |r| \times |\cos\theta_0|$
   if $|Y_A| \le |b_{max}|$ && $|Z_A| \le |c_{max}|$
   go to step 8 below
   end if
   $|r| = |r| - 0.01$
   repeat else if

8. **sub-algorithm** Fine search for a $Q_0(\theta_0, \phi_0)$
   $|r| = |r| + 0.01$
   do
   $|X_A| = |r| \times |\sin\theta_0 \cos\phi_0|, |Y_A| = |r| \times |\sin\theta_0 \sin\phi_0|,\ |Z_A| = |r| \times |\cos\theta_0|$
   return $|b|$ and $|c|$ for $|X_A| \cong |X_{REF}|$
   if $|Y_A| \le |b|$ && $|Z_A| \le |c|$
   go to step 9
   end if
   $|r| = |r| - 0.01$
   repeat do

9. **Return** *gain_3d* as described in step 7, section 5.4.3
   end Return_3D_Antenna_Gain
   Plug *gain_3d* value into communication feasibility module to obtain coverage contour point

Chapter 6
Operational Examples

6.0 Overview

This chapter provides a few operational examples of SMT 7.0. Section 6.1 describes the process of abstraction done for a warehouse drawing. Section 6.2 provides coverage contour plots for certain types of directional antennas.

6.1 Example of Abstraction

This section provides an example of the process of abstraction explained in section 3.1.5. A warehouse drawing adapted for AutoCAD in shown in Figure 39(a). When the SMT tool was used to predict coverage, inaccurate results were obtained. Later, measurements were taken in the warehouse to find the average attenuation of the signal through various racks. This was done by transmitting a signal of known strength from multiple locations on one side of the rack and measuring the signal on the other side. It was seen that the number of partitions supported by SMT were insufficient to characterize the attenuation characteristics of the racks. Hence the partitions were increased from two to four. The racks were then categorized to be one of the four partition types. Racks were manually replaced by straight lines to prevent the tool from thinking that one rack was multiple partitions. The new drawing after this process of abstraction is shown in figure 39(b). The coverage prediction with this new drawing yielded much more accurate results. This was verified by actual measurements taken. Note that the SMT version at that point did not support 3D patterns.

6.2 Operational Examples

This section gives representative plots, shown in figures 40-48 obtained from three different antenna pattern types supported by SMT 7.0. Note that all plots are

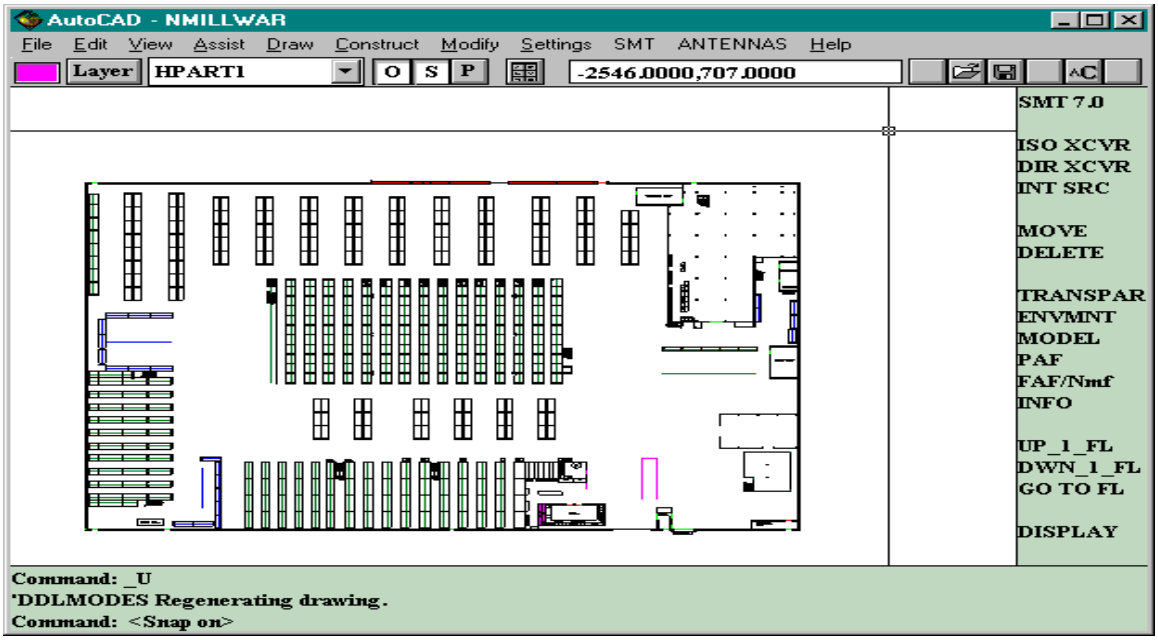

(a)

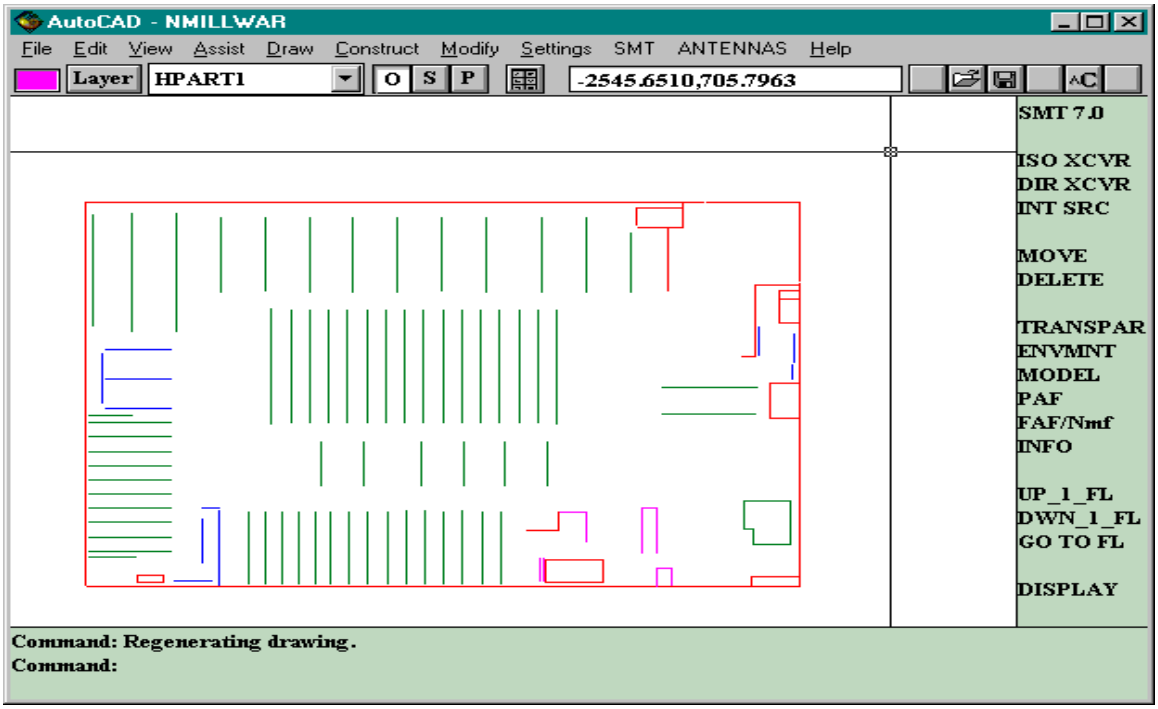

(b)

Figure 39. *The abstraction process. (a) Warehouse floor layout. (b) Result of abstraction process. This was carried out on (a) to increase prediction accuracy.*

drawn with the warehouse drawing in Figure 39 as reference. Also, each figure has a table underneath it explaining the antenna parameters and other key SMT 7.0 parameters chosen for that plot. There are nine example figures, Figures 40 to 48.

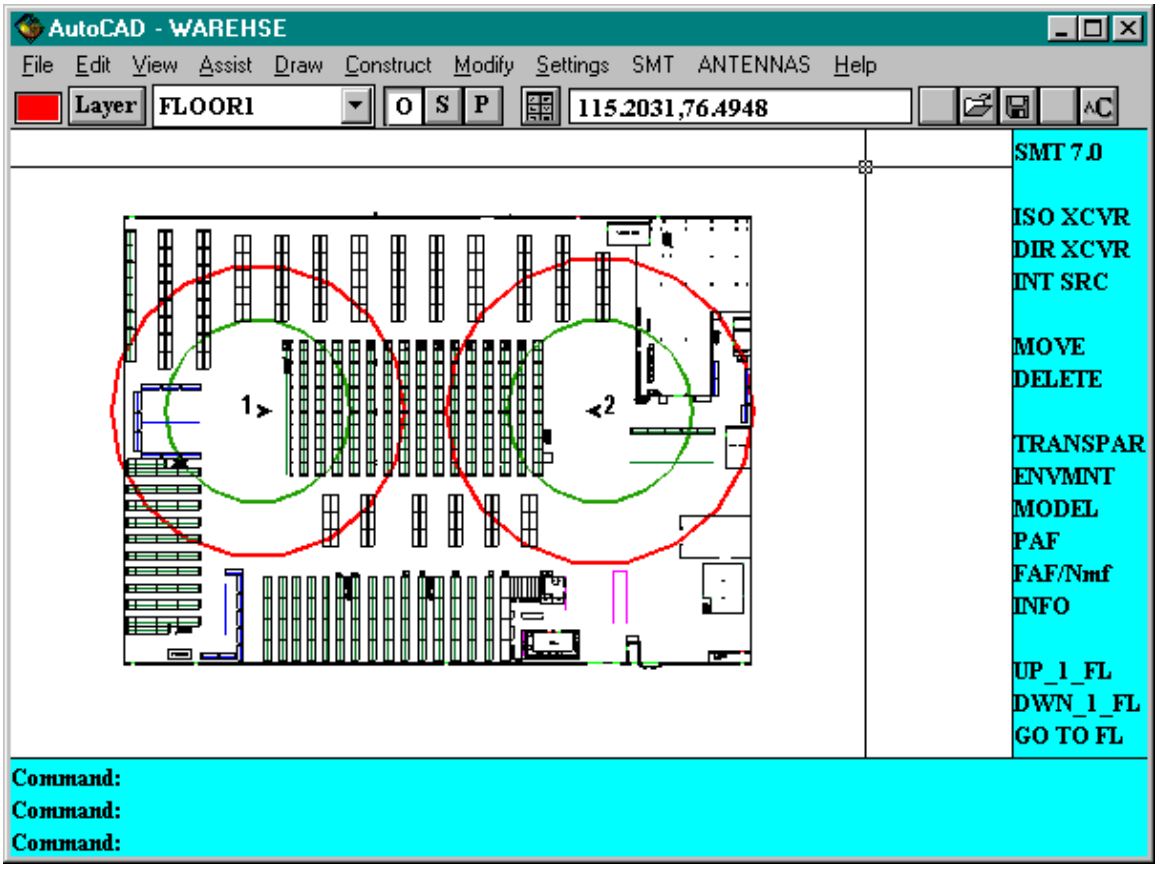

Parameter	Pattern # 1	Pattern # 2
Attenuation model	*n* value (*n* = 2)	*n* value (*n* = 2)
Height of transmitter and receiver in meters	(1.5, 1,3)	(1.5, 1.3)
Orientation of the pattern (azimuth, elevation, slant) in degrees	(0^0, 0^0, 0^0)	(180^0, 0^0, 0^0) (see icon arrow)
Pattern type	Quarterwave dipole	Halfwave dipole

Figure 40. *Example of coverage obtained from two different antenna patterns selected from the "Omnidirectional patterns" menu. The area of coverage obtained from pattern 1 was 1422 m^2 while the one obtained from pattern 2 was 1558 m^2. This is due to the fact that the halfwave dipole (pattern 2) has more directional gain than a quarterwave dipole (pattern 1), all other parameters remaining constant.*

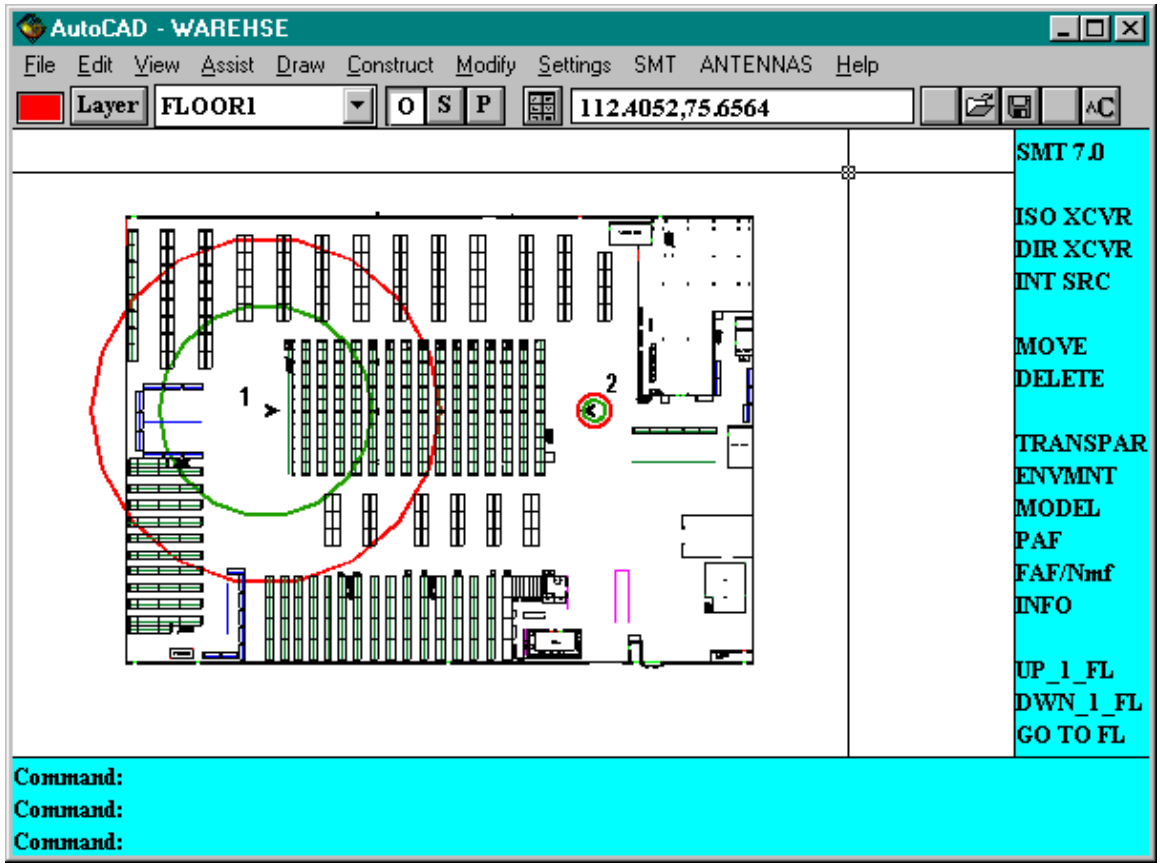

Parameter	Pattern # 1	Pattern # 2
Attenuation model	*n* value (*n* = 2)	*n* value (*n* = 2)
Height of transmitter and receiver in meters	(1.3, 1,5)	(1.5, 1.3)
Orientation of the pattern (azimuth, elevation, slant) in degrees	(0^0, 0^0, 0^0)	(180^0, 0^0, 0^0)
Pattern type	Quarterwave discone	Quarterwave discone

Figure 41. *Example of coverage obtained from a quarterwave discone selected from the "Omnidirectional patterns" menu. Both antennas are identical with respect to the model and pattern, but there is a dramatic difference in the coverage obtained when the heights of the transmitting and receiving antennas are reversed. This is due to the fact that, for the given orientation, the radiation is downward from the transmitting plane. Hence, when the receiver is located above the transmitter, hardly any coverage is obtained.*

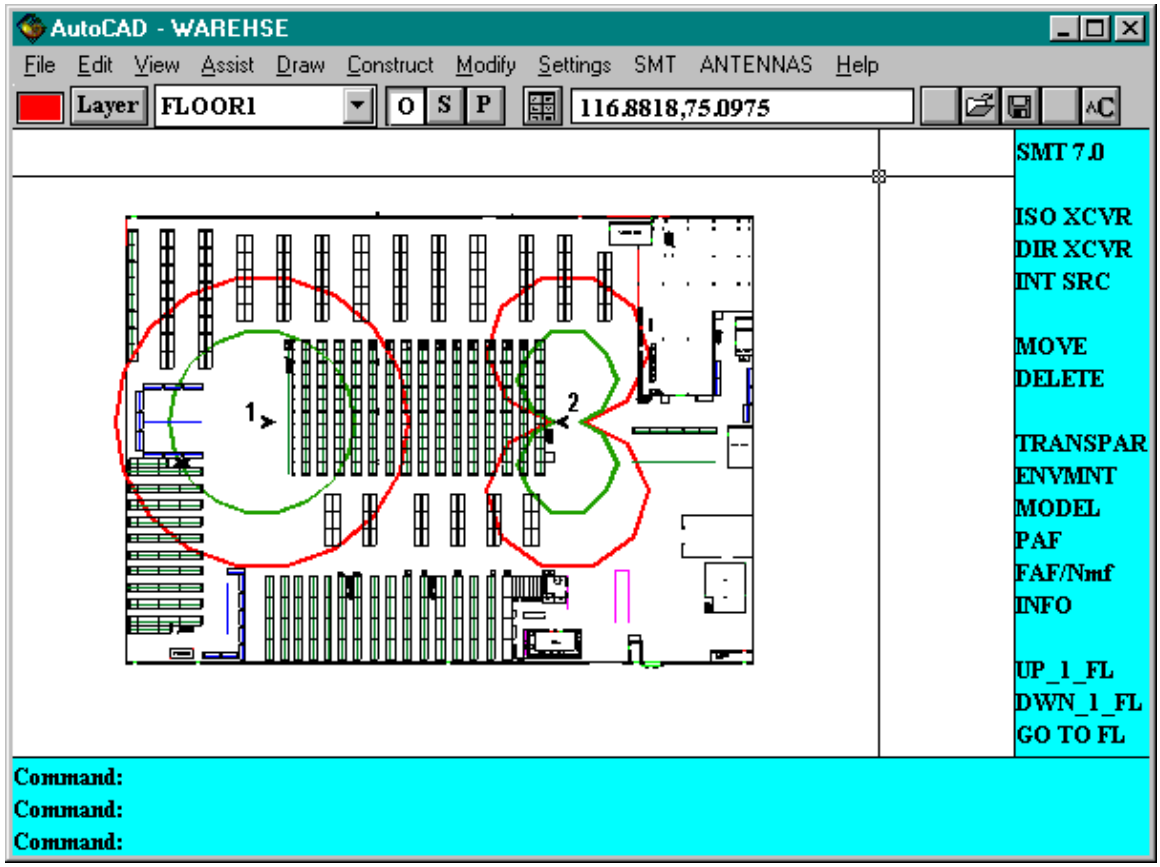

Parameter	Pattern # 1	Pattern # 2
Attenuation model	*n* value (*n* = 2)	*n* value (*n* = 2)
Height of transmitter and receiver in meters	(1.5, 1,2)	(1.5, 1.2)
Orientation of the pattern (azimuth, elevation, slant) in degrees	(0^0, 0^0, 0^0)	(180^0, 90^0, 0^0)
Pattern type	Quarterwave dipole	Quarterwave dipole

Figure 42. *Example of coverage obtained from a quarterwave dipole selected from the "Omnidirectional patterns" menu. The attenuation model, location, contour resolution, and patterns are the same for contours 1 and 2. The figure shows the change in the coverage obtained on the receiver plane for pattern 2, when the elevation of the pattern was changed from 0^0 to 90^0. Since the pattern in 1 is a donut in 3D, it is easy visualize the projection of this shape as seen in 2, after the change in elevation.*

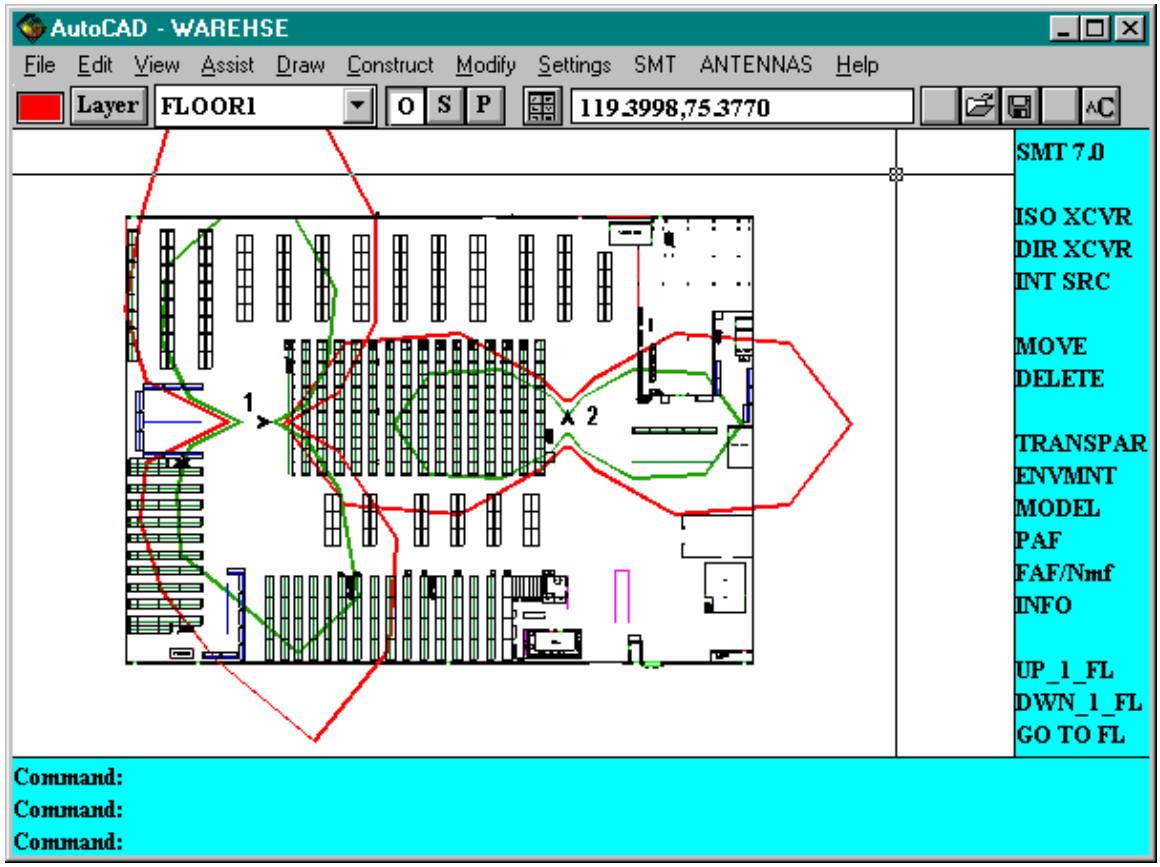

Parameter	Pattern # 1	Pattern # 2
Attenuation model	partition attenuation	*n* value (*n* = 2)
Height of transmitter and receiver in meters	(1.5, 1,2)	(1.5, 1.2)
Orientation of the pattern (azimuth, elevation, slant) in degrees	(0^0, 90^0, 0^0)	(90^0, 90^0, 0^0)
Pattern type	Halfwave biconic	Fullwave biconic

Figure 43. *Example of coverage obtained from two different antenna patterns selected from the "Omnidirectional patterns" menu. The attenuation models used are different. The key item to note here is the variation of the coverage obtained on the receiver plane, when the elevation is changed for pattern 1 without changing the azimuth, as against pattern 2 where both elevation and azimuth are changed. With omni patterns being donuts in 3D this change should be easy to visualize.*

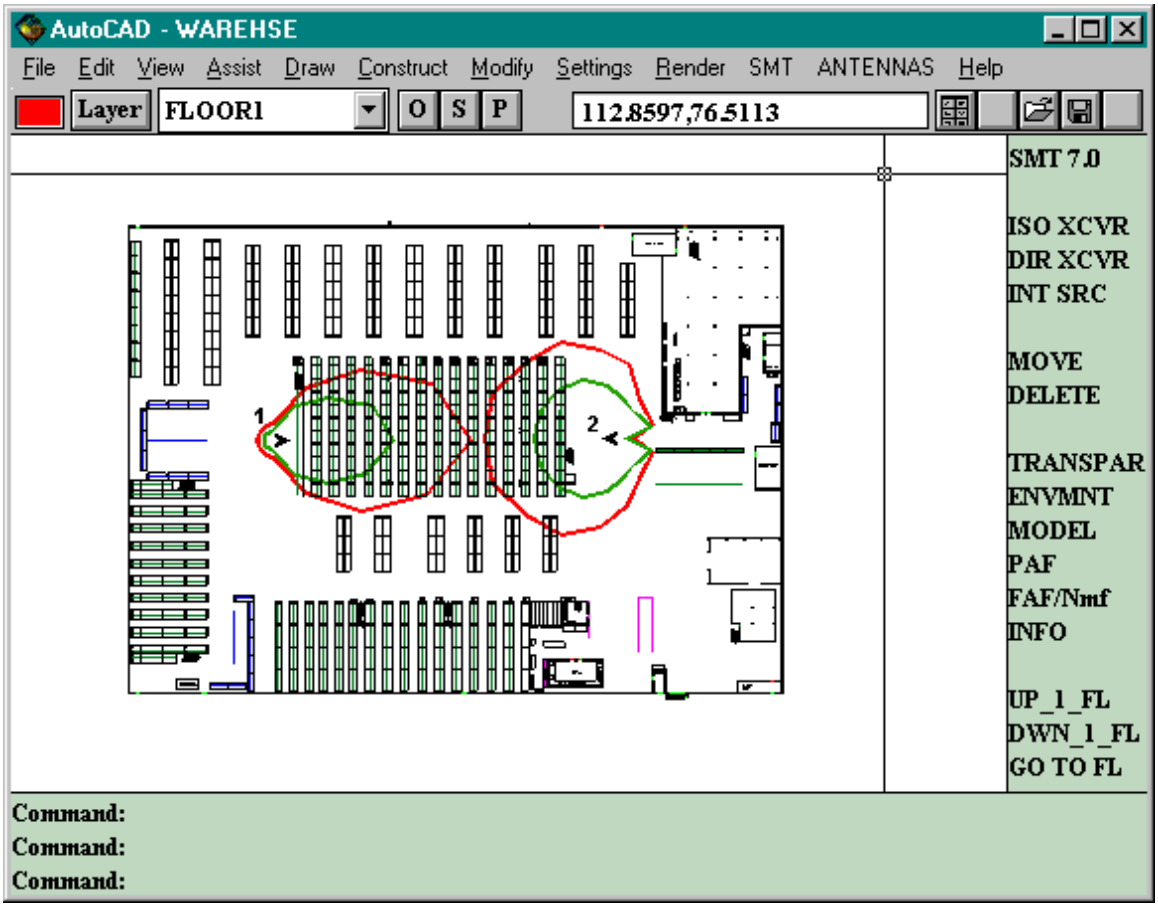

Parameter	Pattern # 1	Pattern # 2
Boresight gain	5 dB	0 dB
Attenuation model	n value (n = 2)	n value (n = 2)
Height of transmitter and receiver in meters	(1.5, 1,3)	(1.5, 1.4)
Orientation of the pattern (azimuth, elevation, slant) in degrees	(0^0, 0^0, 0^0)	(180^0, 0^0, 0^0) (Icon arrow indicates change in azimuth)
Pattern type	Azimuth = ellipse (w = 0.6) Elevation = ellipse	Azimuth = cardiod (a = 0.5) Elevation = cardiod

Figure 44. *Example of coverage obtained from two different antenna patterns selected from the "Other directional patterns" menu. This figure is a simple illustration of two different pattern types, where the azimuth and elevation cuts use the same closed form equations. The interpolation algorithm is used to calculate the coverage for pattern 1 which uses an ellipse equation for both cuts and pattern 2 which uses a cardiod equation for both cuts.*

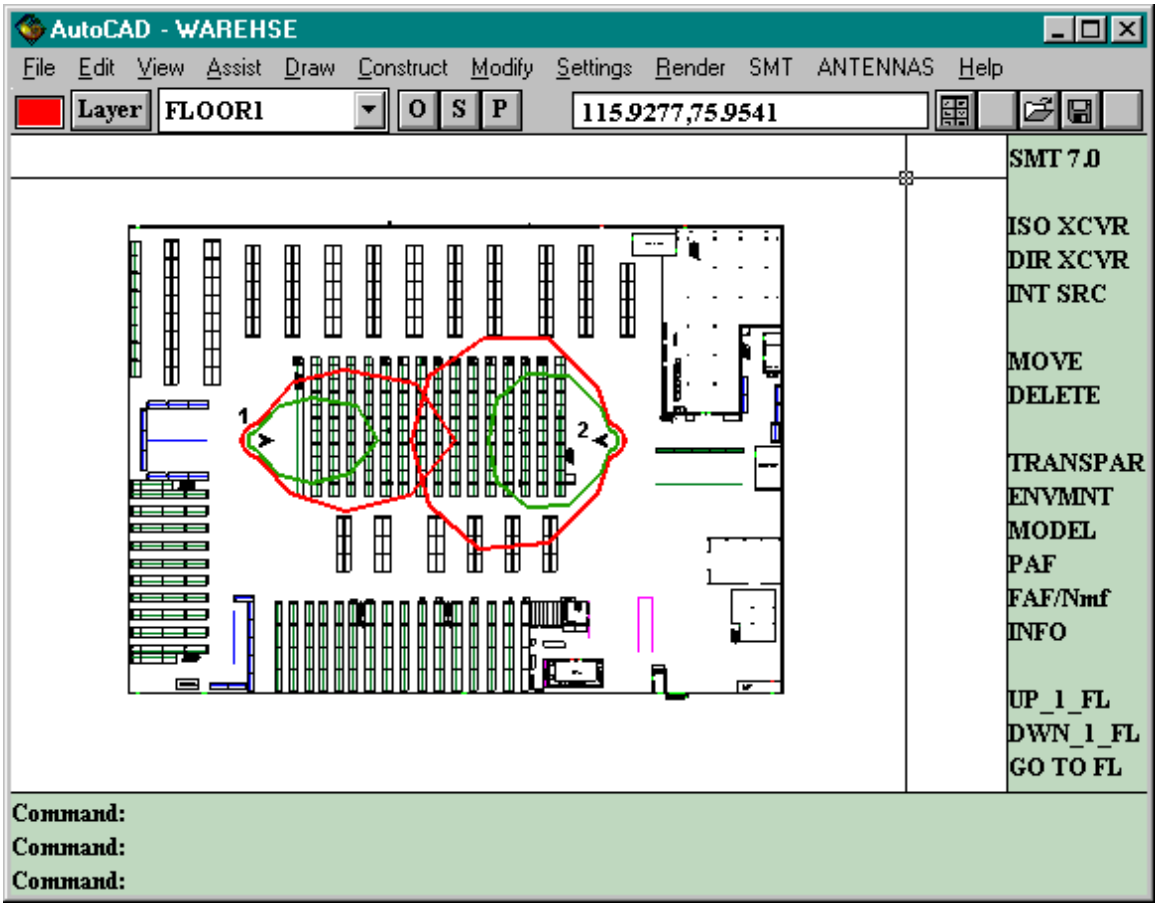

Parameter	Pattern # 1	Pattern # 2
Boresight gain	5 dB	5 dB
Attenuation model	*n* value (n = 2)	*n* value (n = 2)
Height of transmitter and receiver in meters	(1.5, 1,4)	(1.5, 1.4)
Orientation of the pattern (azimuth, elevation, slant) in degrees	(0^0, 0^0, 0^0)	(180^0, 0^0, 0^0)
Pattern type	Azimuth = ellipse (w = 0.6) Elevation = sine	Azimuth = sine (n = 1) Elevation = ellipse

Figure 45. *Example of coverage obtained for two different antennas selected from the "Other directional patterns" menu. The azimuth and elevation pattern cuts used for each antenna are different. Also, the cuts used for pattern 2 are reversed from that of pattern one. As seen, the closed form equation selected for the azimuth cut is the dominating pattern shape since no changes have been made to the default elevation or slant values.*

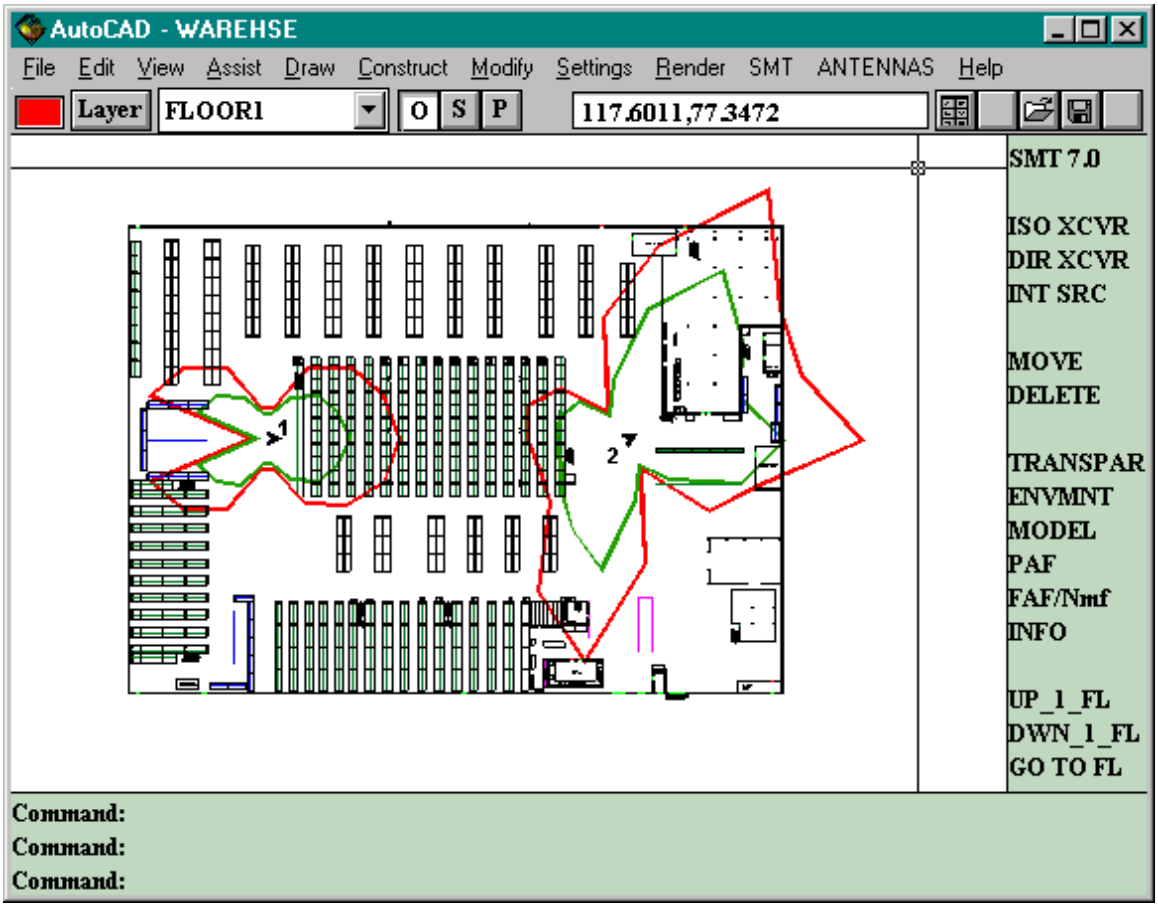

Parameter	Pattern # 1	Pattern # 2
Boresight gain	0 dB	0 dB
Attenuation model	*n* value (n = 2)	partition attenuation
Height of transmitter and receiver in meters	(1.5, 1,4)	(1.5, 1.4)
Orientation of the pattern (azimuth, elevation, slant) in degrees	$(0^0, 0^0, 0^0)$	$(30^0, 30^0, 0^0)$
Pattern type	Az. = bidirectional cosine El. = cardiod	Az.= bidirectional cosine El. = cardiod

Figure 46. *Example of coverage obtained from antennas selected from the "Other directional patterns" menu. The azimuth and elevation plane equations are different. Pattern 2 is simply a rotated version of pattern 1. Pattern 2 is using the partition attenuation model.*

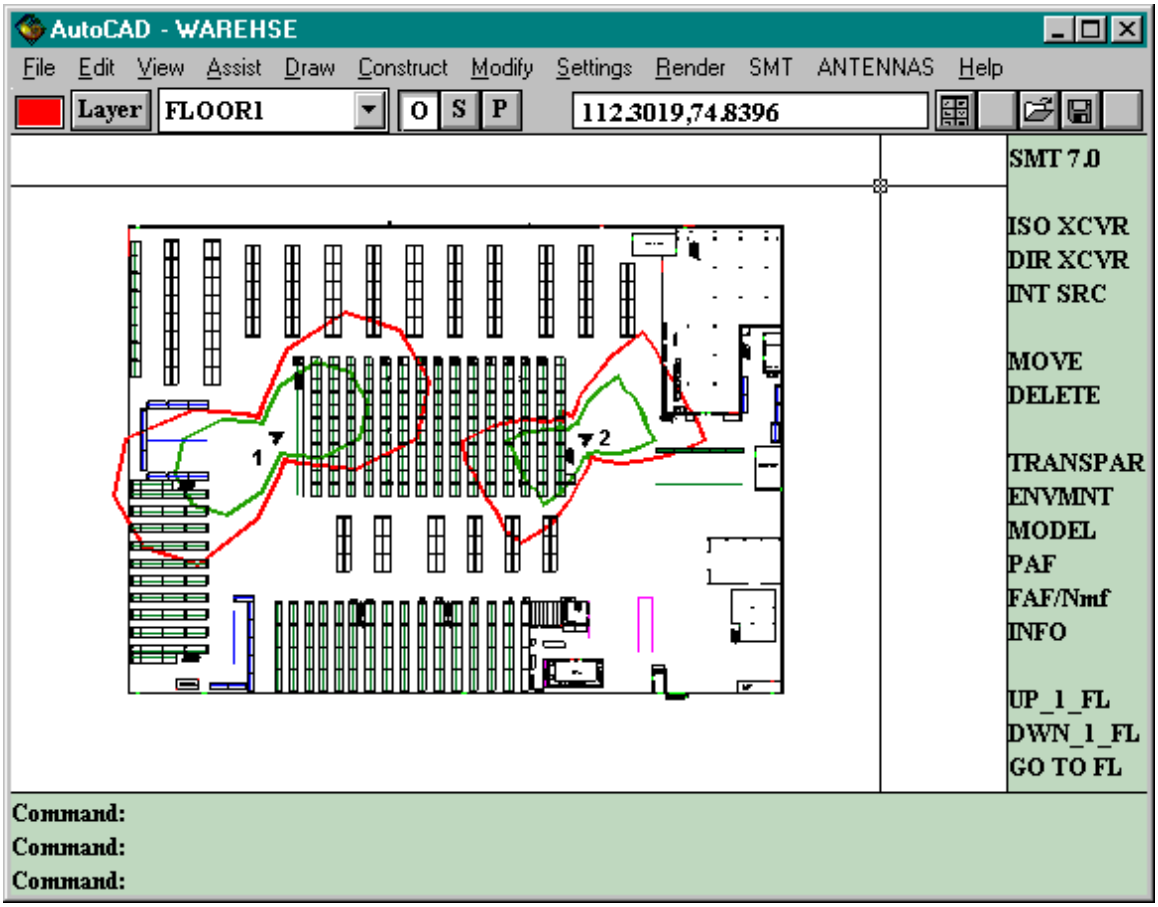

Parameter	Pattern # 1	Pattern # 2
Boresight gain	4 dB	4 dB
Attenuation model	*n* value (n = 2)	*n* value (n = 2)
Height of transmitter and receiver in meters	(1.5, 1,4)	(1.5, 1.4)
Orientation of the pattern (azimuth, elevation, slant) in degrees	(30^0, 30^0, 0^0)	(30^0, 60^0, 0^0)
Pattern type	Azimuth = pattern type 6 Elevation = pattern type 7	Azimuth = pattern type 6 Elevation = pattern type 7

Figure 47. *Example of coverage obtained from antennas selected from the "Other directional patterns" menu. The azimuth and elevation plane equations are different. Pattern 2 is similar to pattern 1 except that the elevation has been further increased. It is interesting to see how the coverage footprint on the receiver plane decreases as the elevation of the pattern is increased.*

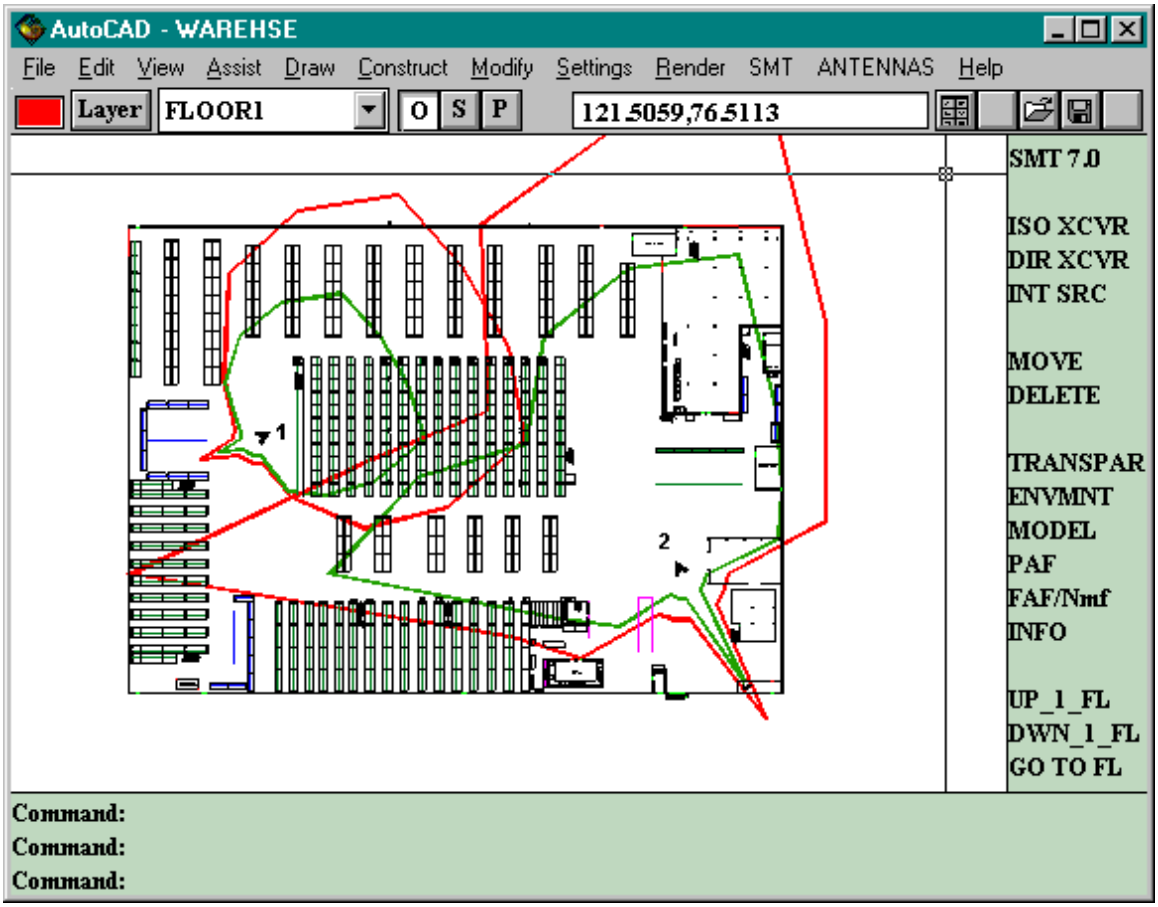

Parameter	Pattern # 1	Pattern # 2
Attenuation model	*n* value (n = 2)	partition attenuation
Height of transmitter and receiver in meters	(1.5, 1,3)	(1.5, 1.3)
Orientation of the pattern (azimuth, elevation, slant) in degrees	(30^0, 30^0, 0^0)	(120^0, 45^0, 0^0)
Pattern type	User provided data	User provided data

Figure 48. *Example of coverage obtained from user provided data for azimuth and elevation planes. The changes in pattern 2 due to orientation and model changes are evident. The data used was from an actual microstrip antenna designed for indoor use.*

Figures 49 and 50 provide examples of coverage obtained from 3D “Other directional patterns” using the partition model of SMT 7.0. The combination of this model plus a good choice of pattern, its location, its direction and gain parameters can yield amazingly selective floor coverage with good coverage accuracy. Figure 49 uses an open plan building, a warehouse in this case. Figure 50 is a closed plan and one of the floors of a building on the school campus. The table under each figure explains the key parameters used for a given pattern.

Pattern 1 in Figure 49 is a good example how the directional antenna can be used to avoid signal spill over. The position, direction and gain parameters of the antenna pattern have been carefully chosen to make use of the partitions and ensure coverage just up to the edge of the building. One can also slightly decrease the gain on pattern 2 to obtain coverage for only the center racks in the building.

Pattern 1 in Figure 50 is another example of directionality where coverage is only along the corridor of the building floor. The other two patterns, one a cardiod and the other an ellipse show how directionality can be used to focus on certain parts of a floor plan and avoid signal spill over.

Figures 51 (a) through (g) provide snap shots of the interpolation process. These seven figures are snapshots for elevation angle changes from 0^0 to 90^0, in steps of 15^0. The azimuth angle is constant at 45^0, and the slant is 0^0. The azimuth pattern chosen is the pattern type 6 from the “Other pattern” menu while the elevation pattern is type 7. The receiver plane is 0.2 meters under the transmitter plane. It is easy to visualize the changes taking place for the coverage on the receiver plane as the 3D orientation of the antenna pattern varies on the transmitter plane. The *n* value model is used in all cases, to facilitate easier visualizing as compared to the partition attenuation model.

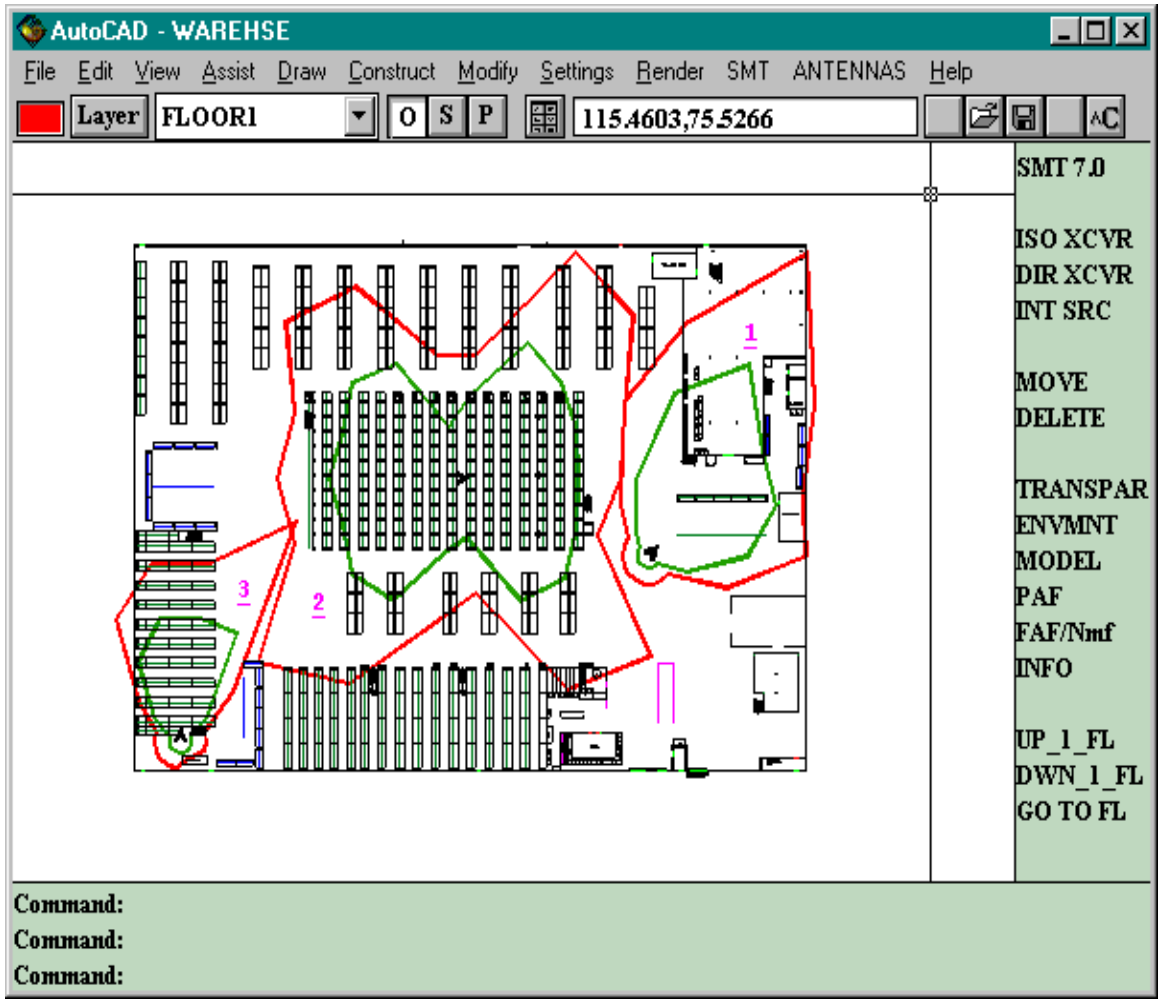

Parameter	Pattern # 1	Pattern # 2	Pattern # 3
Attenuation model	partition	partition	partition
Height of transmitter and receiver in meters	(1.5, 1.5)	(1.5, 1.5)	(1.5, 1.5)
Pattern type (Azimuth and Elevation)	Other 1 and 1	Other 7 and 7	Other 2 and 2
Orientation of the pattern (azimuth, elevation, slant) in degrees	(45^0, 0^0, 0^0)	(0^0, 0^0, 0^0)	(90^0, 0^0, 0^0)
Contour resolution	18	18	18

Figure 49. *Examples of coverage obtained by selecting the "3D display" option from the "Other directional patterns" menu. Partition attenuation model is used.*

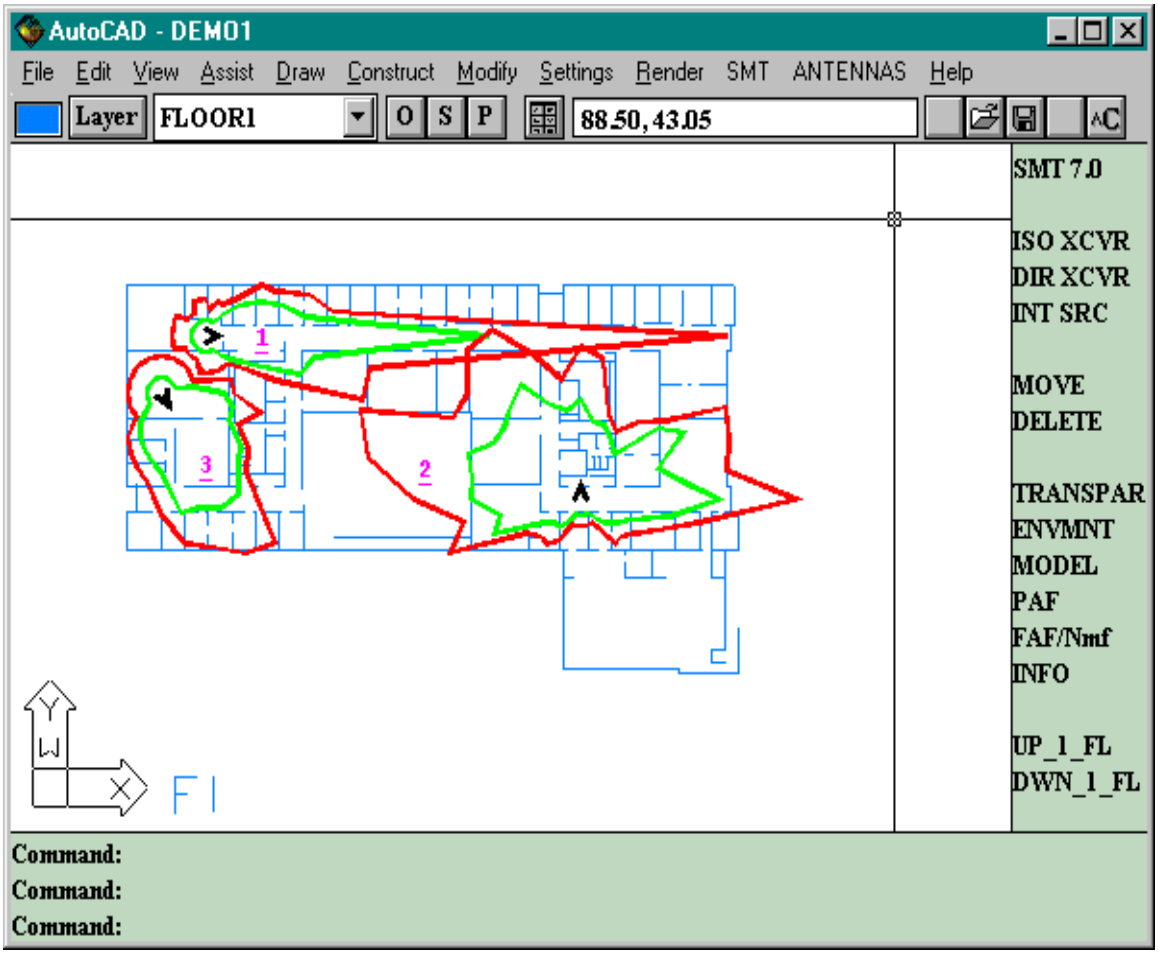

Parameter	Pattern # 1	Pattern # 2	Pattern # 3
Attenuation model	partition	partition	partition
Height of transmitter and receiver in meters	(1.5, 1.5)	(1.5, 1.5)	(1.5, 1.5)
Pattern type (Azimuth and Elevation)	Other 1 and 1	Other 4 and 4	Other 2 and 2
Orientation of the pattern (azimuth, elevation, slant) in degrees	(0^0, 0^0, 0^0)	(90^0, 0^0, 0^0)	(300^0, 0^0, 0^0)
Contour resolution	36	36	36

Figure 50. *Examples of coverage obtained from selecting the "3D display" option from the "Other directional patterns" menu. Partition attenuation model is used.*

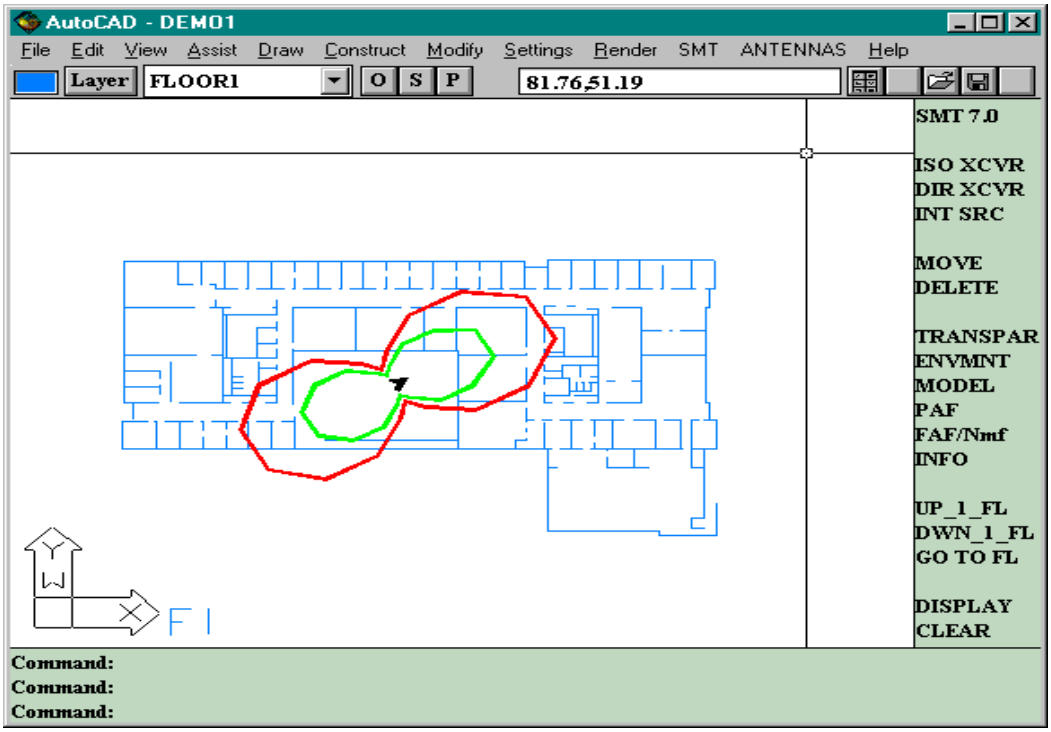

Figure 51. (a)

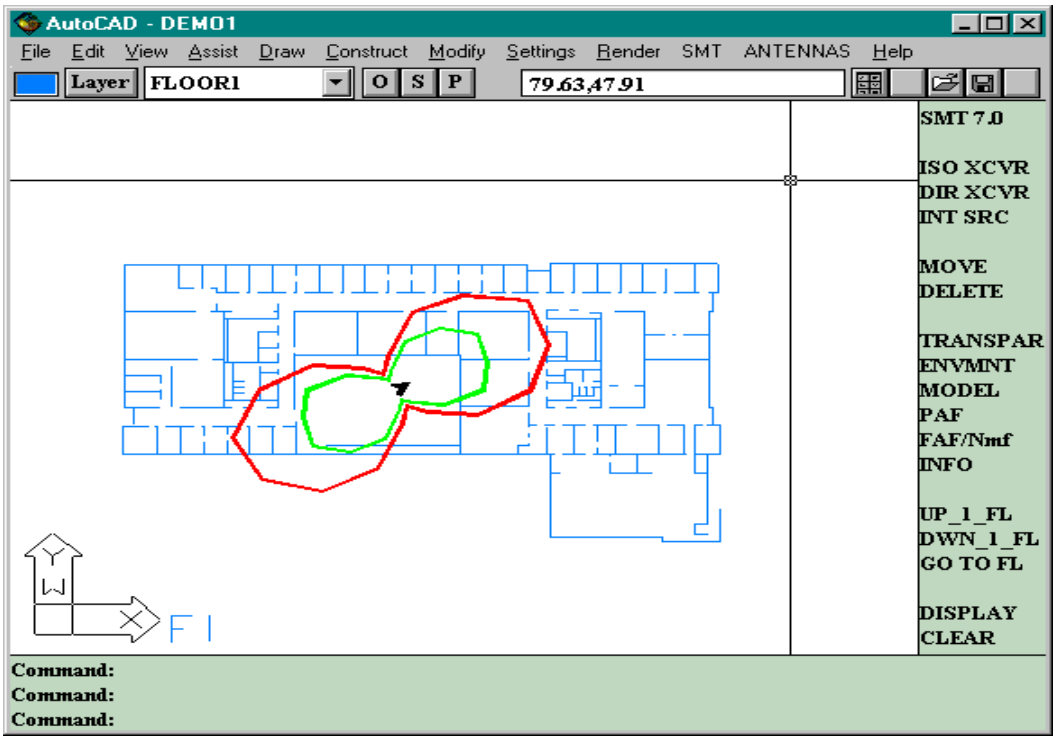

Figure 51. (b)

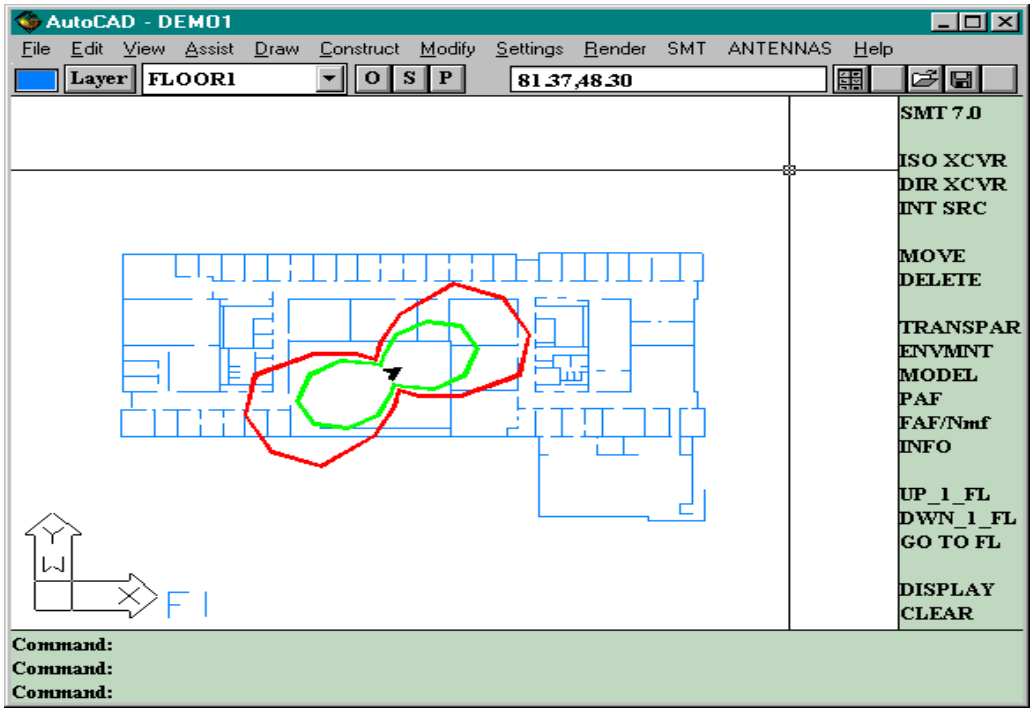

Figure 51. (c)

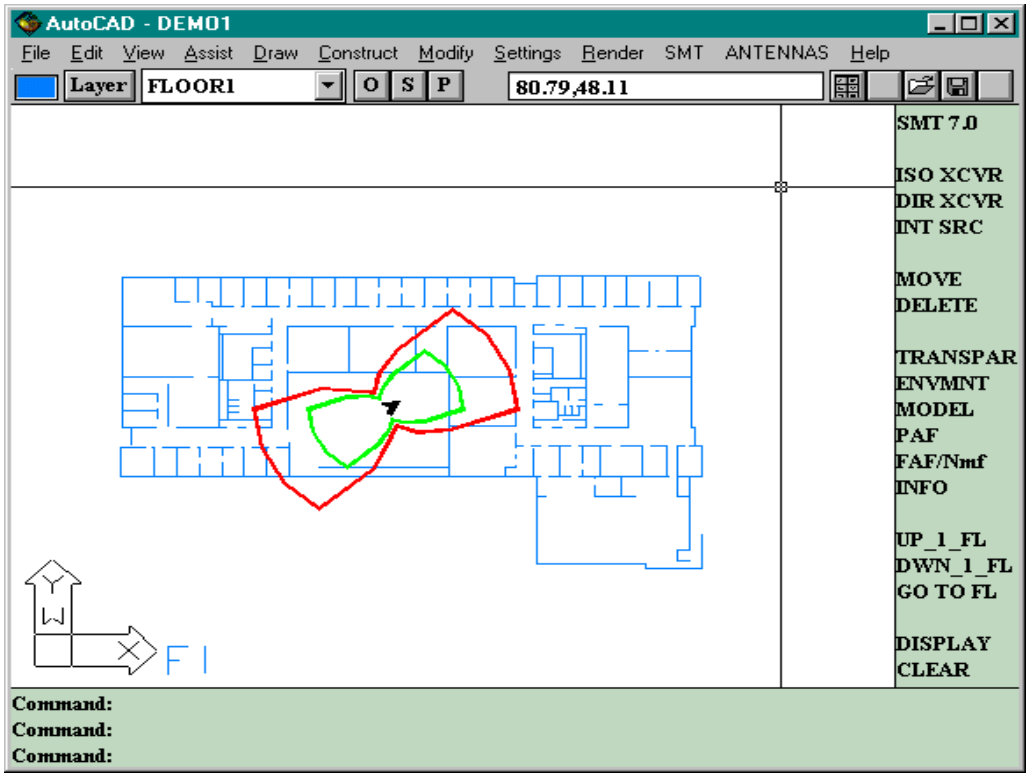

Figure 51. (d)

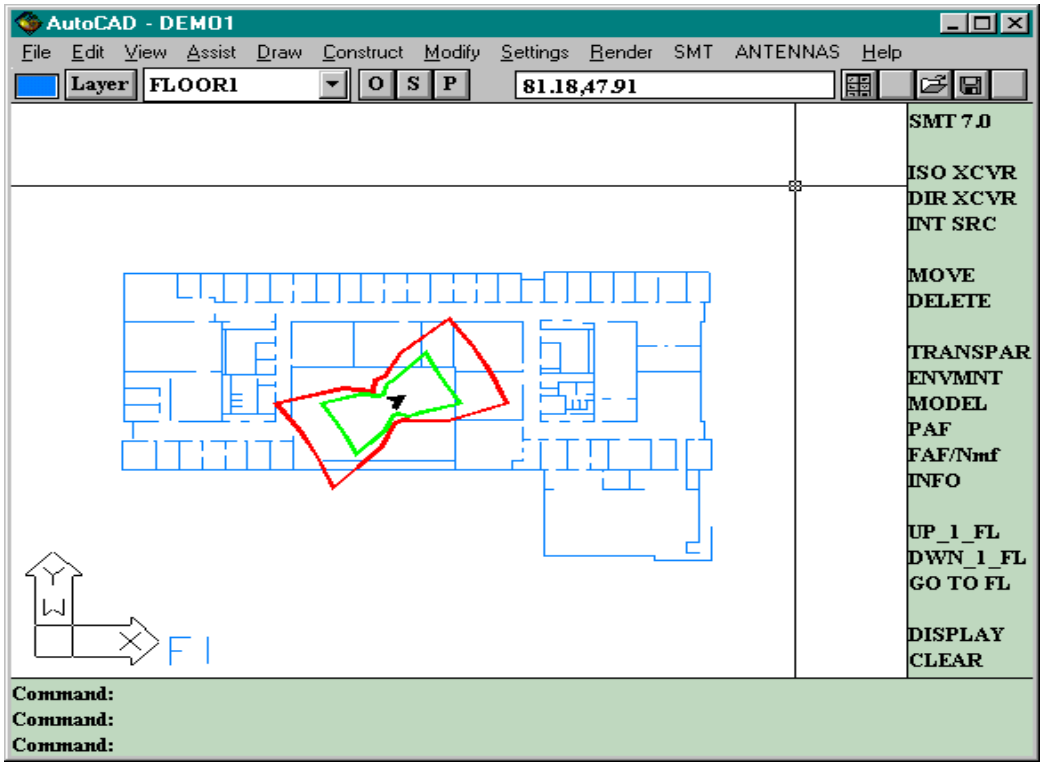

Figure 51. (e)

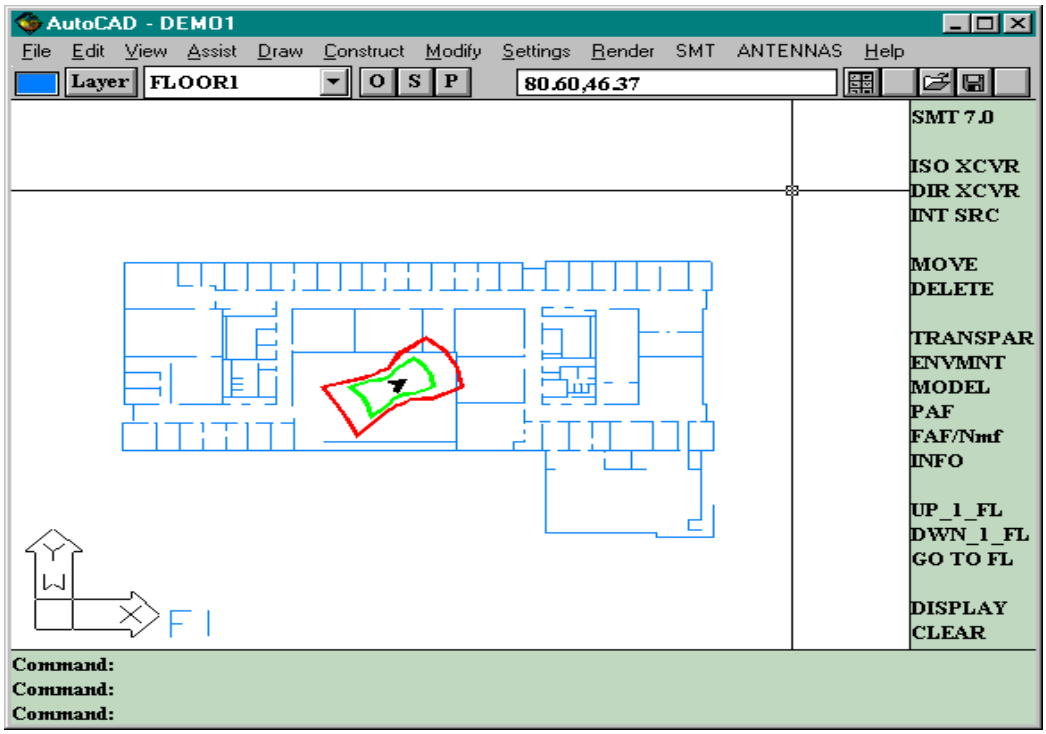

Figure 51. (f)

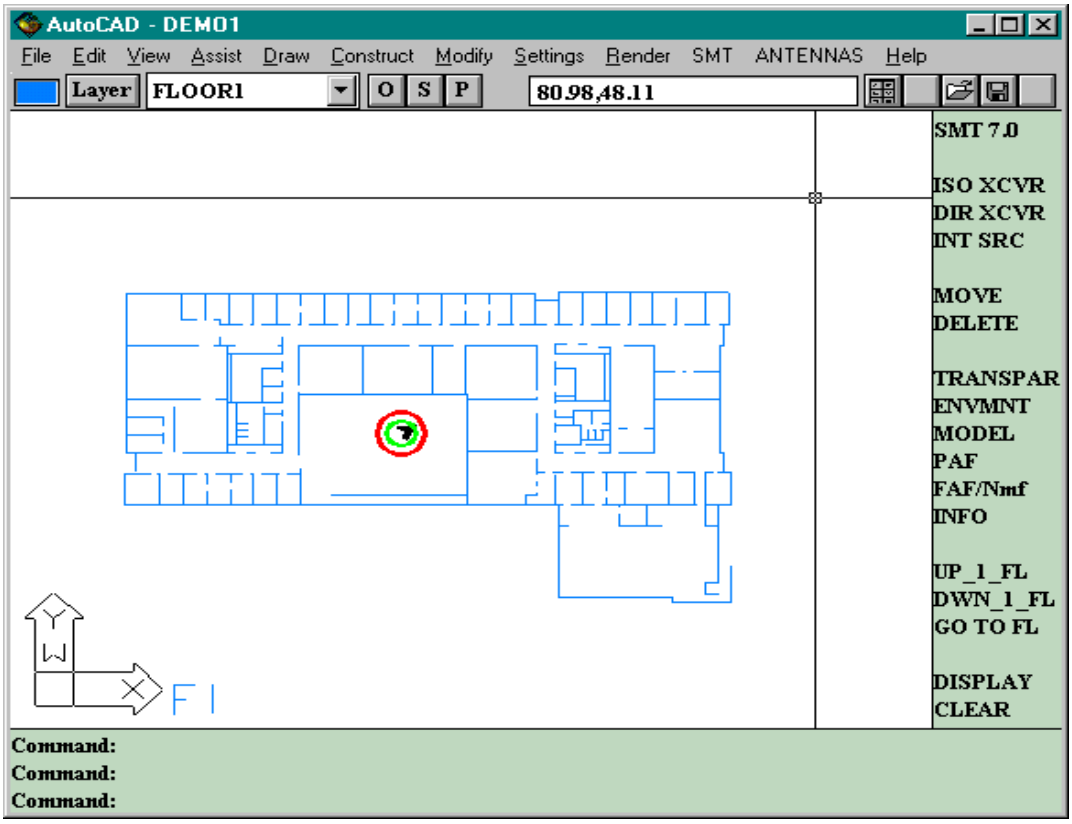

Figure 51. (g)

Figure 51. *Snapshots of the interpolation process obtained by choosing the 3D-display option from the "Other directional patterns" menu. With the azimuth held constant at 45^0 for the transmitting antenna, the elevation angle is varied in steps of 15^0. (a) The elevation at 0^0. (g) The elevation at 90^0. The corresponding coverage as seen on the receiver plane is shown in the figures.*

6.3 Error Analysis

This section deals with error analysis for SMT 7.0. As we know, omnidirectional patterns do not employ interpolation techniques. Hence, information about omnidirectional pattern can be fed in as user provided data and the two compared. This will provide us a direct measure of the accuracy of the interpolation technique. Table 7 is the user pattern file input data used as reference for error analysis. Since all the eight omnidirectional patterns yield a circle for their coverage contour in their default position

(Azimuth =0^0, Elevation=0^0, Slant=0^0), different orientations were chosen for accuracy comparison. Examples 1, 2 and 3 provide analysis information for three such orientations. Tables 8 to 10 provide comparison between expected and interpolated data for the three examples. Table 11 is the summary of observations for the three examples. Figures 52(a) to 52(c) provide coverage plots for the three examples. From the figures and the summary table, it is easy to see that the interpolation technique yielded quite satisfactory results.

Note 1: All three examples use the half wave dipole omnidirectional pattern. To recap from chapter 4, the azimuth and the elevation plane equations for this antenna are:

In the azimuth plane: $G_{AZ}(\phi) = 2.15$ [dB]

In the elevation plane: $G_{EL}(\theta) = 20 \log_{10} \left| \frac{\cos(0.5\pi \cos\theta)}{\sin\theta} \right|$ [dB]

Note 2: In all the three examples, the *n* value model is used for gain value comparisons. This avoids any errors that may creep in due to location and partition effects for a given antenna.

Note 3: In all the three examples, there are two columns that compare the gain in dB for the omni data and the user data. It is important to understand how these were obtained. As we know, the SMT 7.0 returns the gain value $G_T(\theta,\phi)$, which gets plugged into the communication feasibility equation. There are hundreds of such values returned for a given contour calculation. However, we are interested in finding for a given contour, only the last gain value returned for a given radial search angle. To do so, all the gain values returned were printed into an AutoCAD log file for each antenna type. From that list, only the ones which are the final gain values for a radial search line were selected. The radial search angles were also printed into the log file to ease the gain search of what is an otherwise a painstaking process! A contour with 18 points was used for both the omni and user pattern.

Note 4: Table 7 provides information on the gain pattern data used for error analysis. The user data is input in 5^0 increments. As is obvious, the azimuth plane pattern data is simply

2.15 dB as the omni pattern is circular with this boresight gain in the azimuth plane. The elevation gain data is obtained from the equation for the elevation pattern for the omni. Since this equation is normalized, 2.15 dB is added to each entry. This ensures that the user data scales the file data properly and the right boresight gain is obtained.

Table 7. *User pattern file input data*

Angle in 5^0 increments	**Azimuth plane data**	**Elevation plane data**
0	2.150000	-25.000000
5	2.150000	-21.125700
10	2.150000	-15.089300
15	2.150000	-11.543100
20	2.150000	-09.014220
25	2.150000	-07.043870
30	2.150000	-05.430760
35	2.150000	-04.070290
40	2.150000	-02.902680
45	2.150000	-01.891730
50	2.150000	-01.014810
55	2.150000	-00.257570
60	2.150000	00.389087
65	2.150000	00.930904
70	2.150000	01.371384
75	2.150000	01.712610
80	2.150000	01.955762
85	2.150000	02.101461
90	2.150000	02.150000
95	2.150000	02.101461
100	2.150000	01.955762
105	2.150000	01.712610
110	2.150000	01.371384
115	2.150000	00.930904
120	2.150000	00.389087
125	2.150000	-00.257570
130	2.150000	-01.014810
135	2.150000	-01.891730
140	2.150000	-02.902680
145	2.150000	-04.070290
150	2.150000	-05.430760
155	2.150000	-07.043870
160	2.150000	-09.014220
165	2.150000	-11.543100
170	2.150000	-15.089300

175	2.150000	-21.125700
180	2.150000	-25.000000
185	2.150000	-21.125700
190	2.150000	-15.089300
195	2.150000	-11.543100
200	2.150000	-09.014220
205	2.150000	-07.043870
210	2.150000	-05.430760
215	2.150000	-04.070290
220	2.150000	-02.902680
225	2.150000	-01.891730
230	2.150000	-01.014810
235	2.150000	-00.257570
240	2.150000	00.389087
245	2.150000	00.930904
250	2.150000	01.371384
255	2.150000	01.712610
260	2.150000	01.955762
265	2.150000	02.101461
270	2.150000	02.150000
275	2.150000	02.101461
280	2.150000	01.955762
285	2.150000	01.712610
290	2.150000	01.371384
295	2.150000	00.930904
300	2.150000	00.389087
305	2.150000	-00.257570
310	2.150000	-01.014810
315	2.150000	-01.891730
320	2.150000	-02.902680
325	2.150000	-04.070290
330	2.150000	-05.430760
335	2.150000	-07.043870
340	2.150000	-09.014220
345	2.150000	-11.543100
350	2.150000	-15.089300
355	2.150000	-21.125700
360	2.150000	-25.000000

Example 1: Bow Tie Pattern in Elevation Plane

In this example, the orientation of the 3D pattern on the transmitter plane is chosen with an elevation of 90^0. Thus, the interpolation technique is essentially using the elevation plane pattern of an omni. The azimuth and slant are left at their default values of 0^0. The receiver and transmitter are on the same plane.

Table 8. *Error analysis for a bow tie pattern on elevation plane*

Number	Angle in Degrees	Omni Antenna Gain (Non Interpolated) dB	User Antenna Gain (Interpolated) dB	Difference (δ)
1	0^0	– 22.8500000	– 22.850000	0.000000
2	20^0	– 09.0142222	– 09.497300	0.483078
3	40^0	– 02.9026830	– 02.180488	– 0.722195
4	60^0	00.3890870	01.484300	– 1.095213
5	80^0	01.9557620	02.141700	– 0.185938
6	100^0	01.9557620	02.141700	– 0.185938
7	120^0	00.3890870	01.484300	– 1.095213
8	140^0	– 02.9026830	– 02.180488	– 0.722195
9	160^0	– 09.0142222	– 09.497300	0.483078
10	180^0	– 22.8500000	– 22.850000	0.000000
11	200^0	– 09.0142222	– 09.497300	0.483078
12	220^0	– 02.9026830	– 02.180488	– 0.722195
13	240^0	00.3890870	01.484300	– 1.095213
14	260^0	01.9557620	02.141700	– 0.185938
15	280^0	01.9557620	02.141700	– 0.185938
16	300^0	00.3890870	01.484300	– 1.095213
17	320^0	– 02.9026830	– 02.180488	– 0.722195
18	340^0	– 09.0142222	– 09.497300	0.483078

The mean absolute error, $\overline{X} = \dfrac{\sum|\delta|}{n} = \dfrac{9.945696}{18} = 0.5525$

The standard deviation σ is given by $\sqrt{S^2}$ where $S^2 = \dfrac{1}{n-1} \sum_{i=1}^{n} (X_i - \overline{X})^2$.

$S^2 = 0.3337262$ and therefore, $\sigma = 0.5776904$.

Also, the area of coverage obtained for the outer contour was 817.17 m^2 for the user pattern, while the omni pattern yielded an area of coverage of 737.14 m^2.

Example 2: Oval pattern

In this example, the orientation of the 3D pattern on the transmitter plane is chosen with an elevation of 30^0. Thus, the interpolation technique is using both the azimuth plane pattern and elevation plane pattern equations of the omni. The azimuth and slant are left at their default values of 0^0. The receiver and transmitter are on the same plane.

Table 9. *Error analysis for an oval pattern*

Number	Angle in Degrees	Omni Antenna Gain (Non Interpolated) dB	User Antenna Gain (Interpolated) dB	Difference (δ)
1	0^0	0.3890	0.3864	0.0026
2	20^0	0.6155	0.5385	0.0077
3	40^0	1.1618	1.4440	– 0.2822
4	60^0	1.7426	1.4440	0.2986
5	80^0	2.1018	2.1060	– 0.0042
6	100^0	2.1018	2.1060	– 0.0042
7	120^0	1.7426	1.4440	0.2986
8	140^0	1.1618	1.4440	– 0.2822
9	160^0	0.6155	0.5385	0.0077
10	180^0	0.3890	0.3864	0.0026
11	200^0	0.6155	0.5385	0.0077
12	220^0	1.1618	1.4440	– 0.2822
13	240^0	1.7426	1.4440	0.2986
14	260^0	2.1018	2.1060	– 0.0042
15	280^0	2.1018	2.1060	– 0.0042
16	300^0	1.7426	1.4440	0.2986
17	320^0	1.1618	1.4440	– 0.2822
18	340^0	0.6155	0.5385	0.0077

The mean absolute error, $\overline{X} = \frac{\sum|\delta|}{n} = \frac{2.376}{18} = 0.132$

The standard deviation σ is given by $\sqrt{S^2}$ where $S^2 = \frac{1}{n-1} \sum_{i=1}^{n} (X_i - \overline{X})^2$.

$S^2 =$ 0.0397127 and therefore, σ = 0.19928.

Also, the area of coverage obtained for the outer contour was 1302.67 m^2 for the user pattern, while the omni pattern yielded an area of coverage of 1309.34 m^2.

Example 3: Bow Tie Pattern in Azimuth Plane

In this example, the orientation of the 3D pattern on the transmitter plane is chosen with an elevation of 90^0 and an azimuth of 90^0. Thus, the interpolation technique is essentially using the elevation plane pattern of an omni but now oriented to lie on the azimuth plane. The slant is left at its default values of 0^0. The receiver and transmitter are on the same plane.

Table 10. *Error analysis for a bow tie pattern on azimuth plane*

Number	Angle in Degrees	Omni Antenna Gain (Non Interpolated) dB	User Antenna Gain (Interpolated) dB	Difference (δ)
1	0^0	02.150000	02.150000	0.0000
2	20^0	01.371384	02.058130	– 0.6867
3	40^0	– 01.014813	00.103600	– 1.1184
4	60^0	– 05.430762	– 05.256730	– 0.1740
5	80^0	– 15.089391	– 15.409024	0.3196
6	100^0	– 15.089391	– 17.169926	2.0805
7	120^0	– 05.430762	– 05.256730	– 0.1740
8	140^0	– 01.014813	00.103600	– 1.1184
9	160^0	01.371384	02.058130	– 0.6867
10	180^0	02.150000	02.150000	0.0000
11	200^0	01.371384	02.058130	– 0.6867
12	220^0	– 01.014813	00.103600	– 1.1184
13	240^0	– 05.430762	– 05.256730	– 0.1740
14	260^0	– 15.089391	– 15.409024	0.3196
15	280^0	– 15.089391	– 17.169926	2.0805
16	300^0	– 05.430762	– 05.256730	– 0.1740
17	320^0	– 01.014813	00.103600	– 1.1184
18	340^0	01.371384	02.058130	– 0.6867

The mean absolute error, $\overline{X} = \dfrac{\sum|\delta|}{n} = \dfrac{12.7166}{18} = 0.7064$

The standard deviation σ is given by $\sqrt{S^2}$ where $S^2 = \dfrac{1}{n-1} \sum_{i=1}^{n} (X_i - \overline{X})^2$.

$S^2 =$ 0.9023 and therefore, σ = 0.95.

Also, the area of coverage obtained for the outer contour was 810.30 m^2 for the user pattern, while the omni pattern yielded an area of coverage of 730.30 m^2.

Error analysis summary

Table 11. *Tabulation of key comparison parameters for the three examples*

Example #	Difference in % of Area Coverage	Mean Absolute Error [dB]	Standard Deviation [dB]
1	**9.8**	**0.5525**	**0.58**
2	**0.5**	**0.1320**	**0.20**
3	**9.8**	**0.7064**	**0.95**

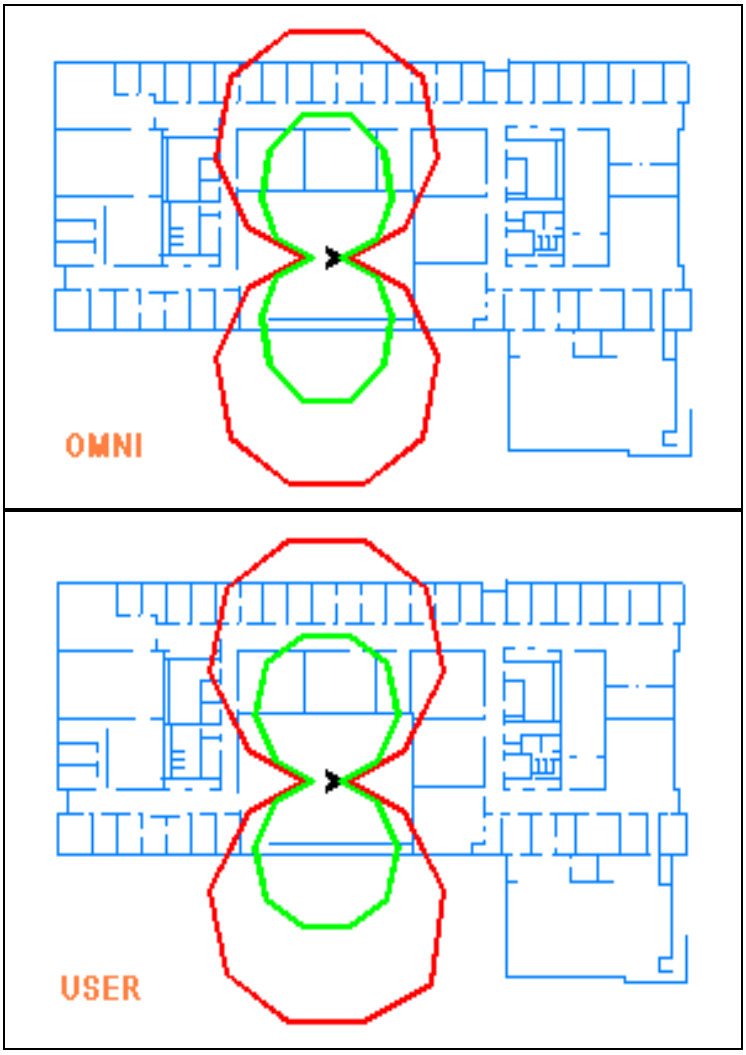

Figure 52. (a)

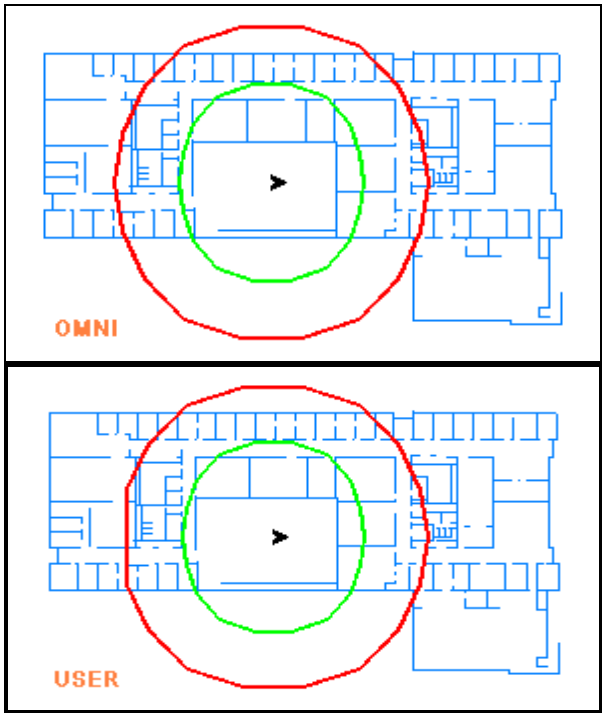

Figure 52. (b)

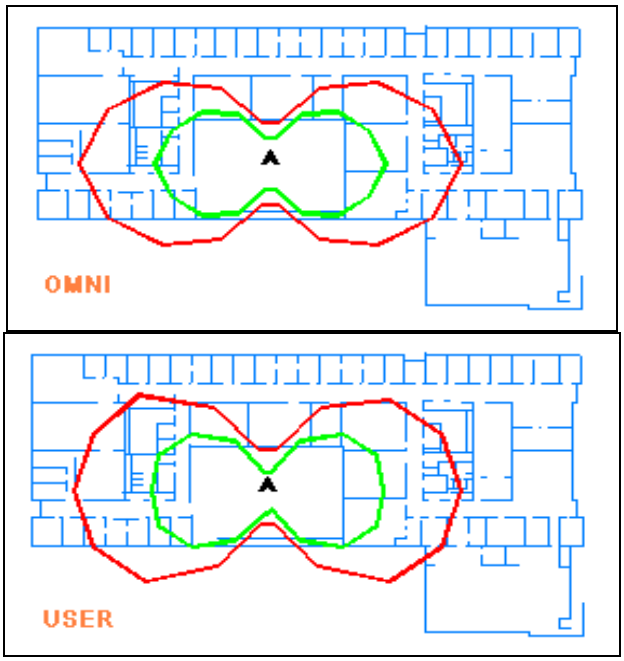

Figure 52. (c)

Figure 52. *Coverage plots corresponding to the three examples used for error analysis. As can be seen, the expected (omni) and actual (user) coverage plots very closely resemble.*

Chapter 7
Conclusion

7.1 Summary of Research Contribution

Here is a recap of what the thesis has described:

1) A mathematical foundation has been developed which allows prediction coverage to include any directional antenna pattern which admits a closed form representation. The antennas patterns have been categorized as “User provided patterns”, “Omnidirectional patterns” and “Other directional patterns”.
2) A set of closed form two dimensional pattern equations for practically deployable antenna types was compiled. These equations form the basis for 3D calculations. A study was made on the most useful range of parameter values for the pattern equation variables. Some of these equations were used by the Antenna*Builder* of SMT *Plus*.
3) The standard industrial format for user generated two dimensional directional antenna patterns was used, which permits the user to input data in the same file format for SMT calculations. The SMT coverage contour resolution is independent of the resolution of the file format data.
4) The tool allows the user to work with three dimensional patterns. This implies that the user can orient the patterns in any direction by rotating them in 3D. He can also place the transmitter antenna at a different height than the receivers. A mathematical foundation based on homogeneous coordinate transformations was developed for the same. Note that the coverage prediction is done in 2D on the receiver plane for any arbitrary orientation of 3D antenna pattern on the transmitter plane.
5) An interpolation method was developed to work with two dimensional patterns, and convert the same into three dimensional patterns. An algorithm was worked out to accomplish the same, after looking into various interpolation techniques.
6) The user interface was enhanced by addition of a directional antenna menu and icon. The tool was embellished by allowing the user to view the area of coverage. This

area coverage feature was also ported to SMT *Plus* during the initial phases of its development.

7) AutoCAD features were exploited, to make the prediction models more dynamic by providing the ability to specify an increased number of partitions (from 2 to 4). This idea was used by SMT *Plus* and the number of partition types increased to 6.

7.2 Recommendations for Future Work

The features added in SMT 7.0 provide a rich addition to the existing suite of SMT *Plus* marketed by Virginia Tech. The features make the tool complete by providing the user an ability to work with 3D antenna patterns. However, as with any tool, there is research potential which can be further explored. The next paragraph outlines certain enhancements that can be carried out on the features that presently exist in SMT 7.0 or SMT *Plus*.

Features specific to antennas that can be added are:

1) The present tool does not take polarization into effect. It is straightforward to add a "polarization mismatch factor" as a part of the antenna height and orientation dialog box if so desired and correspondingly change the gain pattern equation. Also, the user can specify the polarization type for transmitting and receiving antennas.
2) The receiving antenna is presently isotropic. Making it a directional is a challenging task, but allowing the user to choose from a menu of omnidirectional patterns for the receiving antenna would be comparatively less rigorous, but will dramatically improve the functionality the tool. Anyway, practical applications normally have omnidirectional antennas for receivers.
3) The tool presently handles pattern data provided for two principal planes. If more data is available for accurate modeling, the 3D interpolation technique will have to be changed. Also, at the present time, the technique employed is very well suited for

indoor antennas but not for outdoor antennas like YAGI which have many strong side lobes.

4) A leaky feeder antenna seems to be gaining popularity as a valid antenna for indoor wireless communications. Presently, SMT 7.0 does not support this antenna type. In this type of antenna, a coaxial cable will be laid in an indoor environment at a specific height with insulation stripped off at equally spaced points. Even though this may be awkward in many situations, it has its advantages by supporting multiple wireless technologies to share the same medium and in essence acting as multiple point source antenna. A simplistic modeling of this into SMT 7.0 would mean *n* number of equally spaced *similar* directional antennas. The modeling problem would get complicated if all these points need to represent a collective source. One approach would be to scale the antenna gain as a factor of the number of point sources.
5) To avoid repetition, improvements already suggested in [Panj95] and [Skid97] are not covered. However, the key feature which needs to be expanded upon, is the IEEE 802.11 standard support. Since this will be the standard for all indoor wireless LAN networks, special attention will have to be paid for the provisions made in this standard. All vendor offering will soon meet this standard and inter operability among various vendor offerings cited in chapter 2 is expected by the end of the year. The key things which need to be incorporated into the SMT *Plus* tool are:

- The standard supports wireless data transmission in the 2.4 GHz band. This needs to be incorporated into the tool. The standard allocates 83 MHz of spectrum in the US with a maximum power of 1 W for the 2.4 GHz range. Similar specs are available for Europe, Japan, Spain and France.
- A very useful addition to the SMT *Plus* tool would be support for IR. Since this is only line of sight, modifications will have to be done to the program to support this feature. However, the addition of this feature will make the tool complete as 802.11 supports diffuse IR over 850-950 nm.
- Another feature which can be a useful addition to the SMT tool would be a display of maximum data rate supported for a given standard where the modulation scheme at

the RF level is known. For example, the IEEE standard specifies that for DS (direct sequence) systems, DBPSK (differential binary phase shift keying) will be the modulation scheme for data rate of 1 Mbps. Similarly, for 2 Mbps operation, DQPSK (differential quadrature phase shift keying) will be the modulation scheme. If FS (frequency hopping) systems are used, 2-level GFSK will be the modulation scheme for data rate of 1 Mbps and 4-level will be the modulation scheme for data rate of 2 Mbps.

Bibliography

Related to propagation prediction tools:

[Fort95] S.J. Fortune, D.M. Gay, B.W. Kernighan, O. Landron, R.A. Valenzuela, and M.H. Wright, "WISE Design of Indoor Wireless Systems," *IEEE Computational Science and Engineering*, vol. 2, no. 1, pp. 58-68, Spring 1995.

[Panj95] M.A. Panjwani, "An Interactive Site Modelling Tool for Estimating Coverage Regions for Wireless Communication Systems in Multifloored Indoor Environments," M.S. Thesis, Department of Electrical Engineering, Virginia Polytechnic Institute and State University, Blacksburg, VA, May1995.

[Panj96] M.A. Panjwani, A.L. Abbott, and T.S. Rappaport, "Interactive Computation of Coverage Regions for Wireless Communication in Mutifloored Indoor Environments," *IEEE Journal on Selected Areas in Communications*, vol. 14, no. 3, pp. 420-430, April 1996.

[Rapp91] T.S. Rappaport, S.Y. Seidel, and K. Takamizawa, "Statistical channel impulse models for factory and open plan building radio communication system design," *IEEE Transactions on Communications*, vol. COM-39, no. 5, pp. 794-806, May 1991.

[Skid97] R.R. Skidmore, "A Comprehensive In-Building and Microcellular Wireless Communication System Design Tool," M.S. Thesis, Department of Electrical Engineering, Virginia Polytechnic Institute and State University, Blacksburg, VA, June1997.

Related to wireless communication:

[Abbo95] A.L. Abbott, N. Bhat, and T.S. Rappaport, "Interactive Computation of Coverage Regions for Indoor Wireless Communication" *Proceedings of the SPIE conference on wireless data communication*, vol. 2601, pp. 178-189, October 1995.

[Ande95] J.B. Andersen, T.S. Rappaport, and S. Yoshida, "Propagation Measurements and Models for Wireless Communications Channels," *IEEE Communications Magazine*, vol. 33, no. 1, pp. 42-49, January 1995.

[Fleu96] B.H. Fleury and P.E. Leuthold, "Radiowave Propagation in Mobile Communications: An Overview of European Research," *IEEE Communications Magazine*, vol. 34, pp. 70-81, no. 2, February 1996.

[Hash93] H. Hashemi, "The Indoor Radio Propagation Channel," *Proceedings of the IEEE*, vol. 81, no. 7, pp. 943-968, July 1993.

[Mull95] N.J. Muller, *Wireless Data Networks*, Artech House, 1995.

[Nemz95] M. Nemzow, *Implementing Wireless Networks*, McGraw-Hill Book, 1995.

[Padg95] J.E. Padgett, C.G. Gunther, and T. Hattori, "Overview of Wireless Personal Communications," *IEEE Communications Magazine*, vol. 33, no.1, pp. 28-44, January 1995.

[Rapp95] T.S. Rappaport, *Wireless Communications: Principles and Practice*, Prentice Hall, 1995.

[Sant94] A. Santamaria and F.J.L. Hernandez, *Wireless LAN Systems*, Artech House Inc., 1994.

Related to antennas:

[Bala97] C.A. Balanis, *Antenna Theory*, 2nd Edition, John Wiley and Sons, 1997.

[Chat88] R. Chatterjee, *Antenna Theory and Practice*, John Wiley & Sons, 1988.

[Elli81] R.S. Elliott, *Antenna Theory and Design*, Prentice-Hall, N.J., 1981.

[Fuji94] K. Fujimoto and J.R. James, *Mobile Antenna Systems Handbook*, Artech House, 1994.

[Gupt88] K.C. Gupta and A. Benella, *Microstrip Antenna Design*, Artech House, 1988.

[Hall92] G. Hall, *The ARRL Antenna Book*, 10th edition, ARRL publishers, 1992.

[Jasi84] H. Jasik and R.C. Johnson, *Antenna Engineering Handbook*, 2nd Edition, McGraw-Hill Book Company, 1984.

[Krau88] J.D. Kraus, *Antennas*, 2nd Edition, McGraw-Hill Book Company, 1988.

[Kuma91] A. Kumar, *Fixed and Mobile Terminal Antennas*, Artech House, 1991.

[Love76] A.W. Love, *Electromagnetic Horn Antennas*, IEEE Press, 1976.

[Mill85] T.A. Milligan, *Modern Antenna Design*, McGraw-Hill Book Company, 1985.

[Stut81] W.L. Stutzman and G.A. Thiele, *Antenna Theory and Design*, John Wiley & Sons, 1981.

Related to robotics:

[Crai86] J.J. Craig, *Introduction to Robotics - Mechanics & Control*, Addison-Wesley Publishing Company, 1986.

[Nagy87] F. N. Nagy and A. Siegler, *Engineering Foundations of Robotics*, Prentice-Hall International, 1987.

[Shab94] A.A. Shabana, *Computational Dynamics*, John-Wiley & Sons, 1994.

Related to mathematics:

[Krey83] E. Kreyszig, *Advanced Engineering Mathematics*, 5th edition, Wiley Eastern Limited, 1993.

[Rade90] L. Rade and B. Westergren, *Beta-Mathematics Handbook*, 2nd edition, CRC Press, 1990.

Related to programming:

[Kern88] B.W. Kernighan and D.M. Ritchie, *The C Programming Language*, 2nd edition, Prentice Hall, 1988.

Related to computer vision and computer graphics:

[Scot93] Scott Anderson, *Morphing Magic*, Sams Publishing, 1993.

[Ponc89] J. Ponce, D. Chelberg and W.B. Mann, "Invariant Properties of Straight Homogeneous Generalized Cylinders and Their Contours," *IEEE Transactions on Pattern Analysis and Machine Intelligence*, vol. 11, no. 9, pp. 951-966, September 1989.

Appendix A
Minimum System Requirements

This appendix provides the minimum system requirements for SMT version 7.0.

Software:

- DOS 3.3 or later.
- Microsoft Windows 3.1 running in enhanced mode or Windows95.
- AutoCAD release 12.0 for Windows. (Any version is acceptable, e.g. U.S. [Student or Professional] or International, although the International version requires a hardware lock to be installed) .

Hardware:

- PC with 80386™ processor or higher and a math coprocessor.
- Color Monitor. (The bigger the monitor the better. With 14 inch or bigger, all the SMT screen menu commands are visible and accessible. For smaller monitors the user may be required to use the pull down menu, as certain commands on the screen menu may go beyond the visible area of the screen)
- Keyboard, mouse, and a 1.4 MB, 3 1/2-inch floppy drive.
- RAM, 8 MB at least, 16 MB preferred. 8 MB is the minimum specified by AutoCAD, but higher RAM reduces computation time.
- AutoCAD itself requires 37 MB disk space for installation. An additional 20 MB free disk space is recommended.

Appendix B

List of Files and Suggested Placement during Installation

This appendix provides a list of files and suggestions on their placement during installation of SMT version 7.0. Note that the file list below is the *minimum* a user would require to successfully run the SMT. If the user has access to the source code, additional files are required to compile the code. These files are listed in Appendix C.

Even though the placement of files is flexible, it is recommended that the user choose from the following two options.

1. Place all the files listed below onto one directory (e.g. c:\research). Make this directory the working directory for AutoCAD. This can be done by selecting the *properties* from the *program manager* for the AutoCAD icon and editing the working directory.
2. Place the *smt.exe* in c:\acadwin. Place all the **.dcl* files in c:\acadwin\support. Place the **.dwg* and **.dat* files onto one directory (e.g. c:\research). Make this the working directory for AutoCAD.

Installation may be broken down into following steps:

- The original acad.mnu in c:\acadwin\support is to be replaced by the *acad.mnu* file provided with SMT version 7.0. The original file may be renamed acadorij.mnu. It is assumed that AutoCAD is installed in c:\acadwin which is the default installation.
- Copy the *smt.exe* file into the corresponding directory.
- Copy the following **.dcl* files into the corresponding directory.

1) Afval.dcl	2) Alert.dcl	3) Chmodeq.dcl
4) Clsdpat2.dcl	5) Cntr_res.dcl	6) Envpar.dcl
7) Fafval.dcl	8) Faterr.dcl	9) Intsinfo.dcl
10) Nmfval.dcl	11) Omnipatn.dcl	12) Patinfo.dcl

13) Transinfo.dcl 14) Transpar.dcl 15) Txrxheit.dcl

16) Userpatn.dcl 17) Warn.dcl 18) Warn1.dcl

- Copy the **.dat* files. These are the files which contain the user provided antenna pattern data. During SMT compilation the following files were used. 1) Gainxy.dat 2) Gainxz.dat and 3) Gainyz.dat
- Copy the **.dwg* files. During SMT compilation the following files were used. 1) Demo1.dwg and 2) Demo2.dwg.

Appendix C
SMT 7.0 code compilation

The SMT version 7.0 was developed with only 8 MB of RAM which is the minimum required by AutoCAD. The earlier version used Borland C++ compiler for windows (Version 3.1). The program was also compiled on a DOS command line by using the *make* command. Subsequently the compilation was upgraded to Borland C++ compiler for windows (Version 5.02) Also the compilation was done by using the IDE (Interactive Development Environment) which provides the user great flexibility in terms of code additions or modifications.

Other than the standard directories and library files of AutoCAD and Borland C++ which are included during compilation, the SMT project file (called *smt.ide*) consists of the following files:

- The source code files, **.c* and **.h*, which are

  1) Smt.c 2) Smt.h 3) Edm_bldg.h
  4) Edm_comm.h 5) Comm.h 6) Uim_cmd.h
  7) Uim_dlog.h 8) Scm_cntr.h 9) Scm_disp.h
  10) Antenna.h

- *smt.rc*, the resource file for the linker. This file binds an icon and a string to the executable for display in the windows program groups.
- *smt.def*, the module definition file. This file is used to set linker options for the executable.

Appendix D
SMT 7.0 Command Reference

This appendix outlines the various SMT 7.0 commands available to the user via the screen menu or pull down menu or the AutoCAD command prompt. The commands which were not there is the previous versions of SMT or were modified are in italics. All commands are listed in alphabetical order.

ANTENNA HEIGHT AND ORIENTATION Opens up a dialog box which allows the user to set the height of transmitting and receiving antenna above the floor level in meters. Also the orientation of the antenna pattern can be set by selecting the azimuth, elevation and slant angle in degrees.

AREA Prompts the user to select a coverage contour using the mouse. The area enclosed within the contour in square meters and the perimeter of the contour in meters is displayed. This command is not limited to coverage contours, as any closed polygon may be selected with the same result.

CANCEL Any AutoCAD command may be terminated by invoking this screen selection. Its effect is the same as entering ^C on the command line.

CLEAR Erases all coverage contours on the currently displayed floor.

CLEAR_1 Erases the coverage contour on the displayed floor for a selected transmitting source.

CNTR_RES Invoking this command displays the SMT "Contour Resolution" dialog box. The user may then edit the distance resolution and/or the number of contour polygon

points to be calculated. The default settings for the SMT are 1 m for the distance resolution and 18 points for number of points.

DIR XCVR This command allows the user to place any number of SMT directional transmitters on the current floor. Transmitters placed on a different floor are visible in a block outline (➢) and those on the current floor are displayed by a bold block outline (➢)

DISPLAY Displays the inner and outer coverage contour. Coverage is calculated and displayed starting with the most recently placed transceiver. If the coverage region of a transceiver is already on display, it is first erased and is then recalculated.

DELETE Any transmitting source on the current floor can be deleted by invoking this command. The user is prompted on the command line to select the source to delete, which he/she may then do by a mouse click. For a source being deleted, its current coverage region, if already displayed, is also erased.

DOWN_1_F Selecting this menu option moves the displayed floor down by one level for a multi-story floor plan. If the user is currently on the lowest floor of a drawing, invoking this selection displays an SMT message (Invalid floor) dialog box.

ENVMNT Invoking this command displays the SMT "Environment Type" dialog box. The user may then select any environment type and thus set a value for the path loss exponent *n*. This value for *n* is used only for the same-floor distance-dependent path loss model.

FLOORHT This command allows the user to vary the ceiling height of a multi-story building. The default SMT value for all ceiling heights in a building is set at 3 m. Different floors cannot be assigned different ceiling heights.

FAF/Nmf Invoking this command displays the SMT "Floor Attenuation Factor" dialog box if the floor-attenuation-factor model is the active multi-floor model. The user may then set any values for these building parameters.

GO_TO_FL Invoking this command prompts the user to enter the number on the command line of the new floor to display. If the user enters an invalid floor number, SMT displays the SMT message (Invalid floor) dialog box.

GN_MARGIN This command allows the user to vary the threshold margin (in dB) between the two contours. The default SMT margin is currently 6 dB.

ISO XCVR This command allows the user to place any number of isotropic sources on the current floor. Transceivers on the current floor are displayed by a bold block outline ( ). Transceivers that have been placed on a different floor are visible in a block outline ( ).

INTSRC Using this command, the user can place any number of single-tone interference sources on the current floor. Interference sources on the current floor are displayed by a bold block outline (✧)and those placed on a different floor are displayed in a block outline (✧).

INFO Upon invoking this command, the user is prompted to select a source with a mouse click. The corresponding parameters are then displayed in a dialog box. For a transceiver, this information is simply its location coordinates on the floor plan. For an interference source, its current status (whether turned “on” or “off”), transmitting frequency, and power are also displayed and can be edited.

MODEL Displays a dialog box which allows the user to select which propagation model discussed in section 3.7.1 will be used for coverage prediction.

MOVE This command allows the user to reposition any source previously placed onto the current floor by the ISOXCVR or INTSRC or DIRXCVR commands. The user is prompted (on the command line) to select the source to move and then select the new location by a mouse click. For a transceiver being moved, its current coverage region, if already displayed, is first erased and the region around the new location is then automatically calculated and displayed.

OMNIDIRECTIONAL PATTERN This command opens up a dialog box to allow the user to select from a menu of eight omnidirectional patterns.

OTHER DIRECTIONAL PATTERN This command opens up a dialog box to allow the user to select from a menu of other directional patterns. The user selects one from a list of seven elevation plane patterns and one from a list of seven azimuth plane patterns. The user can also assign a boresight gain for the pattern.

PAF Invoking this command displays the SMT "Partition Attenuation Factor" dialog box. The user may then set any value for the four partition types supported for SMT 7.0.

SELECT_1 This command may be invoked to calculate and display the coverage region of a selected transmitting source on the current floor. The user is prompted to select the source with a mouse click.

TRANSPAR Invoking this screen command displays the SMT "Transceiver Parameters" dialog box. The user may then change any or all of the transceiver communication parameter values for all subsequent coverage region calculations. All transceivers on the floor plan, irrespective of whether they were placed before or after invoking this command, are assigned the communication parameters of the selected SMT transceiver type.

UP_1_FL Selecting this menu option moves the displayed floor up by one level for a multi-story floor plan.

USER PROVIDED PATTERN This command opens up a dialog box to allow the user to type in the path name to indicate the location of the two files containing the azimuth and elevation plane data.

WSCALE This command prompts the user to enter a scaling factor for the icon placed on the floor plan. The default factor is 10. Increasing or decreasing this number makes any of the three icons present on the floor plan (isotropic transceiver, directional transmitter, interference source) to grow or shrink in size.

Vita

Nitin Bhat was born on January 24, 1966, in Ratnagiri, India. He received the Bachelor of Engineering degree in Electronics and Communication (Honors) from Regional Engineering College, Suratkal (KREC) in June 1987. From July 1987 to November 1993, he worked in India and Japan as a Senior Engineer in Consumer Electronic Industries (BPL-Sanyo, Videocon-Toshiba). He received the Master of Science degree in Electrical Engineering from Virginia Polytechnic Institute and State University in March 1998. He is a member of IEEE.

Since March 1996, Mr. Bhat has been working as an Systems Engineer with Hughes Network Systems, a wireless communications company, based at Germantown, Maryland.